THE EFFECT OF PARTICLE SIZE SEPARATION ON THE ENRICHMENT AND RECOVERY OF RARE EARTH ELEMENTS FROM SOUTH AFRICAN COAL FLY ASH

UNIVERSITY *of the*
WESTERN CAPE

A dissertation submitted to the University of the Western Cape in the fulfilment of the degree of Magister Scientiae (M.Sc)

By

BONGIWE VINITA SELEKA

Department of Earth Sciences

Faculty of Natural Sciences

Supervisor:

Dr. Sumaya Clarke

Co-supervisor:

Dr. Lehlohonolo Mokhahlane

August 2021,

Bellville, South Africa

ABSTRACT

There has been increasing interest in finding alternative sources for Rare Earth Elements (REEs) due to their application in green energy and Coal Fly Ash (CFA) has been found to be a viable potential source. Thus investigations on the feasibility of recovering REEs from CFA and the possibility of optimizing the current recovery techniques have become popular. The main focus in the investigations has been to use equipment and products that are environmentally sustainable and economically efficient. In addition, studies have shown that there is a relationship between the particle size of CFA and the REE concentration, which can potentially increase the recovery of REEs. However, there have been inconsistencies in the findings of this relationship. Thus, this study aimed to assess the effect of particle size separation on the enrichment and recovery efficiencies of REEs from South African CFA. CFA from Duvha and Tutuka power stations was sampled and the objectives were to qualitatively and quantitatively characterize the morphology, mineral and elemental composition of CFA; to assess the relationship between REEs with the particle size of CFA; to determine REE recovery efficiencies; and characterize, the morphology, mineral, as well as the elemental composition of solid residues obtained after alkali-fusion acid leaching. The samples were analysed using SEM-EDS, XRF, TIMA, LA:ICP-MS and ICP-MS analytical techniques.

The morphological analyses of the raw CFAs of Duvha and Tutuka CFA revealed that the majority of the particles were typically spherical with some irregular shaped structures in agglomerated form. Tutuka CFA exhibited numerous ferrospheres, while Duvha CFA displayed more cenospheres and plerospheres. Quartz and mullite were identified as the major mineral phases in both CFAs, while maghemite, microcline and calcite were present in low quantities. The ΣREE content in Duvha and Tutuka CFA was measured to be 573.77 ppm and 546.25 ppm, respectively. The distribution of ΣREEs with particle was determined for both CFAs and a moderate positive correlation and substantial relationship existed between the particle size of Duvha CFA with the ΣREE content (R = 0.68). In Tutuka CFA, there was a very high positive correlation and dependable relationship (R = 0.99) between the particle size of Tutuka CFA with the ΣREE content. In Duvha CFA, the abundance of ΣREE recovered in the leachates of the whole (un-sieved) samples was in the order of Ce > La > Nd > Y in Duvha CFA, while in Tutuka CFA it was Ce > Y > La > Nd. REEs in the leachates of the sieved particle size fractions of Duvha and Tutuka CFA revealed a slight increase in the recovery of ΣREE with a decrease in particle size. A positive moderate correlation and substantial

relationship between the particle size of Duvha CFA with the ΣREE recovered in the leachates (R = 0.66), while there was a very high positive correlation and dependable relationship (R = 0.94) between the particle size of Tutuka CFA with the ΣREE content recovered in the leachates. In both Duvha and Tutuka CFA, the highest α for ΣREEs was observed in the smallest size fraction (< 25 μm) with α of 38.31 % and 36.39 % respectively.

The morphology of the particles of the leached solid residues of both CFAs was different in shape and structure compared to the raw CFAs. The particles of the leached solid residues appeared to have been crusted, etched and corroded. SiO_2 and Al_2O_3 remained the major elements retained in the leached solid residues of both CFAs. The analyses of the REEs retained in the leached solid residues showed minimal variation in the amounts of REEs retained between the leached solid residue of Duvha and Tutuka CFA, except for Ce. The REE Ce was retained more in Tutuka CFA compared to Duvha CFA leached residue with 88.42 ppm (44.81%) and 75.40 (34.75%) ppm retained, respectively.

DECLARATION

I, Bongiwe Vinita Seleka, declare that the full dissertation titled '**The Effect of Particle Size Separation on the Enrichment and Recovery of Rare Earth Elements from South African Coal Fly Ash"**, is my work, has not been submitted before for any degree or examination in any other university and that all the sources I have used or quoted have been indicated and acknowledged by complete references.

Full Name: Bongiwe Vinita Seleka 20 August 2021

Signature

ACKNOWLEDGEMENTS

First and foremost, I would like to thank Almighty God for his favour and my parents for their love and support, through my education.

I would like to express my sincerest gratitude to my supervisors Dr Sumaya Clarke and Dr Lehlohonolo Mokhahlane for their support and guidance. I truly consider myself very privileged for being under the supervision of such passionate and encouraging supervisors. Thank you for allowing me to grow as a research scientist and for your financial contributions to this research.

The National Research Foundation (NRF) of South Africa is acknowledged for its financial contribution (Grant No. MND190704452899) to this master's research.

To Dr Alechine Ameh, thank you for your technical assistance in the laboratory. You were very keen to avail yourself from the first day I met you. I am truly grateful that there are people like you in our institution.

Special thanks go to my colleagues, who have become like siblings for their advice, and support.

Sincere deepest gratitude goes to Kamohelo Mokoena, your encouragement and support through this journey is appreciated and duly noted. Thank you for allowing me to brainstorm ideas and giving me a safe creative space to do so. This journey was a rollercoaster ride, and experiencing it with you made it worthwhile. Friend, we did it.

ACRONYMS AND ABBREVIATIONS

CFA	Coal Fly Ash
REE	Rare Earth Elements
HDPE	High Density Polyethylene
LREE	Light Rare Earth elements
MREE	Medium Rare Earth Elements
HREE	Heavy Rare Earth Elements
SEM-EDS	Scanning Electron Microscope – Energy Dispersive Spectrometry
XRD	X-Ray Diffraction
TIMA	Tescan Integrated Mineral Analyser
XRF	X-Ray Fluorescence
ICPS-MS	Coupled Plasma Mass Spectrometry
LA:I CPS-MS	Laser Ablation: Coupled Plasma Mass Spectrometry

METRIC UNITS OF MEASUREMENT

ℓ	Litre
mℓ	Millilitres
mol/ℓ	Moles per litre
μm	Micrometre
g	Grams
ppm	Parts per million
rpm	Revolutions per minute

LIST OF CONTENTS

LIST OF FIGURES

LIST OF TABLES

LIST OF TABLES

CHAPTER ONE: GENERAL INTRODUCTION

1. Introduction

Rare earth elements (REEs) are a group of 17 chemical elements, which include scandium, yttrium and the 15 lanthanides. These elements are widely used and have become important components in various industries (e.g., clean energy production, health care, oil refining and electronics) (Huang et al., 2018). Furthermore, the demand for REEs continues to increase, however, the availability remains limited (Scott et al., 2015; Rosita et al., 2020). Thus, there is a need to identify new and unconventional sources of REEs. Coal Fly Ash (CFA) is considered a viable source because REEs are retained during coal combustion and is available in large quantities (Dutta et al., 2016; Huang et al., 2018; Taggart et al., 2018b; Yang, 2019).

This chapter aims to provide an outline of the focus of the study. A brief background on the enrichment and recovery of REEs from CFA is provided. Furthermore, the problem statement and the objectives of the study are outlined later in the chapter.

1.1. Research Background

Globally, there has been a shift towards green energy and this has led to an increase in the demand for REEs (Dutta et al., 2016). This is due to their unique electrochemical, magnetic, and luminescent properties, which are essential in the manufacturing of green energy devices. Therefore, a market exists for REEs. China has been the predominant producer of REEs, producing more than 90% in the past two decades (Seredin and Dai, 2012; Josso et al., 2018). Thus, the recovery of REEs from CFA in South Africa will allow the country to compete in the trade of these elements. Moreover, recovering REEs from CFA can potentially reduce the mining and processing costs as these costs will be assigned to the production of CFA (Yang, 2019).

CFA contains a higher fraction of REEs (>30% of total REEs) than REE-bearing ores (Seredin and Dai, 2012; Taggart et al., 2016). In addition, CFA potentially contains the full range of REEs while most conventional REE mines only extract a few of these elements (Wagner and Matiane, 2018). The bulk of REEs have been found to reside within the matrix of the CFA particle in the alumina glass phase. Therefore, obtaining REEs from CFA requires an extraction

process, one that will allow accessibility of the REEs from the matrix (Lin et al., 2018; Zhang and Honaker, 2020). Effective extraction of REEs from CFA is quite difficult due to the complex nature of CFA. The complexity arises from the chemical composition of the coal, the combustion technique and the technology used (Hower et al., 2016; Taggart et al., 2016). CFA could potentially be a source of REEs in the future if cost-effective extraction methods are developed. Further research needs to be conducted to identify the potential of CFA as a source for REEs and to develop the capabilities to economically recover REEs in an environmentally sustainable manner.

Several techniques have been developed for the successful recovery of REEs from CFA and these methods are based on hydrometallurgy processes. Hydrometallurgy is a technique within the field of extractive metallurgy involving the use of aqueous chemistry for the recovery of metals from ores, concentrates, recycled or residual materials (Kashiwakura et al., 2013; Balaram, 2019; Wang et al., 2019). For the recovery of REEs from CFA, various leaching techniques have been developed including direct acid leaching, alkaline leaching, alkaline-acid fusion leaching and bioleaching (Jha et al., 2016; King et al., 2018; Lin et al., 2018; Taggart et al., 2018b).

Recent investigations have shown that with the direct acid leaching and alkaline-acid fusion leaching technique relatively high REE recovery efficiencies (> 70 %) can be obtained (Cao et al., 2018; Tang et al., 2019; Zhang and Honaker, 2020), thus they are often favoured. However, low REE recovery efficiencies are still observed in some CFAs. Taggart et al. (2018b) suggested that not all CFA, particularly those that are enriched in calcium oxide (CaO) should necessarily be subjected to alkali fusion as recovery efficiencies are similar to that of alkali fusion acid leaching can be obtained by direct acid leaching. Thus, this is important to consider when attempting to scale-up these techniques to industrial applications and taking into account that these techniques can consume quite a lot of energy.

Thus current investigations are focussed on optimising the two techniques and lowering the costs and energy consumption (King et al., 2018; Taggart et al., 2018a; Taggart et al., 2018b; Tang et al., 2019; Zhang and Honaker, 2020). A huge part of optimising the techniques is attempting to enrich the CFA with REEs before leaching as literature has shown that physical separation methods can be applied to achieve this (Hower et al., 2013; Blissett et al., 2014; Lin et al., 2017; Pan et al., 2020). These methods have mainly included particle size, magnetic, density and electrostatic separation as well as flotation. However, limited applications of these

methods in the recovery of REEs from CFAs have been reported in recent studies (Lin et al., 2017). Thus, current investigations are focussed on concentrating REEs in CFA before acid leaching by applying physical separation techniques to ensure that the recovering efficiencies are increased (Lin et al., 2017; Taggart et al., 2018a; Tang et al., 2019; Rosita et al., 2020; Pan et al., 2020; Zhang and Honaker, 2020).

1.2. Research Problem

CFA is regarded as a reliable alternative source of REEs, and in recent years, the development of economically, feasible and environmentally friendly approaches for domestic REE recovery has been of great research interest (Taggart et al., 2016; King et al., 2018; Taggart et al., 2018a; Liu et al., 2019; Tang et al., 2019). REE recovery processes from CFA include beneficiation and acid leaching. Beneficiation processes are aimed to enrich CFA with REEs by isolating fractions of CFA that are most likely to be more abundant in REEs. These processes often include, among others, particle sizing, density separation, magnetic separation, and froth flotation (Lin et al., 2017; Lin et al., 2018; Rosita et al., 2020; Rybak and Rybak, 2021).

Literature has shown that there is a relationship between the particle size of CFA and the REE concentration. The content of REEs has been found to increase with a decrease in particle size of CFA, particularly for separates between 100 and 30 micrometres (µm) (Clarke and Sloss, 1992; Seredin and Dai, 2012; Hower et al., 2013; Blissett et al., 2014). However, some literature shows some disagreements in experimental results, which indicates that different CFAs might have different responses to these separation techniques (Scott et al., 2015). In REE recovery, the particle size of CFA is an important parameter because its surface may act as a site for deposition or condensation of various elements during the acid leaching process. Therefore, the effect of the particle size of CFA on the recovery of REEs needs to be thoroughly understood as it may play an important role in addressing the low REE recovery efficiencies. Furthermore, in South Africa, the occurrence, distribution, as well as recovery of REEs from CFA has not been extensively explored (Eze, 2013; Hancox and Götz, 2014; Wagner and Matiane, 2018).

Overall, REE recovery technologies are not well developed and there is still the issue of low recovery efficiencies in some CFAs. This knowledge gap creates a need to better understand the feasibility of CFA as an alternative source of REEs. Furthermore, several studies have

reported on the enrichment of REEs from CFA by particle size separation (Dai et al., 2010; Hower et al., 2013; Dai et al., 2014; Scott et al., 2015; Lin et al., 2017; Pan et al. 2020; Rosita et al., 2020). However, none of these studies particularly using South African CFA have gone further and extracted REEs from the separates, using commonly used techniques such as alkali-fusion acid leaching. Therefore, the purpose of this study was to evaluate the effect of particle size on REE enrichment and recovery efficiencies on South African CFA.

1.3. Significance of the Study

REEs have been recognised as critical raw materials in the development of green energy and advanced technologies (e.g., hybrid vehicles, wind turbines, next-generation rechargeable batteries, etc.) (Franus et al., 2015; Dutta et al., 2016; Balaram, 2019). As the world is slowly shifting towards green energy and advanced clean technologies, the global demand and supply of REEs continue to increase (Balaram, 2019). Thus, there is a need to investigate new sources for these elements (Dutta et al., 2016).

CFA which is often considered waste has been regarded as the viable source of REEs and is enriched in these elements than some REE-bearing ore deposits. In addition, REEs in CFA have been found to increase with a decrease in particle size. However, whether this relationship exists in REE recovery has not been explored. Therefore, it is of paramount importance to develop and understand approaches that can optimise the recovery of REEs from CFA. Thus, knowledge advances in this area of research will have an important contribution to the various applications of REEs (Dutta et al., 2016; Lanzerstorfer, 2018; Gollakota et al., 2019).

Furthermore, it is stated within the South African National Environmental Management Act No. 107 (1998) that everyone has a right to a clean environment, one that is not harmful to their health and well-being (Government Gazette, 1998). On the other hand, the National Water Act No. 36 (1998), states that the nation's water resources need to be protected, used, conserved and managed (Department of Water and Sanitation, 1998). Thus, it is of utmost importance to protect the environment. Therefore, the utilisation of CFA particularly for purposes that would yield environmental and economic benefits may potentially address some of the environmental concerns that are associated with its disposal (Singh and Kalamdhad, 2011; Tiwari et al., 2015; Dalton et al., 2018; Gollakota et al., 2019). This will subsequently align with the National Water and Environmental Management Acts of 1998.

Internationally CFA is generally classified as a by-product or a resource depending on the country. South Africa currently classifies CFA as hazardous waste and this classification is the strictest in the world (Reynolds-Clausen and Singh, 2019). Nevertheless, on the 3rd of February 2020, several companies that produce coal ash had some of their coal by-products such as CFA excluded from the definition of "waste" in terms of the National Environment Management Waste Act No 59 of 2008 (Creecy, 2020). These companies include but are not limited to Eskom Holdings COC (Ltd), Sasol South Africa (Ltd) and Anglo-American Platinum (Ltd).

The exclusion of CFA produced by these companies from the waste classification gives rise to several opportunities in the beneficiation of ash in South Africa, particularly in REE recovery. For the past two decades, China has been the predominant producer of REEs (Seredin and Dai, 2012; Josso et al., 2018). Therefore, the recovery of REEs from South African CFA will allow the country to compete in the trade of these elements and apply them in the development of green energy and technologically advanced devices. Thus, investigations such as this study can provide baseline information on the recovery of REEs from South African CFA as currently this has not been extensively explored.

The findings of this study will contribute to the understanding of the distribution of REEs with particle size and evaluate the efficiency of the alkali-fusion acid leaching technique in recovering REEs. Furthermore, the findings will give insight on whether applying acid leaching techniques in REE recovery results in waste products that are more toxic than the CFA, thus rendering the process environmentally unsustainable.

1.4. Hypothesis

There is an inverse relationship between the particle size of CFA and the concentration of REEs. The concentration of REEs increase with decreasing particle size of CFA.

1.5. Research Questions

i. What effect does the particle size of CFA have on the enrichment of REEs?

ii. What effect does the particle size of CFA have on the recovery efficiencies of REEs?

1.6. Study Aim and Objectives

This study aims to assess the effect of particle size separation on the enrichment and recovery efficiencies of REEs from South African CFA.

The overall objectives of this study can be summarised as:

i. To characterize the raw bulk CFA in terms of morphology, mineral and elemental composition, through the application of various analytical techniques (i.e., SEM-EDS, XRD, XRF, TIMA, ICP-MS and LA-ICP-MS). This will provide an understanding of the initial characteristics of the CFA before particle size separation and leaching.

ii. To assess the relationship between REEs and the particle size of CFA, through particle size separation and analytical analyses of the whole and separated size fractions to determine the total REE concentrations using LA-ICP-MS. As well as to evaluate whether the inverse relationship between the particle size of CFA and REE content found in literature exists in South African CFA (Clarke and Sloss, 1992; Seredin and Dai, 2012; Hower et al., 2013; Blissett et al., 2014).

iii. To determine the REE recovery efficiencies of the whole and separated size fractions of CFA, through the application of a commonly used technique in REE recovery, alkali-fusion acid leaching. As well as assess whether particle size separation enriches REEs in CFA and improve recovery efficiencies.

iv. To characterize the solid residue obtained after alkali-fusion acid leaching in terms of morphology, mineral and elemental composition using various analytical techniques (i.e., SEM-EDS, XRD, XRF, ICP-MS and LA-ICP-MS) and to obtain a better understanding of the REE leaching process in South African CFA. In addition, to allow for the evaluation of the toxicity level of the solid residue compared to the raw CFA.

1.7. Scope and Delimitation of the Study

REE recovery from CFA employs the hydrometallurgy technique which is used in the field of extractive metallurgy involving the use of aqueous chemistry for the recovery of metals from ores, concentrates and recycled or residual materials. The technique involves four distinct phases: preparation, dissolution, extraction and recovery. However, this study mainly focussed

on the dissolution aspect of REE recovery, and the purpose was to evaluate the relationship between particle size and REE enrichment. A relationship between CFA particle size and REE is reported to exist between separates of 100 and 30 µm (Clarke and Sloss, 1992; Seredin and Dai, 2012; Hower et al., 2013; Blissett et al., 2014; Lin et al., 2017; Lin et al., 2018; Rosita et al., 2020). Thus, the particle size fractions investigated in this study ranged between 106 and 25 µm. Throughout the study, a quantitative experimental design was adopted to achieve the objectives. This involved separating CFA into various particle size fractions, subjecting it to alkali-fusion and acid leaching. Standard analytical procedures were applied for the analysis of the raw CFA, supernatant water and the solid leached residues obtained after the experiments.

Ideally, for each particle size fraction, it would have been desired that the total chemistry including REEs be determined for the raw CFAs, leachates and solid leached residues of both CFAs. However, due to funding constraints, this was not done, rather the analysis of the REE content was prioritized. In addition, due to the above-mentioned reason as well as time constraints, the study was unable to investigate optimal alkali-fusion and acid leaching conditions for each CFA used. Therefore, optimal conditions suggested in literature were applied to evaluate the relationship between the particle size of CFA and REE recovery efficiencies.

1.8. Study Site Description and Justification

Two South African coal-fired power stations that are operated by Eskom were chosen as study sites for this research and they are as follows: Duvha and Tutuka. Duvha Power Station is located approximately 15 kilometres (km) east of Witbank in Mpumalanga Province, while Tutuka Power Station is situated 25 km from Standerton in the same province (Eskom Holdings SOC Ltd, 2020).

The CFA disposal mode in the two selected power stations is not the same. Duvha power station operates a wet ashing facility, whereby the ash is mixed with water, then hydraulically pumped into an Ash Dam, while Tutuka makes use of the dry disposal technique whereby the CFA is transported via a conveyor belt to an ash dumpsite. The choice of Duvha and Tutuka Power Stations as study sites was dictated by their accessibility, CFA disposal mode and their likelihood of burning coal sourced from different coalfields, which leads to different chemical compositions of the CFA produced.

Duvha Power Station receives coal from the Witbank Coalfield as feedstock to the power station, while Tutuka receives coal from the Highveld Coalfield. The Witbank and Highveld Coalfield hosts many of the major mine-mouth coal-fired power stations in South Africa (Hancox and Götz, 2014; Hancox, 2016). The above two coal-fired power stations as study sites provide a general view of the types of CFAs resulting from South Africa's largest coalfields.

1.9. Thesis Outline

Chapter one provides a general introduction and research background to the study. In addition, the chapter establishes the problem and the significance of this research. The aim and objectives of the study as well the research questions that the study attempted to answer are provided in this chapter.

Chapter two provides a review of relevant literature concerning the theoretical framework of this study. The review includes studies of a similar nature to this one and has contributed to the understanding of the recovering of REEs from CFA as well as the influence of particle size on the enrichment of REEs and REE recovery efficiencies.

Chapter three provides a detailed description of the study sites and an overview of the methods used to achieve the above-mentioned objectives. The chapter clarifies the methods for data acquisition and describes how this data was processed and analysed using relevant laboratory tools.

Chapter four describes the results obtained through experiments and laboratory analysis. The results are presented in various formats such as tables, graphs, and figures.

Chapter five discusses the findings of the study; the results are compared to previous findings of similar studies (local and international context) as well as other relevant literature and theory outlined in the literature review.

The final chapter of this dissertation concludes the study by summarizing the findings of the study, based on the aim and objectives established in the first chapter. Furthermore, it provides recommendations for future research and management.

CHAPTER TWO: LITERATURE REVIEW

2. Introduction

During coal combustion, mineral impurities in the coal, such as clay, feldspars, and quartz, are fused in suspension and float out of the combustion chamber with exhaust gases (Vadapalli et al., 2008; Jones et al., 2012). As the fused material rises, it cools and solidifies into spherical glassy particles called coal fly ash (CFA) (Kashiwakura et al., 2013). Throughout the world, CFA is an abundant by-product of coal combustion in power stations and is mostly disposed of in landfills and ash ponds; only a small part of it is used constructively.

This chapter reviews relevant literature on the characteristics of CFA and focuses on a research topic that has become popular concerning the utilisation of CFA, which is the recovery of rare earth elements (REEs). Investigations on the effect of particle size separation on the enrichment of REEs are reviewed as a means to better understand the distribution of REEs in CFA and improve recovery efficiencies. REEs, herein include the 15 lanthanides (i.e., Lanthanum (La), Cerium (Ce), Praseodymium (Pr), Neodymium (Nd) Promethium (Pm), Samarium (Sm), Europium (Eu), Gadolinium (Gd), Terbium (Tb), Dysprosium (Dy), Hoetium (Lu)), Ytrium (Y) and Scandium (Sc).

2.1. Coal Combustion Products

Coal is currently the most important energy source in the world after oil (Gollakota et al., 2019; Harris et al., 2019). In addition, coal is one of the cheapest and most abundant energy carriers (Sahoo et al., 2016). China ranked first (1 827 million metric tonnes of oil equivalent) on the world's top ten coal consumption in 2015, while South Africa ranked seventh (143 million metric tonnes of oil equivalent) (Harris et al., 2019).

The combustion of coal by coal-fired power plants generates large quantities of coal combustion by-products (CCPs), which include ashes, slag, and flue-gas desulfurization residues (Vadapalli et al., 2008; Jones et al., 2012). The type of ash produced is a function of the mineral components of the original parent material of the coal and the combustion technique used (Kutchko and Kim, 2006). CFA, bottom ash (BA) and boiler slag (BS) are produced, according to the characteristics derived from the coal combustion methods and

emission controls (Rowland, 2014). **Table 2. 1** provides a detailed description of these CCPs (Luther, 2010; Rowland, 2014). Roughly 80% of the CCPs are released as CFA while the rest are mostly retained within the furnace as bottom ash (Jankowski et al., 2006; Kashiwakura et al., 2013).

Table 2. 1: Types of Coal Combustion Products (Luther, 2010; Rowland, 2014)

Product	Description
Coal Fly Ash (CFA)	Fine powdered ferro-aluminosilicate material captured through a particulate control device in the chimney of coal-fired plants at 1100 - 1400°C. The particles range from cenospheres (hollow particles) to plerospheres (hollow microspheres).
Bottom Ash (BA)	Coarse, gritty material and these ash particles are too large to be carried in the flue gas, hence the particles fall to the bottom of a furnace. Also, the particles have a porous surface structure and grain sizes ranging from fine sand to fine gravel.
Boiler Slag (BS)	Material drained from the wet bottom boilers operated at 1500 - 1700 °C. In contact with significant water molten BS fractures, crystallises and forms small rounded particles. BS material is made up of hard, angular particles that have a smooth, glassy appearance and the particles are uniform in size, hard, and durable, with resistance to surface wear

In South Africa, there are abundant coal resources and large quantities of CCPs are produced both in the generation of electricity (e.g., Eskom Holdings SOC Ltd) and the production of liquid fuel (e.g., Sasol Limited). However, only a small portion of it is made available to be used in various industries (e.g., cement, brick, road construction, etc.). For example, Reynolds-Clausen and Singh (2019) reported that in the year 2014 – 2015 Eskom produced 34.4 million tonnes (Mt) of ash in 13 power stations and of that ash 2.408 Mt was sold to industry. **Figure 2.1** provides further detail on the volumes of ash produced in a few of the power stations in South Africa. Kendal Power Station produced approximately 4.91 Mt of ash and of that ash, 1.91 Mt was used as an effluent sink at the power station to prevent the leaching of toxic elements to the environment. Therefore, 3 Mt was available to be recycled, however, only 0.54 Mt was sold, leaving 2.56 Mt being disposed of on landfill sites. This indicates an opportunity to utilize the ash even further as large volumes remain available for use.

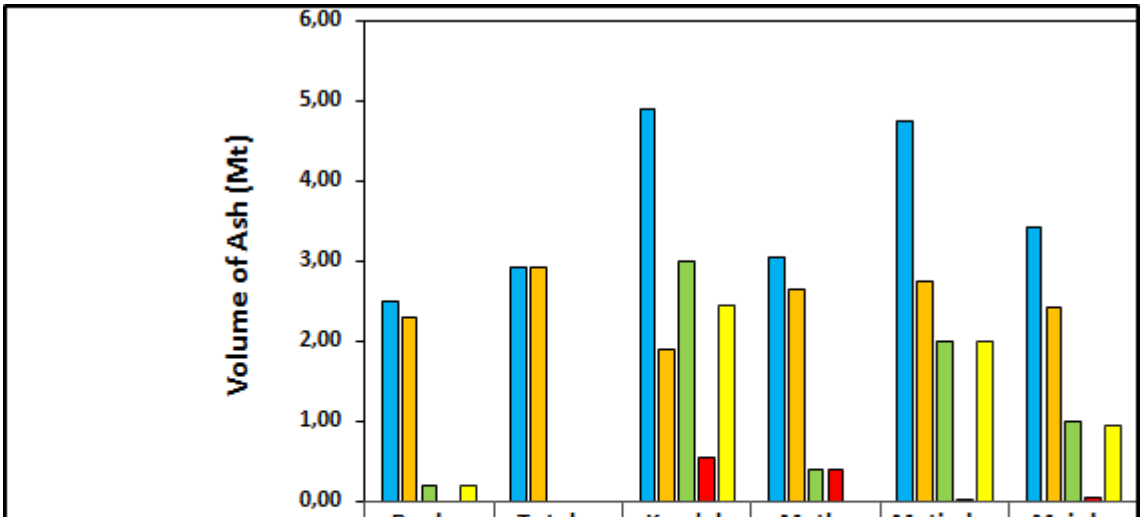

	Duvha	Tutuka	Kendal	Matla	Matimba	Majuba
Ash Produced	2,51	2,93	4,91	3,04	4,75	3,43
Ash used for Effluent Sink	2,31	2,93	1,91	2,64	2,75	2,43
Saleable Ash	0,20	0,00	3,00	0,40	2,00	1,00
Ash Sold	0,00	0,00	0,54	0,40	0,01	0,04
Remaining Ash	0,20	0,00	2,46	0,00	1,99	0,96

Figure 2.1: Estimated ash volumes available in some South African Power Stations (Reynolds-Clausen and Singh, 2019)

2.2. Classification of Coal Fly Ash

CFAs are generally classified into two chemical groups, namely Class F and Class C and this is based on the American Society of Testing of Materials (ASTM) C618 - 95 standards. **Table 2.2** provides some of the major differences between the two classifications. Class F CFAs have low calcium content and are generally produced from the combustion of higher-rank bituminous coals and anthracites. In addition, low-rank coals can meet the Class F requirements (Manz, 1999). On the other hand, the high-calcium Class C CFAs are usually produced from the combustion of low-rank lignites and sub-bituminous coals. Furthermore, ASTM C618 requires that Class F contain a minimum of 70 % pozzolanic compounds (silica oxide (SiO_2) + alumina oxide (Al_2O_3) + iron oxide (Fe_2O_3)), while Class C have between 50 and 70 % of these compounds (**Table 2.2**). Thus, Class F CFAs are more pozzolanic, meaning the CFA has cementitious properties (hardens) when reacted with calcium hydroxide ($Ca(OH)_2$) and water (H_2O), while Class C CFAs can be self-cementing (Vassilev and Vassileva, 2007; Saha, 2018). Generally, most of the CFA generated from South African coals is classified as Class F (Gitari

et al., 2009; Eze et al., 2014; Ameh et al., 2017; Reynolds-Clausen and Singh, 2019; Akinyemi et al., 2020).

Table 2.2*:* Composition of Coal Fly Ash Classes as per ASTM Standards (Jayaranjan et al., 2014)

Differences (%)	Class F	Class C
$SiO_2 + Al_2O_3 + Fe_2O_3$ (minimum)	70	50
SO_3 (maximum)	5	5
Moisture Content (maximum)	3	3
Loss of Ignition (maximum)	6	6
Available Alkalis (as Na_2O) (maximum)	1.5	1.5

2.3. Characteristics of Coal Fly Ash

The mineralogical, physical and chemical properties of CFA depend on the nature of coal, conditions of combustion, type of emission control devices, storage and handling methods (Hood et al., 2017). However, the typical coal feed of most coal-fed utility boilers consists of a blend of many coals. Thus, the CFA characteristics particularly that of chemistry cannot be traced back to a single coal.

2.3.1. Physical features

The colour of CFA ranges from grey to tan to reddish-brown as shown in **Figure 2. 2** and it is often a function of the combustion technique used as well as the amount of unburned carbon present (Jayaranjan et al., 2014). The darker the colour, the higher the carbon content and the opposite of this is true. Bituminous and sub-bituminous coals are the predominant form of coal present and mined in South Africa, while some areas have lignite. Bituminous CFA varies from light to dark grey, whereas, lignite CFA is usually tan in colour (Akinlua et al., 2011).

Figure 2. 2: Variations in the colour of coal fly ash (South African Coal Ash Association, 2020)

CFA mostly consists of silt-size particles (roughly between 0.01-100 micrometres (μm) in diameter, which consist of spherical particles embedded in an amorphous matrix and in general has a silt loam texture. Mehta (1994) found that CFA particles containing high amounts of CaO are finer than those containing low quantities. The particle size distribution of CFA varies over time depending on the coal-burning conditions in the power station.

Vadapalli et al. (2007) analysed the particle size distribution of South African CFA from a local power station and found the particle size distribution to be 14, 42 and 38 weight percent (wt %) for size fractions 75-150, 25-75 and < 25 μm respectively. Similarly, Nathan et al. (1999) investigated the particle size distribution of South African CFA (a by-product of coal from the Witbank Coalfield) and Colombian CFA. The results showed that 80 wt% of the South African and 75 wt % of the Colombian CFA particles studied were found in fractions lower than 45 μm.

Davison et al. (1974) found the trace elements arsenic (As), selenium (Se), cadmium (Cd), zinc (Zn), nickel (Ni), chromium (Cr), and lead (Pb) to significantly increase in concentration with decreasing particle size in two CFAs obtained from a power plant in the United States of America (USA). For example, Ni increased from 100 - 260 ppm, while Zn increased from 500 - 1400 ppm from sizes 74 - <5 μm. This observation was explained by the combustion of coal at high temperatures, where species containing these trace elements are volatilised then preferentially condensed or adsorbed onto smaller size particles. Furthermore, several studies (Scott, 2015; Lin et al., 2017; Pan et al., 2020; Rossita et al., 2020) have reported REEs to be

enriched in the smaller size fractions of CFA and it was found that the smaller content of unburnt carbon in these fractions was one of the contributors to this. For example, Pan et al. (2020) found the ΣREE content in Chinese CFA to increase from 608 micrograms per gram (µg/g) (150-100 µm) to 896 µg/g (< 25 µm). This suggests that smaller size fractions should be of most interest with respect to REE recovery efficiency. In addition, the bulk of CFA can be utilised as it is mostly comprised of smaller fractions that are potentially enriched with REEs.

Morphologically, CFA particles vary in shape and chemical composition (Goodarzi and Sanei, 2009; Sharonova et al., 2015). Cenospheres (hollow alumina-silicate rich spheres), plerospheres (larger hollow spherical particles, encapsulating smaller spheres) and ferrospheres (ferrous rich spherical particles) are the most common particles in CFA (Goodarzi and Sanei, 2009; Sharonova et al., 2015; Liu et al., 2016). Plerospheres, are less common in CFA compared to the other two particles. The presence of cenospheres further increases the specific surface area of CFA and enhances its adsorption ability. They are formed during the combustion of coal when the molten cools; the entrapped gas is emitted and forms pores on the surface of these particles. Cenospheres generally have better mechanical properties and a higher chemical reactivity than plerospheres (Liu et al., 2016; Etale et al., 2018).

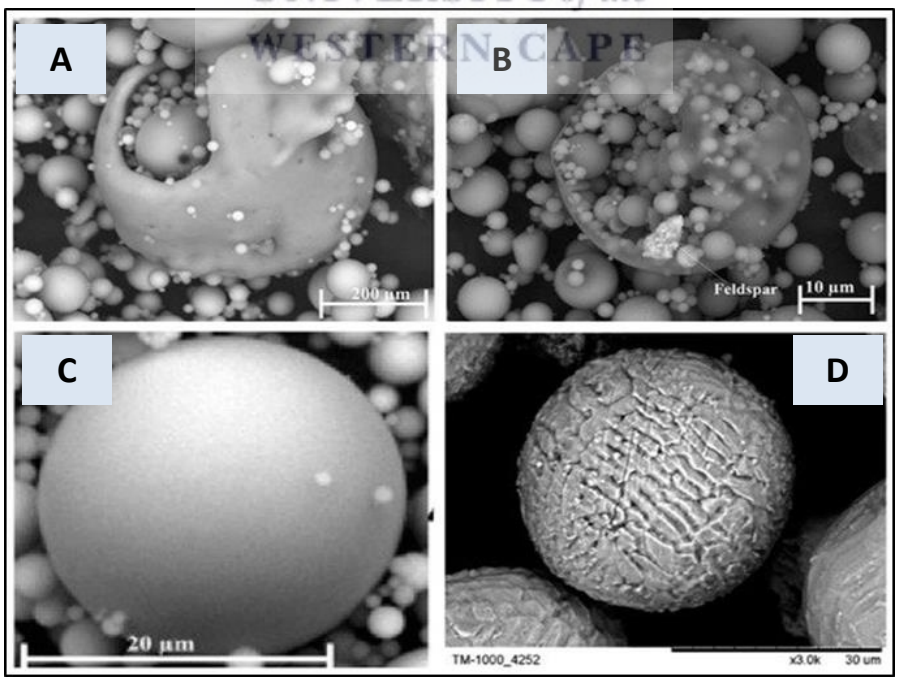

Figure 2. 3: Scanning Electron Microscope (SEM) images illustrating plerospheres (A,B) cenospheres (C) ferrospheres (D) found in CFA adapted from (Goodarzi and Sanei, 2009; Sharonova et al., 2015)

Figure 2. 3A,B shows plerospheres, which are thick and thin-walled. Both the plerospheres have trapped numerous smaller sized spherical particles, along with gases and minerals. While **Figure 2. 3C** depicts cenospheres which are spherical, having mainly Al and Si, along with carbon, on their surface, **Figure 2. 3D** shows ferrospheres, which are ferrous on their surface and have a rough-surfaced and dendritic shape on their surface. Minerals associated with REEs (e.g., monazite, zircon, xenotime, etc.) are found on the surface and within these particles and their presence is dependent on the initial mineralogy of the coal burnt (Goodarzi and Sanei, 2009; Zhang, 2014; Sharonova et al., 2015; Pan et al., 2019).

2.3.2. Mineralogy and Chemical Features

CFA is predominantly comprised of non-crystalline alumina-silicate glasses, mullite-quartz, magnetic and smaller amounts of unburnt coal particles and crystalline minerals (Zhang, 2014). The glassy and spherical occurrence of fine CFA indicates the melting of silicate minerals under high temperatures during the combustion process (Hansen et al., 1981; Mahlaba et al., 2011).

During the combustion of coal, CFA is enriched in all the heavy metals including REEs as they are not combustible. The REEs occur in different forms, namely: as discrete minerals, ion adsorbed forms or native metals (Anand et al., 2020). REE-bearing minerals are much less common in CFA than in the corresponding coal, even though the CFA is REE-enriched. This is due to the melting temperatures of some of these mineral traces (e.g., zircon, monazite, xenotime, etc.) being below the temperature range in which most coal-fired boilers operate (i.e.,1300 - 1700 °C) (Kolker et al., 2017). Nonetheless, traces of these minerals have been observed in CFA, and zircon, as well as monazite, have been the most common ones (Sahoo et al., 2016). Kolker et al. (2017) suggested several possible explanations for REE enrichment in CFA with the disappearance of REE mineral phases: (i) persistence of trace phases but with size reduction due to thermal shock, (ii) localized diffusion of REE from trace phases to the glass; and (iii) occurrence of REE as nanoparticles or REE-enriched domains at the nanometer scale. The boilers of the CFAs used in this study (i.e., Tutuka and Duvha Power Stations) operate at temperatures of ~ 540 °C (Eskom Holdings SOC Ltd, 2020) Therefore, it is expected that REE-bearing trace phases will be preserved in these CFAs as operating temperatures are well below the melting temperatures of the phases.

Smolka-Danielowska (2010) observed mineral grains of monazite, xenotime, and zircon, in Polish CFAs, which were associated with the REE content, and the Light Rare Earth Elements (LREES) correlated with the aluminosilicate glass phase. While Dai et al. (2014) encountered REE-bearing calcite, possibly of the mineral parasite and zircon trapped within the alumina-silicate glass phase of CFA from Jungar Power Plant, China. On the other hand, Kolker et al. (2017) reported REE-bearing Fe-oxides in several CFAs from the USA and China which were associated with plerospheres observed in the particles.

Thompson et al. (2018) found grains of REE-bearing minerals in CFA encapsulated within glassy (aluminosilicate rich) particles and were typically <2 μm. Aluminosilicate glass particles were abundant, with some being solid and a few being cenospheres and plerospheres. In addition, the mineral monazite was also found embedded in aluminosilicate glass particles, while the cenospheres were rich in iron, and it was reported that the mineral source was likely hematite. A mineral grain that was not capsulated was found, which mostly contained light rare earth elements (LREEs) with no Al and little Si. The authors suggested that this was the mineral apatite with LREE impurities.

These studies have illustrated that REEs are mostly distributed throughout the aluminosilicate glass phase of CFA, in form of cenospheres and plerospheres. Furthermore, REEs have been observed to be adsorbed on the surfaces and absorbed within these mineral phases. This suggests that for the successful liberation of REEs from CFA, the aluminosilicate glass phase should be targeted. The presence of plerospheres in CFA may restrict reactivity during leaching as they contain particles within larger particles. Therefore, to improve the reactivity of CFA that is abundant in plerospheres milling or grinding needs to be considered to break the spheres. However, due to cenospheres being porous and the predominant particle form in CFA, the specific surface area is increased and in turn, reactivity is enhanced. This suggests that overall CFA has substantial reactivity when reacted with an acid to release REEs.

Table.3 presents the common range of elemental composition of bituminous and sub-bituminous CFAs as these are the type of coals mined and used in power generation in South Africa. The elemental oxides SiO_2, Al_2O_3, and Fe_2O_3 are the predominant ones in these two types of CFAs (Klein et al., 1975; Hansen and Fisher, 1980; Mahlaba et al., 2011) and this corroborates with the major minerals found in CFA. Bituminous coal has a higher weight percentage (wt %) range of Fe_2O_3 compared to sub-bituminous coal with elemental oxide composition of 10 - 40 wt % and 4 - 10 wt % respectively.

Table 2.3: Typical range of elemental composition of Coal Fly Ash (Sahoo et al., 2016)

Parent Coal	Bituminous	Sub-bituminous
Element	**%**	**%**
SiO_2	20 - 60	40 - 60
Al_2O_3	5 -35	20 - 30
Fe_2O_3	10 - 40	4 - 10
CaO	1 - 12	5 - 30
MgO	0 - 5	1 - 6
SO_2	0 - 4	0 - 2
Na_2O	0 - 4	0 - 2
K_2O	0 - 3	0 - 4
Loss of ignition	0 - 15	0 - 3

CFA contains basic soluble oxides such as calcium oxide (CaO) and magnesium oxide (MgO) and has been found to have a pH range of 10 – 12.5 thus, can act as a sink of toxic metals (Choi et al., 2002; Gitari et al., 2008; Gitari et al., 2010; Akinyemi et al., 2011; Rowland, 2014). These metals include but are not limited to arsenic (As), beryllium (Be), boron (B), cadmium (Cd), chromium (Cr), chromium VI, cobalt (Co), lead (Pb), manganese (Mn), mercury (Hg), molybdenum (Mo), selenium (Se), strontium (Sr), thallium (Tl) and Zinc (Zn) (Aljoe et al., 2007). The concentrations of these toxic metals depend on the source of the parent coal and combustion process (Kim, et al., 2003). In addition, these elements tend to be associated with particle surfaces rather than particle core structures (Markowski and Filby, 1985). Thus, they are readily leached in an acid solution.

Radioactive elements Uranium (U) and Thorium (Th) are naturally associated with REEs and this is preserved in CFA (Taggart et al., 2018a). Thus, during REE recovery, these radionuclides are co-recovered. REEs have been found to increase with a decrease in particle size therefore, it is expected that U and Th follow the same trend. In CFA, U is mostly associated with particle surfaces, while Th is associated with the aluminosilicate matrix (Hansen and Fisher, 1980; Vassilev and Vassileva, 2005). When considering the scaling up of REE recovery from CFA it is of paramount importance to be aware that U and Th, and other potentially hazardous elements are mobilized along with REEs during recovery because the process is nonselective.

2.3.3. Rare Earth Elements in Coal Fly Ash

REEs refer to the lanthanides (atomic number 57 -71) on the periodic table as defined by the International Union of Pure and Applied Chemistry (IUPAC) (Huang et al., 2018; Balaram, 2019). The element promethium (Pm) (atomic number 61) is excluded because it is unstable. Often, the element Sc (atomic number 21) and Y (atomic number 39) are included in the category of REEs as a result of similarities in the physical and chemical properties to that of the lanthanides (Taggart et al., 2018b). REEs are not as rare as the name insinuates, however, REEs are rarely concentrated in minable ore deposits (i.e. bastnäsite, monazite, and xenotime). In the Earth's crust, the abundance of REEs is greater than some metals (e.g. silver, gold, platinum) (Cotton, 2006; Moldoveanu and Papangelakis, 2012). REEs do not naturally occur as metallic elements but rather as mineral compounds that are grouped into oxides, halides, phosphates, carbonates and silicates due to the geochemical environment they occur in (Kanazawa and Kamitani, 2006).

Generally, REEs are classified based on their geochemistry, this classification divides the REEs into three groups: light (LREEs - La, Ce, Pr, Nd, and Sm), medium (MREEs - Eu, Gd, Tb, Dy, and Y), and heavy (HREEs - Ho, Er, Tm, Yb, and Lu). The various REEs are not equally abundant or equally valuable hence they have been further classified into three economic clusters as critical (Y, Nd, Eu, Tb, Dy, Er), uncritical (La, Pr, Sm, Gd), or excessive (Ce, Ho, Tm, Yb, Lu) based on abundance and utilization (Seredin and Dai, 2012; Pan et al., 2018; Taggart et al., 2018a). The classification is based on the Dudley Kingsnorth prediction of the relationship between demand and supply of individual REEs in past years (Seredin and Dai, 2012).

REEs are also present in coals, with many reported having concentrations equal to or higher than their average content available in the upper continental crust (UCC) (Seredin and Finkelman, 2008; Das et al., 2018). This is a result of coal basins being enriched with REEs at different stages of evolution by various ore formation processes. These processes are: (i) input by surface waters; (ii) connected with falling and leaching of acid and alkaline volcanic ash; (iii) input by meteoric and groundwater; (iv) connected with ascending flows of thermal mineral water and deep fluid (Seredin and Dai, 2012). In CFA, REE content may be approximately three times higher than the UCC, due to their non-volatile character during coal combustion (Kolker et al., 2017; Wagner and Matiane, 2018). The world average ΣREE content in CFA is ~404 ppm (Dai et al., 2016; Balaram, 2019).

CFA has been found to contain a higher fraction of REEs (>30% of total REEs) than REE-bearing ore deposits (Seredin and Dai, 2012; Taggart et al., 2016). For example, ion adsorption REE deposits have been reported to have ΣREE content ranging from 300 – 3500 ppm (Estrade et al., 2019). Bern et al. (2017) observed ΣREE content of 581 ppm in a similar REE deposit in South Carolina, USA. On the other hand, Zhang et al. (2015) found the ΣREE concentration in Chinese bottom ash to be 794 ppm, while Seredin and Dai (2012) reported values above 4000 ppm for some Russian CFA. The abovementioned findings suggest that CFA can potentially be regarded as a more viable source of REEs and is available in large quantities.

Table 1.4 compares the concentrations of REEs in the UCC to that of coals and CFAs found in China and South Africa. The Jungar Chinese CFA was reported to have total ΣREE content of 338.6 ppm while Tutuka and Matla South African CFA was found to have 517.8 and 455.37 ppm respectively. These values were far higher than the average UCC and higher than the global average of CFA content (i.e., ≈ 400 ppm). Although the three CFAs varied in the ΣREE content, they displayed quite similar REE distribution trends; REEs were abundant in the order of Ce > La > Nd > Y > Pr and these elements are typically grouped within the LREEs. In addition, these REEs are the most common among all REEs and in the natural environment they are often present in greater amounts than silver (Ag) and lead (Pb) (Franus et al., 2015).

Over the past two decades, China has been the predominant producer of REEs, producing more than 90% (Seredin and Dai, 2012; Franus et al., 2015; Josso et al., 2018). Nevertheless, literature has also shown that the REE abundance of some South African CFA compared to some of the Chinese is relatively higher (**Table 1.4**), this shows that an opportunity exists for South Africa to compete with China in the trade of these elements.

In South Africa, past investigations on the utilization of CFA have been centred on the characterization, production of synthetic zeolites, polymer composites and mine water treatment (Gitari, 2006; Musyoka, 2009; Eze et al., 2014; Ameh et al., 2017; Alegbe et al., 2018; Akinyemi et al., 2020). Therefore, there is still limited literature on REEs occurrence and recovery in the majority of South African coals and CFAs (Wagner and Matiane, 2018). Thus, this study is focused on REE enrichment by size separation and REE recovery. This will provide a better understanding of the distribution of REEs with particle size and the effect it has on REE recovery.

Table 1.4: Comparison of concentrations of REEs in the UCC, world coals, ash and coal fly ash from China and South Africa (Wagner and Matiane, 2018)

REES	UCC (ppm)	JUNGAR, CHINA (ppm)		TUTUKA, SA (ppm)		MATLA, SA (ppm)
		Coal	*CFA*	*Coal*	*CFA*	*CFA*
La	30	41.2	85.4	39.9	91.4	81.5
Ce	64	71.8	141	91.6	182.4	189.78
Pr	7.1	8.2	17.3	9.5	19.7	18.35
Nd	26	27.6	58.5	30.8	71.8	63.35
Sm	4.5	5.2	10.6	5.3	14.4	11.93
Eu	0.88	0.9	1.8	0.9	2.7	2.35
Gd	3.8	4.7	9.1	4.2	12.6	10.4
Tb	0.64	0.7	1.4	0.6	1.9	1.6
Dy	3.5	4.2	8.6	3.3	11.9	9.5
Ho	0.8	0.8	1.7	0.7	2.4	1.97
Er	2.3	2.4	4.9	1.9	6.7	5.38
Tm	0.33	0.3	0.7	0.3	1	0.77
Yb	2.2	2.3	4.8	1.8	6.5	5.27
Lu	0.32	0.3	0.7	0.3	1	0.72
Y	22	20.4	42.1	17.5	64.9	52.3
Sc	11	-	-	9.7	26.5	24.94

* **REE concentration is in parts per million (ppm)**

2.4. Disposal of Coal Fly Ash

Globally, only a small portion of CFA is utilised productively (approximately 30%), the remainder is disposed of in landfills and ash basins (Yao et al., 2015). For example, approximately 750 million tons (Mt) of CFA is generated annually worldwide (Yao et al., 2015), whilst in South Africa, about 50 Mt is produced with only about 10% of it utilised (Wagner and Matiane, 2018; Reynolds-Clausen and Singh, 2019).

2.4.1. Coal Fly Ash Disposal Mechanisms

The bulk of CFA is currently disposed of by dry and wet methods. The aforementioned methods effectively lead to the dumping of CFA on landfills and ash basins **(Figure 2. 4)**

(Hansen et al., 2002; Haynes, 2009; Luther, 2010; Renew et al., 2017). A combination of both of these techniques is possible. In dry disposal, CFA is often transported by a conveyor system or even trucks from the power plant to the landfill where it is dumped. The landfill sites may be lined or unlined (Hansen et al., 2002).

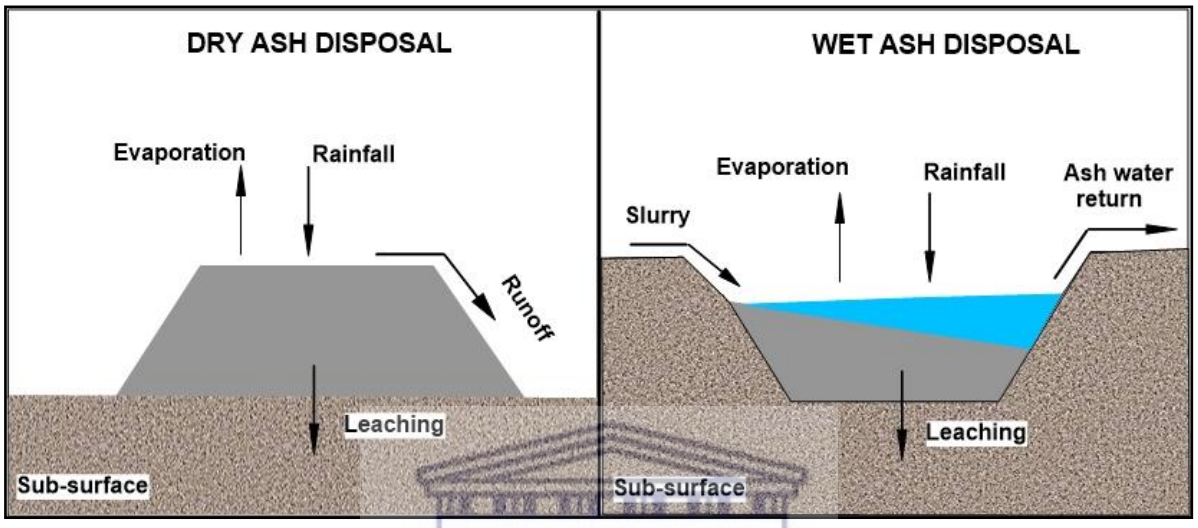

Figure 2. 4: Schematic diagram of dry and wet ash disposal, adapted from (Hansen et al., 2002)

In wet methods, CFA is washed out with water and piped as a slurry into artificial dams, settling ponds or lagoons and over time the water is allowed to drain. Once the CFA is piped into the dam the particles settle to the bottom of the dam and the effluent is either discharged to receiving waters or pumped back to the power station for reuse as shown in **Figure 2. 4.** The advantages of ash pond disposal are dust and noise minimization. Ash disposal ponds may be lined or unlined. The unlined ponding process often produces supernatant water with high concentrations of dissolved solids, trace elements and metals exceeding background concentrations, which may pose potential groundwater contamination problems.

Over time with both these disposal mechanisms, CFA is expected to weather as it is exposed to several environmental factors such as; precipitation, evaporation ingressed carbon dioxide (CO_2) and oxygen (O_2). Weathering is the process of weakening and breaking down of rocks, soil, and minerals through interaction with the earth's atmosphere, water, and biological organisms. The overall processes of weathering are not reversible even though individual reaction steps are often treated as reversible equilibria (McBride, 1994). There are three main types of weathering processes: mechanical, chemical and organic. Chemical weathering affects

the chemical composition of CFA over time the most and usually occurs through the process of leaching (Akinyemi et al., 2011).

2.4.2. Leaching of Coal Fly Ash

Leaching is a process of extracting a substance from a solid material that has come into contact with a liquid, it is a process that occurs during chemical weathering. In the leaching of CFA, rainwater plays an important role, as it facilitates the ability to remove, or extract, chemical constituents from the solid particles of CFA. The major processes that affect the leaching process when CFA interacts with water are dissolution of primary solids, precipitation of secondary solids, as well as redox, sorption, and hydrolysis reactions (Akinyemi et al., 2011; Akinyemi et al., 2012).

The leaching of trace elements from any type of CFA is a slow and often complex process. This process is strongly dependent on the pH developed during interaction with the leaching solutions (Plank and Martens, 1973; Jankowski et al., 2006). Numerous heavy metals and trace elements are soluble in water under acidic conditions and can move downward with water through the soil, and in some cases move to aquifers, surface streams, or lakes (Singh et al., 2012). Nontoxic soluble elements leach out first in water or weak acids (Green and Manaban, 1978), however, the long-term leaching of toxic trace elements is associated with slow mobility of elements from the aluminosilicate glass phase, magnetite, and related minerals (Hulett et al., 1980). Thus, chemical interactions of CFAs with infiltrating rainwater ingressed O_2 and CO_2 at ash dumps are expected to take a long time to remove mobile trace metals from the solid phase. For this reason, a possibility exists for REEs not to be leached to the environment while the CFA is on the disposal sites thus, resulting in the bulk of the CFA on landfills viable for REE recovery.

2.4.3. Leaching of Rare Earth Elements

There is limited literature on the mobility of REEs from CFAs, thus studies of REE-bearing rocks and minerals ores are used to understand their mobility as similar processes might occur during the weathering of CFA. This is due to CFA containing similar minerals to these rocks.

REE-bearing rocks and minerals also go through weathering in the environment and this leads to the mobilisation of REEs. The pH of a solution passing through a REE-bearing medium is

an important parameter controlling REE mobility, with the highest levels in acidic conditions. Under acidic conditions, REEs can easily leach whereas under neutral to alkaline conditions REEs may often be adsorbed onto oxide and clay minerals (Zhu et al., 2019). Heavy-REEs often appear to be more leachable than Light-REEs, due to Heavy-REEs tendency of forming soluble carbonate complexes than the LREE in solution, thus, are easily leached (Galbarczyk-Gasiorowska, 2010).

The behaviour of REEs during rock weathering depends on the intensity of weathering and the stability of primary minerals. REEs may be immobilised by various mechanisms such as (i) retention in primary minerals which are resistant to weathering, (ii) incorporation in newly-formed crystalline or amorphous phases, and (iii) adsorption by clays (Braun et al., 1993).

Galbarczyk-Gasiorowska (2010) investigated the mobilisation of REEs during weathering and fractionation between the rock, soil, and solutions percolating the host rock. The author reported that during sequential extraction of the soils, REEs were generally associated with the organic matter and Fe-Mn oxides and hydroxides fractions. de Sá Paye et al. (2014) reported similar observations when investigating REE contents in Brazilian soils. Braun et al. (1993) found the majority of the REEs to be leached from Fe-rich upper soil horizons. Ganne and Feng (2017) reported that Mn-Fe hydroxides and secondary phosphate minerals are the main hosts of acid leachable REEs. In addition, mobility of REEs was characterized by more HREEs leaching than LREEs, this is consistent with the observations of Galbarczyk-Gasiorowska (2010) and Price et al. (1991) found Nb to be the least leached element.

These studies have demonstrated that in soils and rocks REEs are associated with Fe-oxides and this coincides with an investigation by Kolker et al. (2017) who reported REE-bearing Fe-oxides in several CFAs from the USA and China. It is possible that the aluminosilicate glass phase is not the only REE enriched phase in CFA, and that Fe-oxides should also be targeted particularly in CFAs that exhibit plerospheres (i.e., Fe-rich particles). Furthermore, these studies found HREEs to leach more than LREEs. Therefore, it can be expected that in the recovery of REEs from CFA a similar trend will be observed, especially when the leaching conditions applied are more aggressive than the one used in these studies.

One of the most consistent highlights of the literature is that the mobility and fractionation of REEs during weathering needs further clarification (Ganne and Feng, 2017). Also, there is

limited literature on the mobility of REEs in CFA during weathering. This might be one of the crucial factors that play a role in the recovery efficiencies of REEs from CFA.

2.4.4. Environmental Impacts of Coal Fly Ash Leaching

Coal is known to contain every naturally occurring element, so it is expected that many trace elements are found in CFA (e.g., As, B, Cd, Pb, Cu, Mo, Ni, Se, Zn, etc.). Thus, the leaching of trace elements during CFA disposal is of concern for possible contamination, especially for the aquatic environment when CFA comes in contact with water. Severe exposure (short-term, high concentration) of these elements can kill aquatic organisms directly, whereas chronic exposure (long-term, low concentration) can result in either mortality or non-lethal effects such as stunted growth, reduced reproduction, and deformities (Singh and Kalamdhad, 2011). The disposal of dry ash often results in air pollution as the fine ash particles are easily mobilised by wind, however, this does not persist because dust suppressors are used and rainfall plays a role in suppressing the fine particles (**Figure 2. 4**).

Dalton et al. (2018) conducted a study around a large coal-fired power plant in Mpumalanga province and found that the deposition of CFA from the flue stacks and ash dump enriched soils with trace metals. Concentrations of As, Cu, Mn, Ni and Pb exceeded local screening levels. With the percolation of rainwater into the subsurface, it is evident that these trace metals can potentially end up in groundwater systems, subsequently contaminating the water resource. Poor management of CFA is responsible for, the loss of plants and reduction of biodiversity (Vadapalli et al., 2008). The weathering of CFA over time is the major process responsible for the release of various elements to the environment during dry ash disposal on landfills, due to the exposure of CFA to atmospheric conditions. Therefore, there is a need to find alternative ways to sustainably utilize CFA.

Currently, there are gaps in the literature on the leaching of REEs from CFAs from landfill sites as well as the possible effects on the environment. However, due to the increase in the interest in utilizing REEs in various applications (e.g., generation of green energy and technologically advanced devices), it is important to better understand these effects as they may impede these applications. Nonetheless, substantial investigations have been conducted on the various techniques that can be applied in the recovery of REEs. Furthermore, these

studies have focussed on identifying REE recovery techniques and conditions that can potentially yield higher recovery efficiencies.

2.5. Rare Earth Element Enrichment in Coal Fly Ash

REE recovery processes from CFA include beneficiation and leaching. Beneficiation processes are aimed to enrich CFA with REEs by isolating fractions of CFA that are most likely to be more abundant in REEs and this is generally done before leaching. Lin et al. (2017) showed that REEs in CFA could be enriched by simple physical separation methods, namely, particle size separation, density or float-sink separation, and magnetic separation. Previous studies have demonstrated that there is an inverse relationship between the particle size of CFA and the concentration of REEs for separates between 100 µm and 30 µm (Clarke and Sloss, 1992; Seredin and Dai, 2012; Hower et al., 2013; Blissett et al., 2014).

2.5.1. Effect of Particle Size on the Enrichment of Rare Earth Elements:

The distribution of particle size and surface area of CFA give preliminary insight into the interactions between the CFA and aqueous solutions. Generally, leaching of CFA with an acid occurs at the interface between a solid and liquid phase, and sometimes gaseous phase, therefore, the surface of a CFA particle may act as a site for deposition or condensation of various elements (Shemi, 2013). CFA has been found to have a relatively high specific surface area of 200 – 300 square meters per kilogram (m^2/kg), this offers a high potential reactivity (Gitari, 2006; Musyoka, 2009). The smaller the particle diameter, the greater the surface area relative to the volume available for the adsorption of liquid and gaseous materials.

Lin et al. (2017) investigated the enrichment of REEs from various CFA samples when separated into the following size fractions: 150, 75, 53, 45, 38, 25 and < 20 µm. Despite some variations, the results showed that the REE concentrations in particle size-fractioned CFA samples generally increased as the particle size decreased showing moderate enrichment of REEs in the smaller CFA particles. Also, the findings suggested that regardless of the CFA sources, the samples had a very similar particle size distribution, which may further imply the same CFA formation mechanism during coal combustion.

Rosita et al. (2020), subjected three Indonesian CFAs to a physical separation process by sieving to enrich the REE content in the CFA. It was found that the REE content increased as

the particle size of the CFA decreased. The highest enrichment factor and REE recovery were observed in the finest size fraction (< 38 µm) with an enrichment factor of 1.1 and 58.69 % REE recovery.

Pan et al. (2020) physically separated CFA from China employing wet sieving into the following size fractions: 150-100 µm, 100-74 µm, 74-55 µm, 55- 35 µm, 38-25 µm and < 25 µm. The findings showed that the REE content increased from 608 to 896 microgram per gram (µg/g) with decreasing particle size, and the highest REEs content was measured at the <25 µm size fraction. This trend coincided well with the trends concluded by the previous studies (Taggart et al., 2016; Lin et al., 2017; Dai et al., 2014).

In contrast, Scott et al. (2015) findings did not display a similar trend when looking at the enrichment of REEs after dry sieving CFA from three power stations in the United States into the following size fractions 1000, 100, 10, 5 and < 5 µm. Instead, no relationship between particle size and REE enrichment was observed. The suggested reason for these findings was the different size ranges used compared to other studies and the possibility of there being a limit to REE enrichment with decreasing grain size or for that particular study a finer increment of sampling was needed. Regardless, the study confirmed that REEs are depleted in the coarse fraction (> 100 µm) relative to the whole ash. Furthermore, the 100 µm fraction was found easiest to separate. Conversely, the 5 µm and < 5 µm fractions were increasingly more difficult to separate, due to the fine grain size and represented an insignificant part of the total mass in each of the three fly ash samples.

Overall, these studies have demonstrated that an inverse relationship exists between the particle size of CFA and the concentration of REEs. The successful enrichment of REEs by the application of particle size separation technique can potentially have a positive impact on the recovery efficiencies of REEs.

2.6. Hydrometallurgy: Recovering Rare Earth Elements from Coal Fly Ash

Hydrometallurgy is a technique within the field of extractive metallurgy involving the use of aqueous chemistry for the recovery of metals from ores, concentrates and recycled or residual materials (Kashiwakura et al., 2013; Balaram, 2019; Wang et al., 2019). This process involves four distinct phases (i.e., preparation, dissolution, extraction and recovery) as shown in **Figure**

2. 5. Firstly, the solid material is prepared by granulation, grinding and classification to a size fraction most suitable for the technique to be applied. Secondly, the metal of interest is transferred from the solid material into an aqueous solution. Thirdly, the metal-bearing solution is concentrated and purified. Finally, the metal is recovered from the purified solution into a solid-state. Similarly, REE recovery from CFA employs hydrometallurgical techniques (King et al., 2018; Yang et al., 2019).

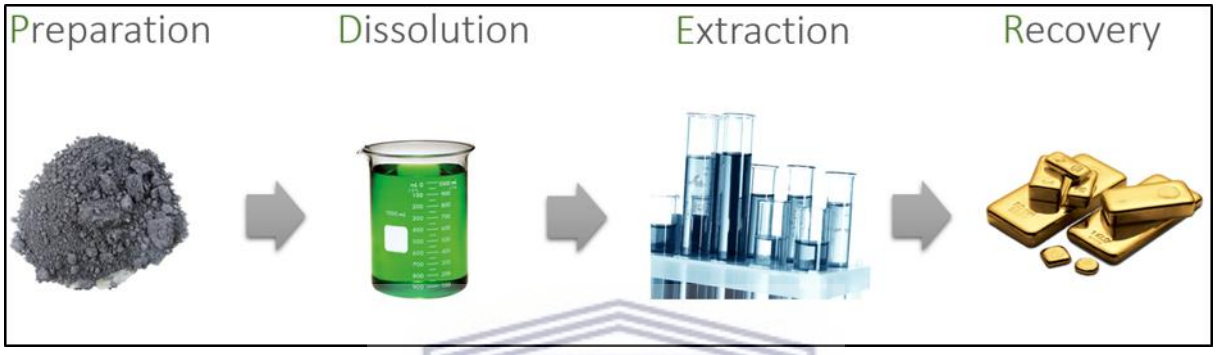

Figure 2. 5: Flow diagram of the general procedure followed in hydrometallurgy for recovering metals from waste material

The predominant phase in CFA is the aluminosilicate glass, which forms the matrix of the CFA particles and REEs are distributed throughout this aluminosilicate glass (Taggart et al., 2018b). Several methods have been well developed for recovering alumina (Al_2O_3) from CFA, these methods are a rational starting point for the recovery of REEs from CFA because they target the alumina-silicate glass where REEs reside. The recovery of Al_2O_3 from CFA is based on the application of hydrometallurgical processes such as acid or base leaching, precipitation, solvent extraction and re-crystallization (Matjie et al., 2005).

The bulk of Al_2O_3 extraction literature follows two main paths, direct acid leaching using hydrochloric acid (HCl) or sulphuric acid (H_2SO_4) or sintering (known as alkaline acid –fusion leaching) with calcium oxide (CaO), sodium hydroxide (NaOH), sodium carbonate (Na_2CO_3), and or ammonium sulphate $(NH4)_2SO_4$ followed by acid leaching. However, other leaching techniques exist for the recovery of REEs such as alkaline leaching and bioleaching (Jha et al., 2016; King et al., 2018; Lin et al., 2018; Taggart et al., 2018a). Direct acid leaching and alkali-fusion acid leaching are further discussed in detail in the sections below.

2.6.1. Direct Acid Leaching

Direct acid leaching requires no intervention before the leaching process and an acid, known as a lixiviant is used to selectively extract the desired elements from the CFA. Three commonly used acids in leaching processes are hydrochloric acid (HCl), nitric acid (HNO_3) and sulphuric acid (H_2SO_4). Knowledge of the characteristics of these lixiviants is necessary for the selection of suitable conditions for acid leaching processes (Shemi, 2013). Moreover, it is important to note that all these acids are corrosive, thus posing some limitations to acid leaching. However, acid leaching is successful for the most part in the recovery of REEs from CFA as it allows for the dissolution of numerous elements from CFA (Tang et al., 2019).

2.6.2. Alkali Fusion Acid Leaching

The purpose of the alkali fusion is to activate the inert material in CFA based on the reaction with alkali carbonate at high temperature, in which phases of quartz and mullite can be transferred or decomposed into a series of soluble silicates such as nepheline, and noselite, to provide good materials for subsequent acid leaching (Tang et al., 2019).

Honaker et al. (2019) compared the leaching characteristics of REEs from coal when sintering is performed before acid leaching to that of direct acid leaching. The authors observed that REE recovery significantly improved when the coal was sintered, approximately 80 % of REEs were leached. However, without sintering, the REE recovery was relatively low; for example, only 25% of the REEs were leached.

2.6.3. Kinetics of Leaching

The most common model considered in leaching is that illustrated in **Figure 2. 6a**, where the reaction takes place on the exposed surface of the particle and the product completely dissolves in the liquid and this is the "shrinking particle model". If the product does not dissolve in the liquid, the particle size would not change but the reacting core shrinks inside the particle (**Figure 2. 6b)** and this is the "Shrinking Core–Constant" model. Lastly, if the reaction proceeds and the unreacted core of the particle shrinks while the product layer forms around the core (**Figure 2. 6c)** it is called the "Shrinking Core–Shrinking Particle" model. However, the product layer is soft and breaks apart when the particles collide (Wen, 1968; Seidel and Zimmels, 1998; Gbor and Jia, 2004; Safari et al., 2009).

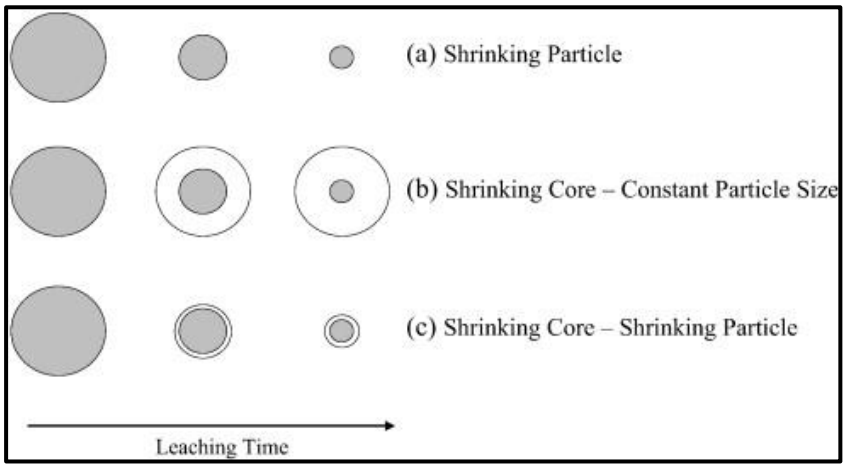

Figure 2. 6: Schematic diagram of different mechanisms of acid leaching (Safari et al., 2009)

The shrinking core model has been found to best describe the leaching process of CFA with an acid (Shemi, 2013; Wanta et al., 2020). The model assumes that the particles are spherical and that during leaching, the particles shrink uniformly, thus, maintaining their spherical shape (Gbor and Jia, 2004; Safari et al., 2009). Furthermore, the process is heterogeneous and involves several fundamental steps that are simultaneously involved and affect each other (Gbor and Jia, 2004; Wanta et al., 2020)

The surface reaction of the solid and fluid during leaching can be considered to consist of the following three mechanisms: diffusion through the liquid film layer, diffusion in solid (product layer) and chemical reaction at the unreacted core. These mechanisms occur consecutively, therefore, if any of them is slower than all the others, it becomes the rate-determining mechanism (Safari et al., 2009; Wanta et al., 2020). Thus, identifying this mechanism and understanding the factors that can influence it is very important.

Considering the shrinking core model in the leaching process of CFA with HCl; it is possible that if the migration of H^+ in the solution is not restricted by its concentration and the solid−liquid ratio, then the H^+ are expected to react with REEs at the surface as well as within the CFA particles as the majority are porous. This should result in the dissolution of REEs from within the core and at the surface of the particles. In addition, the dissolution of the REEs should then take place layer by layer. The aluminosilicate phase along with quartz are two of the major mineral sources of silica in CFA. Therefore, in the leaching of CFA with HCl, it is expected that silica is one of the major products which will most likely be in a form of a gel.

Over time this silica gel in solution may act as the product layer in the shrinking core model (**Figure 2. 6c)**, thereby limiting the reaction as the surface area will be reduced. Thus, reducing the transport of reactants to the surface of CFA particles. For this reason, the product layer would possibly be the rate-determining step.

Numerous studies have investigated factors (e.g., acid concentration, stirring speed, solid-liquid ratio, etc.) that play an important role in the leaching of REEs from CFA. Understanding these factors will aid in the selection of the most suitable combination that will potentially yield higher leaching efficiencies. The section below provides further detail on these factors.

2.7. Factors Controlling the Recovery of Rare Earth Elements from Coal Fly Ash

Systematic studies of leaching of REEs from CFA produced in several coal plants in certain parts of the world have been conducted using hydrometallurgical methods. This was done for the purpose to overcome the issue of low recovery efficiencies by direct leaching. It is important to highlight that only a few of these studies have been conducted using South African CFA (Eze, 2014; Ripfumelo, 2012). Several authors (Guo et al., 2013; Taggart et al., 2018a; Tang et al., 2019) have developed a two-step hydrometallurgical process, which combines alkali fusion and acid leaching. Furthermore, these studies have investigated the different parameters that affect the recovery of REEs from CFA as well as suggested optimum conditions of recovery.

2.7.1. Effect of Sintering Additives and Temperature

Thermochemical sintering or roasting processes are often employed in REE recovery to decompose the aluminosilicate glass phases in CFA into acid-soluble forms, and this allows accessibility of REEs that reside within and throughout this glass phase. In CFA, oxides such as SiO_2 and Al_2O_3 which exist in mineral phases of aluminosilicate glass, quartz and mullite have low activity and high-temperature alkali sintering can greatly increase their activity (Guo et al., 2013). During sintering with alkaline additives (e.g., NaOH, Na_2CO_3 and Na_2O_2), the crystal structure of these minerals phases are decomposed to their active forms which are acid-soluble (i.e., nepheline ($NaAlSiO_4$), sodium silicate (Na_2SiO_3) and jadeite ($NaAlSi_2O_6$)) (Guo et al., 2013; Pan et al., 2021). Thus, during acid leaching, the products of alkali sintering are

decomposed further and in turn, liberate REE-bearing particles which can easily be dissolved. The decomposition of these mineral phases during sintering can be summarized with the following equations (Guo et al., 2013; Pan et al., 2021):

$$6NaOH + 3Al_2O_3{\cdot}2SiO_2\ (mullite) + 10SiO_2\ (quartz) \rightarrow 6NaAlSi_2O_6\ (jadeite) + 3H2O \quad (1)$$

$$3Na_2CO_3 + 3Al_2O_3{\cdot}2SiO_2\ (mullite) + 4SiO_2\ (quartz) \rightarrow 6NaAlSiO_4\ (nepheline) + 3CO2 \quad (2)$$

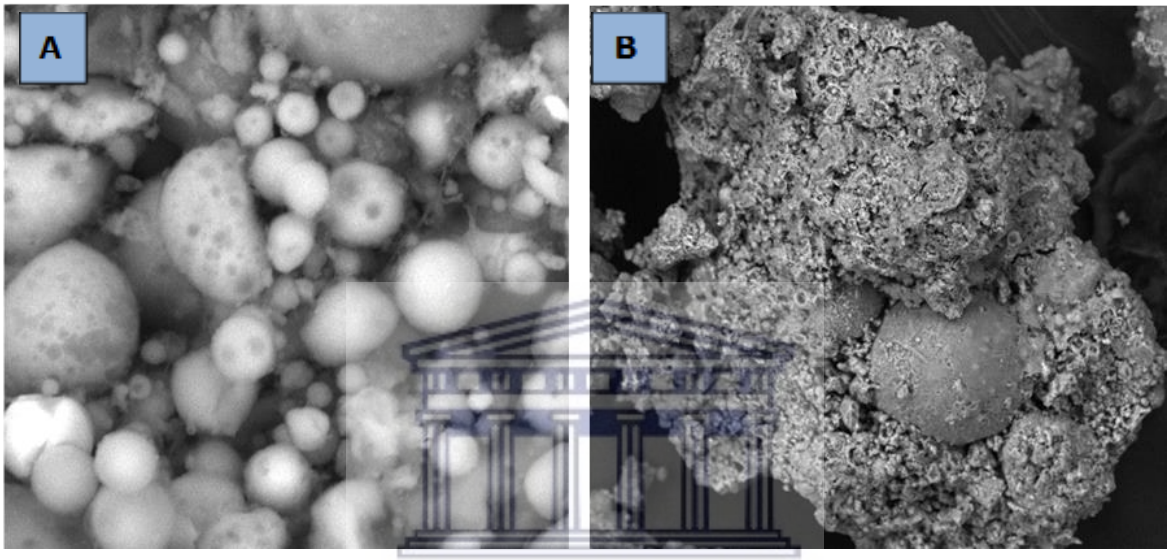

Figure 2. 7: Scanning Electron Microscope (SEM) images illustrating CFA particles (A) before and (B) after NaOH sintering

Figure 2. 7 illustrates CFA from a coal-fired power station in South Africa before **(Figure 2. 7A)** and after (**Figure 2. 7B**) sintering with NaOH. In **Figure 2. 7A**, the CFA was comprised of smooth spherical particles with minimal agglomeration. However, in **Figure 2. 7B**, the particles had more agglomeration and appeared to have melted. The absence of the original morphology in the sintered CFA indicates that the inherent mineral composition was destroyed (Bai et al., 2018); localized melting between particles occurred to break bonds and form new compounds (Shemi, 2013). Also, alkali sintering plays an important role in the decomposition of plerospheres found in CFA which are particles within a particle and have low reactivity (Goodarzi and Sanei, 2009; Sharonova et al., 2015). Overall, alkali sintering facilitates the liberation of REEs during acid leaching because the mineral phases which contain REEs are transformed into soluble forms.

Taggart et al. (2016) found that Na_2O_2 and NaOH were the most effective roasting additives for extracting REEs, as recovery efficiencies of > 105% and > 90% was achieved for the two CFAs investigated in the study. In another study where NaOH was used as a sintering additive of CFA, NaOH was found to improve the alumina extraction and decreased the thermal activation temperature greatly when using hydrochloric acid as the lixiviant (Guo et al., 2013)

Taggart et al. (2018a) investigated the effects of roasting temperature when sintering with NaOH and their results suggested that the optimal NaOH roasting temperature for REE extraction is 350 °C, though higher recoveries are possible at 450 °C. In CFA, mineral phases such as aluminosilicate glass, quartz and mullite are difficult to react with NaOH at lower temperatures due to their low activity. Therefore, roasting at higher temperatures, specifically temperatures above the melting point of NaOH (i.e., 318 °C) is necessary (Taggart et al., 2018a). This stimulates the activity of these mineral phases as well as decompose them into soluble forms (Shemi, 2013). The authors further explained that going beyond 450 °C will not result in a significant increase in recovery efficiency. Furthermore, these findings are supported by research on NaOH as a CFA additive, in which alumina extraction efficiency improved only marginally when sintering temperature was beyond 400 °C (Guo et al., 2013).

Furthermore, Taggart et al. (2018a) investigated the effectiveness of roasting techniques to improve extraction of REEs from CFA using Appalachian, Illinois, and Powder River basins CFA as representatives of ash in the United States of America. It was observed that roasting with NaOH often recovered >90% of total REEs while the use of other additives recovered < 50% of total REEs. Additionally, approximately 100 % recoveries were observed for the Powder River Basin CFA sample regardless of the roasting agent and the CFA to the additive ratio used. This suggested that acid leaching alone was sufficient for recovering REEs from the more soluble Powder River Basin ashes. The explanations provided for this observation were that the Powder River Basin CFA had a higher CaO content than Appalachian CFA and high CaO content thus making the CFA more soluble thereby increasing REE recovery. Additionally, in that particular CFA, the Ca-Fe glass phase was more enriched in REEs and the CFA was subjected to a process similar to alkali fusion during combustion thus, resulting in the CFA being more susceptible to acid leaching.

Although the roasting of CFA prior acid leaching liberates REEs from the aluminosilicate glass phase of the CFA making REEs more soluble during acid leaching, this process might be unnecessary for CFAs that are relatively enriched in CaO (making the CFA more soluble), as

the process consumes quite a lot energy. Thus, it might be worthwhile to explore whether it is necessary to subject a particular CFA to roasting before acid leaching or not, before the scaling up of these techniques for industrial applications.

2.7.2. Effect of Mass Ratio on Sintering

The success of sintering CFA with an alkali additive to decompose the aluminosilicate glass phase is to a certain degree dependent on the mass ratio of the reactant (CFA: alkali additive). The ratio of CFA to the alkali additive can either enhance or limit the decomposition reactions (Taggart et al., 2018a; Tang et al., 2019). Therefore, there needs to be a sufficient mass of CFA to additive for the desired decomposition reactions to occur. In the past when comparing roasting agents, excess additives relative to CFA were used to identify the most successful additives (Taggart et al., 2018a). However, the processing of CFA for REEs recovery at an industrial scale will require a much more economical use of reagents. Thus, Taggart et al. (2018a) investigated several CFA-additive mass ratios, to determine whether REE recovery depends on an excess of additive. The authors observed that REE extraction using a mass ratio for alkali fusion of 1:1 with sodium hydroxide (NaOH) as the additive, resulted in recovery efficiencies >70%. The recovery efficiency did not differ significantly from when ratios of 1:5 using NaOH, 1:6 using sodium peroxide (Na_2O_2), or 1:1 using Na_2O_2 were used. The findings suggest that using less NaOH does not necessarily compromise REE extraction efficiency. In support of the mass ratio of 1:1 Tang et al. (2019) found the optimum conditions of roasting with sodium carbonate (Na_2CO_3) as the additive to be a solid mass ratio of 1:1. Further experiments conducted by Taggart et al. (2018a) showed that decreasing the mass ratio to 1: 0.5 drastically decreased the REE recovery efficiency from approximately 90% to 50%. This suggests that the threshold for the alkali fusion mass ratio (CFA: additive) is between 1:1 and 1:0.5.

2.7.3. Effect of Solid-Liquid Ratio

In a heterogonous chemical reaction (i.e., solid and liquid), there needs to be a sufficient amount of the reactants to effectively interact with another during the reaction to form products. Therefore, the solid to liquid ratio (S/L) plays a very important role in REE recovery. To investigate the effect of the S/L ratio on REEs Cao et al. (2018) conducted a study to evaluate the effect of the S/L ratio of REEs extraction as well as the optimum condition. The S/L ratios

investigated were 1:5, 1:10, 1:15 and 1:20. The findings indicated that when the hydrochloric acid (HCl) volume was increased, the leaching efficiency of REEs tended to increase. When the S/L ratio was decreased from 1:5 to 1:10, the leaching efficiency of the REEs under investigation rapidly increased from below 40% to above 60%. Furthermore, when the S/L ratio was decreased further, the increase of the leaching efficiency was very small.

Tang et al. (2019) conducted a similar study and found that when the S/L ratio was decreased from 1:5 to 1:20, the leaching efficiencies of Y, La, Ce, Pr, and Nd increased significantly from 43.18, 12.30, 17.44, 19.91, and 24.54 % to 92.49, 60.10, 64.17, 60.69 and 70.79%, respectively. These observations were in agreement with the findings of Cao et al. (2018). Thus, the leaching efficiency was improved by decreasing the S/L ratio. When the S/L ratio was decreased further from 1:20 to 1:30, the leaching efficiencies became stable. However, when the study considered environmental sustainability in the process of leaching, it suggested that a more appropriate S/L ratio to use would be 1:20 due to the acid consumption of the 1:30 ratio.

2.7.4. Effect of Acid Concentration

The rate of a reaction generally varies directly with changes in the concentration of the reactants (Peiravi et al., 2017). Therefore, increasing the concentration of the reactants will increase the rate of the reaction because more of the reacting molecules or ions are present to form the reaction products. Increasing the acid concentration during the leaching of CFA is aimed to assist with the decomposition of the mineral structures that are associated with REEs so that they become soluble.

Cao et al. (2018) examined the effect of HCl concentration on the recovery efficiencies of REEs from CFA. The acid concentrations that were explored are 1, 2, 3, 5, and 7 moles per litre (mol/ℓ). It was observed that the initial concentration of HCl has a great influence on the REE leaching efficiency, especially at lower HCl concentrations. When the HCl concentration was increased from 1 to 3 mol/ℓ a significant increase in the leaching efficiencies of La, Ce and Nd were observed. The efficiencies increased from 27.46, 25.33, and 24.64 % to 75.96, 70.16, and 68.66 %, respectively. Additionally, it was observed that when the concentration of HCl exceeded 3 mol/ℓ, the leaching efficiency of REEs no longer increased significantly. Thus, the study recommended an optimum HCl concentration of 3 mol/ℓ. In a similar study, Tang et al. (2019) investigated the HCl concentrations from 0.1 to 4 mol/ℓ. The authors observed that

when the HCl concentration was raised from 0.1 to 2 mol/ℓ, the leaching efficiency of REEs distinctly increased. The overall leaching rate of REEs increased rapidly from 0.03% to 59.78%. Similarly to the study of Cao et al. (2018), when the HCl was increased from 2 to 4 mol/ℓ a decrease in REEs leaching efficiency was observed. This shows that perhaps the optimum HCl concentration may be 3 mol/ℓ as Cao et al. (2018) suggested.

2.7.5. Effect of Stirring Intensity

Stirring in any chemical reaction plays an important role as it ensures that the reactants remain in motion, thus increasing the chances of collision and increasing the rate of the reaction (Tang et al., 2019). In the recovery of REEs from CFA, stirring is applied to assist in accelerating the breakdown of the alumina-silicate glass phase to liberate REEs. Tang et al. (2019) investigated the influence of stirring intensity on the leaching efficiency of REEs using variable stirring intensities to dissolve CFA samples with the HCl. When the stirring intensity was increased from 0 to 400 revolutions per minute (rpm) a significant and consistent increase was observed in the leaching efficiency of REEs. The significant increase was attributed to the increase of stirring intensity which favours liquid-solid reaction mass transfer in the reaction system. However, when the stirring intensity exceeded 400 rpm, the overall leaching efficiency was observed to slightly decline. Thus, the study recommended an optimum stirring intensity of 400 rpm.

2.7.6. Effect of Leaching Temperature

Temperature plays a very important role to activate any chemical reaction as well as accelerating it. Increasing the temperature of a reaction increases the kinetic energy of the particles and this, in turn, increases the number of collisions so the reaction rate increases (Kumari et al., 2019). Cao et al. (2018) explored the possibility of leaching REEs from CFA under atmospheric pressure and low temperature (under 100 °C) conditions, to attempt to conserve energy. The temperatures that were explored in the study are as follows 20, 30, 45, 60, 75, and 90 °C. The authors observed that at temperatures below 45 °C, the leaching efficiencies were < 30 %, and at 45 - 60 °C the increase in the rate of leaching efficiency was much faster compared to that at below 45 °C, while the rate decreased at the stage of 60 - 90 °C. Although at 90 °C the highest leaching efficiencies were achieved, the author suggested 60 °C as the viable temperature condition concerning energy conservation.

2.7.7. Effect of Leaching Time

In hydrometallurgical leaching processes, contact time can be defined as the duration in which the reactants are in contact, thus resulting in reactions that produce products (El-Mottaleb et al., 2016). Therefore, it can be assumed that the longer the reactants are in contact, the more opportunity there is for products to be formed up until the reactions reach an equilibrium point where no further change in the consumption of reactants and formation of products is to be expected to occur.

The effect of leaching (reaction) time on the leaching efficiency of REEs has been investigated and the overall observation is that an increase in the leaching duration increases the leaching efficiency. Cao et al. (2018) explored this and from the findings noted that changes in leaching efficiency could be divided into four stages: before 60 minutes, during 60-90 minutes, during 90 - 120 minutes and after 120 minutes. During the before 60 minutes stage, the leaching efficiency was found to greatly increase with time. However, during the 60 – 90 minutes stage the leaching efficiency was relatively unchanged. During the 90 – 120 minutes stage, the leaching efficiency was observed to increase and after 120 minutes, the increase rate of the leaching efficiency became very slow. The above findings of Cao et al. (2018) are similar to that of Taggart et al. (2016) where higher REE recovery efficiencies of above 80 % were achieved with a leaching duration of 120 minutes. In addition, Tang et al. (2019) found REE recovery efficiencies to steadily increase from a leaching duration of 20 to 120 minutes and the highest recovery efficiency was recorded at a duration of 120 minutes.

Cao et al. (2018) provided the following explanation for the observed findings. During the before 60 minutes stage, the concentration of hydrogen ions (H^+) in the solution is high and so is the content of REE compounds that are easily dissociated from CFA and this results in rapid reaction processes. After the reactions have taken place for some time, the REE compounds on the surface of the CFA particles are depleted (leached into solution) and the unreacted compounds are likely the ones that are in the matrix of the particle. These compounds only dissociate after H^+ diffusion into the matrix of the CFA particle. Therefore, the 60 - 90 minutes stage is the diffusion process of H^+ into the matrix of CFA particles, during which the increase in the leaching efficiency is very limited. After this process, the leaching efficiency rapidly increases when H^+ comes into contact with now easily dissociated REE compounds in the matrix of CFA. This is the reason for the increase in leaching efficiency during the 90 - 120

minutes stage. After 120 minutes, the remaining H^+ concentration in the solution is low and the unreacted REE compounds that remain are those that are difficult to dissociate from the matrix. This results in the contact probability and contact area between the REE compounds and H^+ being reduced, thus, leading to just a slight increase in leaching efficiency. Therefore, 120 minutes was considered as the optimal duration of leaching because leaching beyond this does not result in a significant increase in the recovery of REEs.

2.8. Benefits of Recovering of Rare Earth Elements from Coal Fly Ash

There are several advantages associated with the utilization of CFA to recover REEs from the REE-bearing ore deposits. Firstly, CFA is a large and more reliable source of these elements across the globe as it is a readily available waste product. Secondly, it is an already mined material therefore, it does not require excavation, which is capital intensive and can degrade the environment. Thirdly, CFA has the potential to reduce environmental and health concerns as no mining of the source rock takes place (Lin et al., 2017; Yang, 2019). Finally, CFA is a fine powder and this makes it ideal for chemical processing (e.g., leaching) as it eliminates several costly ore processing steps and saves the energy required for the comminution of ore (Taggart et al., 2016; Lanzerstorfer, 2018).

The world is slowly shifting towards green energy and advanced technologies, therefore in the upcoming years, the demand for REEs will increase as they are essential in the development of these technologies (Franus et al., 2015; Dutta et al., 2016; Balaram, 2019). Thus, there is a need to investigate new sources for these elements (Dutta et al., 2016). For example, La which is the second most common element among all REEs is an essential component in hybrid cars, while Eu has been used in ultraviolet LED devices and Er in lasers used for medical operations (Franus et al., 2015; Balaram, 2019). In addition, the REEs Nd, Pr, Dy, Tb and Sm are one of the important components in neo-magnets (super-power constant magnets), which are irreplaceable in industrial generators due to their ability to effectively transform any kind of energy (e.g., wind, tidal, thermal, etc.) into electricity (Seredin and Dai, 2012; Balaram, 2019).

Several REEs have been characterized as “critical” due to the geographic location, economic and political stability in the countries that produce them. Therefore, a market exists for REEs in regions where they are relatively abundant. In the last twenty years, China has been the predominant producer of REEs, producing more than 90% (Seredin and Dai, 2012; Josso et al.,

2018). Thus, the recovery of REEs from CFA from other regions such as South Africa will allow the country to compete in the trade of these elements. If CFA can be exploited as a source of REEs, it will greatly promote the comprehensive development and application of CFA to achieve the economic development of coal. Moreover, it can potentially reduce environmental concerns associated with CFA disposal because the volumes disposed of on landfill sites will decrease. In addition, CFA can be used multiple times in the extraction of REE thus, possibly reducing its volume and this is of great significance to the sustainable utilisation of CFA.

2.9. Limitations of Recovering Rare Earth Elements from Coal Fly Ash

The recovery of REEs particularly using acid leaching methods have some limitations in terms of the separation and recovery of materials of interest from undesired species. Consequently, this hinders the ability to achieve high-grade REE concentrates and adds cost, as another process will be required to separate the elements of interest (Honaker et al., 2019). Moreover, the REEs leaching efficiencies are highly dependent on the type of CFA used. Essentially, it is challenging to obtain exact leaching efficiencies as previous investigations by using the exact methods when a different type of CFA is used. Thus, recovery methods are developed based on CFA characteristics. Additionally, the acids used in the leaching methods are highly corrosive and often costly and this results in concerns regarding scaling up for industrial applications (Zhang and Honaker, 2019). Furthermore, to some extent, these corrosive acids render their use in these processes not environmentally suitable. Consequently, there will always be a compromise between attempting to obtain higher recovery efficiencies and environmental sustainability.

2.10. Summary of Chapter Two

Chapter two reviewed relevant literature on the production of CFA, its properties and highlighted the impacts of the disposal of CFA as well as, the well-known alternative uses of CFA. The properties of CFA such as mineralogy, physical and chemical are dependent on the parent material which is coal, the conditions of combustion, type of emission control devices, storage and handling methods.

The current disposal methods of CFA raises a lot of environmental concerns as CFA is mostly disposed of on landfills and ash dams. The major environmental concerns are associated with

the potential leaching of toxic elements from landfill sites as a result of weathering. Due to the increase in population growth, the electricity demand will inevitably increase. This will result in a higher demand for coal, consequently an increase in the production of CFA. Therefore, there is a need for alternative disposal methods and utilisation of CFA, which are optimal and will yield environmental benefits.

Although CFA is a waste material, it is enriched in REEs in some areas of the world, hence is a potential valuable secondary source. Globally, there has been an increase in the demand for REEs, thus alternative sources besides REEs bearing ores have been investigated. Furthermore, REEs are essential in the manufacturing of high-technological devices which can be used in various applications that will yield positive impacts on the social and economic society. Ideally, CFA is a viable alternative source of REEs as it is readily available in large quantities across the globe.

Although in several parts of the world the occurrence of REEs in coal and CFA have been extensively explored, there is still limited literature on South African coals and CFAs. Additionally, literature has highlighted that REEs in CFA could be enriched by simple physical separation methods and that an inverse relationship between the particle size of CFA and the concentration of REEs exists. However, some literature shows some disagreements of experimental results, which indicates that different CFAs might give different responses to these separation techniques that are supposed to enrich REEs.

Hydrometallurgical methods which often involve leaching, extraction, separation and purification are generally used in the recovery of REEs from waste material, particularly in CFA. The direct acid leaching and alkaline-acid fusion leaching technique are the most favoured as they yield relatively high REE recovery efficiencies. Over the years the methods of recovering REEs from CFA have been investigated and modified to overcome low recovery efficiencies as well as to scale-up for industrial application and achieve environmental sustainability. However, very little progress has been made towards finding the optimum recovery conditions that may suit the bulk of the CFA available in South Africa and the world. This is predominantly a consequence of CFA being chemically different due to the combustion of coal sourced from different regions as well as the combustion techniques and technologies used.

Furthermore, several other factors that may potentially influence the recovery efficiencies of REEs need to be explored. One of the factors that have not been extensively investigated particularly in South Africa is the effect of particle size of CFA on the enrichment and recovery efficiency of REEs. This is of utmost importance to investigate as it can lead to greater REE recovery efficiencies. Also, methods that are best suited for recovering REEs from South African CFA or the various CFA produced by the various power stations are yet to be found. Thus, this study aims to assess the effect of particle size of CFA on the enrichment and recovery efficiency of REEs from CFA. Findings from this study will improve the understanding of the recovery of REEs and methods and specific conditions that accelerate and favour greater recovery of REEs from South African CFA for beneficiation.

CHAPTER THREE: SITE DESCRIPTION AND METHODS

3. Introduction

This chapter begins with a detailed description of the study sites. The research methods used to assess the effect of the particle size of coal fly ash (CFA) on the enrichment and recovery of rare earth elements (REEs) are described in detail. The research methods explained in this chapter are those that were applied during sampling, experimental and analytical analyses. The experimental procedure is described in detail, while the quality assurance and quality control measures adhered to during sampling and analyses are outlined.

3.1. Description of Study Site

Two South African coal-fired power stations that are operated by Eskom were chosen as study sites for this research and they are as follows: Duvha and Tutuka. The choice of Duvha and Tutuka Power Stations as study sites was dictated by their accessibility, CFA disposal mode and their likelihood of burning coal sourced from different coalfields, which potentially could result in CFA of varying chemical compositions.

3.1.1. Duvha Power Station

Duvha Power Station is located approximately 15 kilometres (km) east of Witbank in Mpumalanga Province. Construction of the power station began in 1975 and the last unit was commissioned in 1984. In 1993 Duvha became the first power station in the world to be retrofitted with pulse jet fabric filter plants on three of its six units. The power station is situated on the Witbank Coalfield thus, coal from this coalfield is often used as feedstock at Duvha Power Station. Approximately 2.5 million tons (Mt) of CFA is produced annually at the power station (Reynolds-Clausen and Singh, 2019).

The station operates a wet ashing facility, which means the ash is mixed with water at a ratio of 10:1 and then the wet ash slurry is hydraulically pumped into an ash dam. Here, the ash is allowed to settle out of solution and the water is decanted to a Low-Level Ash Water Return Dam (LLAWRD) (**Figure 3. 1**), before it is pumped back to the station for reuse (Eskom Holdings SOC Ltd, 2020). All impacted stormwater generated on-site is contained and

managed on-site whilst clean water is diverted around the site to a tributary and ultimately drains to the Witbank Dam.

Figure 3. 1*:* Aerial view of Duvha Power Station and the Ash Dam

3.1.2. Tutuka Power Station

Tutuka Power Station is situated in Mpumalanga Province 25 km away from Standerton. Tutuka's construction phase began in 1980 and the first unit was commissioned in 1985 while the plant was fully commercialised by 1991 (Eskom Holdings SOC Ltd, 2020). The power station is located on the Highland Coalfield thus, coal from this coalfield is often used as power station feedstock at Tutuka. Wagner and Matiane (2018) reported coal used as feedstock at the power station to have ΣREE content of 218.3 ppm and the CFA of this coal was found to have ΣREE content of 517.8 ppm, indicating that REEs were enriched in the CFA compared to the coal. Approximately 2.93 Mt of CFA is produced annually at the power station, (Reynolds-Clausen and Singh, 2019).

Tutuka Power Station uses the dry disposal technique to dispose of the CFA. The ash dumpsite of the power station is in the vicinity and the dry ash is transported by a conveyor belt to the dumpsite. Sections of the dumpsite with ash that was dumped approximately 30 ages ago have been rehabilitated and this can be seen on the aerial image below (**Figure 3. 2**).

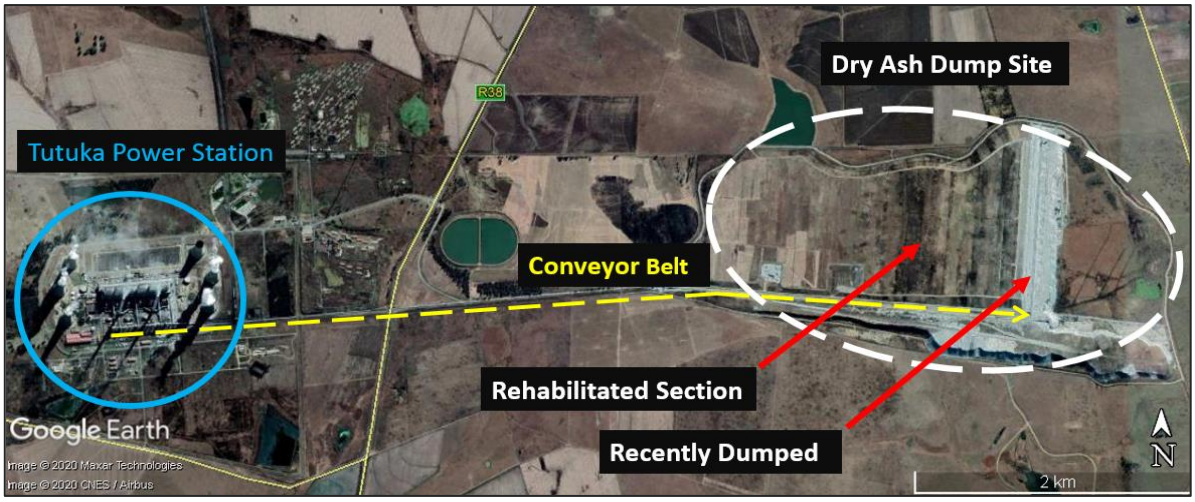

Figure 3. 2: Aerial view of Tutuka Power Station and the Ash Dump Site

3.2. Sample Collection

Fresh CFA samples were collected at Tutuka and Duvha Power Station. The leachates (supernatant water obtained after leaching experiments) and the solid residue samples were collected after the leaching experiments were concluded. The materials that were used for field and laboratory sample collection and storage are presented in **Table 3. 1**.

Table 3. 1: Materials used for sample collection and storage

Material	Use
Plastic bags	Storing of raw CFA samples
High- density Polyethylene (HDPE) Buckets (25 ℓ)	Storing of raw CFA samples
High-Density Polyethylene (HDPE) Sampling Bottles (250 mℓ)	Storing of leachate
Ziploc Bags	Storing of solid residue

In Tutuka power station, fresh CFA samples were collected from the conveyor belt, while in Duvha power station the samples were collected from the precipitators. The samples were collected in plastic bags which were filled to the top to prevent the ingress of CO_2 and then sealed. The samples were then stored in 25 ℓ high-density polyethylene (HDPE) buckets and labelled accordingly. The 25 ℓ buckets with CFA samples were stored in a dark cool place far away from any source of heat, out of direct sunlight. A subset of the CFA samples was sent to an analytical lab at the University of the Witwatersrand for chemical analysis.

3.3. Experiment Set-Up and Procedure

The study adopted the alkali fusion and direct acid leaching experimental conditions used and suggested by the following authors: Guo et al. (2013), Cao et al. (2018), Taggart et al., (2018a) and Tang et al. (2019) as reviewed in **section 2.7**. The optimum leaching conditions suggested by these studies are not just to improve the recovery efficiencies of REEs, but are also an attempt to conduct these experiments in an environmentally sustainable manner (i.e., using less energy and fewer volumes of corrosive acids). Below is a flow diagram of the experimental procedure that was followed. **Figure 3. 3** depicts a flow chart of the general procedure followed during data collection.

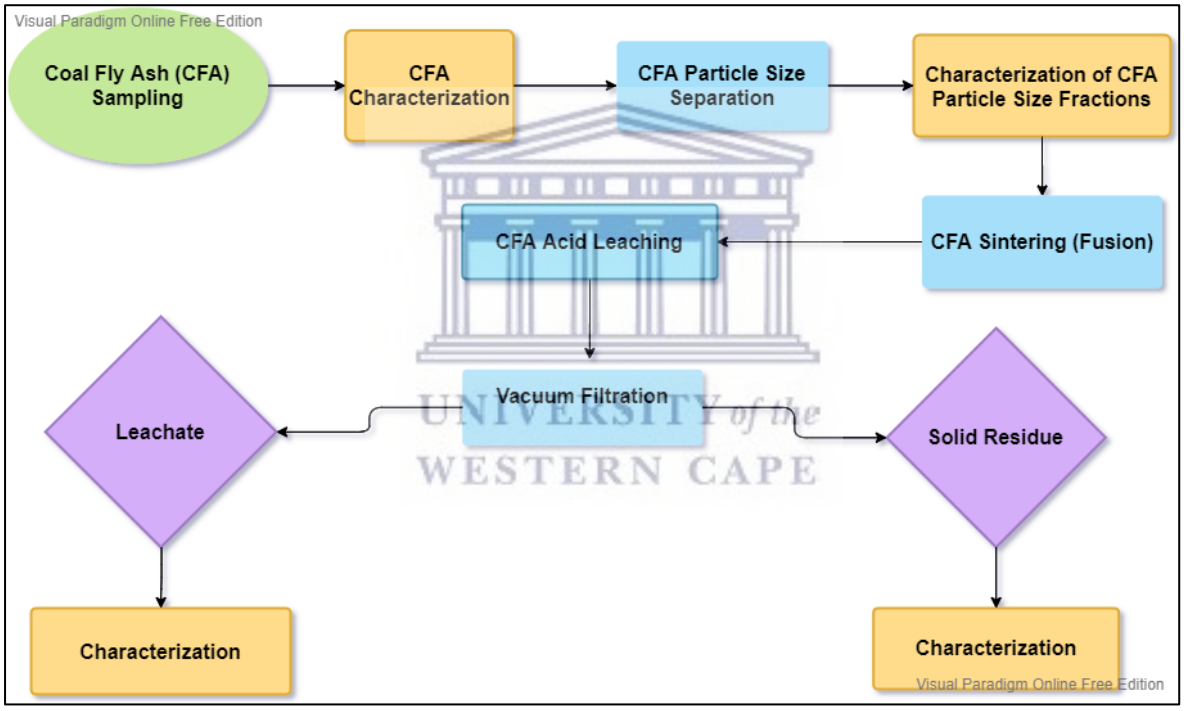

Figure 3. 3: Flow chart showing the overall procedure followed during data collection

3.3.1. Sieving Procedure

The raw collected CFA was oven-dried at 105 °C until a constant mass was reached using dying pans with dimensions that the loading of the CFA did not exceed 1 gram per square centimetre (g/cm^2) to remove moisture content. The moisture content was calculated to be 16 % and 0 % for Tutuka and Duvha CFA respectively. 1000 g of the oven-dried CFA of each power station was sieved into the following fractions: > 106, 106 - 75, 75 – 53, 53 - 50, 50 -

32, 32 - 25, < 25 µm. Previous studies have demonstrated that an inverse relationship between the particle size of CFA and the concentration of REEs exists for separates between 100 and 30 µm (Clarke and Sloss, 1992; Seredin and Dai, 2012; Hower et al., 2013; Blissett et al., 2014; Lin et al., 2017; Lin et al., 2018; Rosita et al., 2020).

3.3.2. Sintering Procedure

The following table consists of all the materials used during the sintering process (alkali-fusion) of CFA with sodium hydroxide (NaOH) per sample.

Table 3. 2: Materials used during the sintering phase of the experiment

Material	Use
10 g of CFA	Medium to be leached
10 g of crushed Sodium Hydroxide (NaOH) pellets	Sintering agent used to promote the breakdown of the aluminium silicate glass phase of CFA.
30 mℓ porcelain crucible	Holds contents to be sintered
Furnace	Instrument used to sinter CFA and NaOH

The sieved oven-dried CFA was subjected to sintering (roasting). For sintering, 10 gram (g) of CFA was thoroughly mixed with 10 g of crushed NaOH pearls (1:1 solid ratio) in a crucible. The crucible along with the contents was placed in a furnace for sintering **(Figure 3. 4)** for 2 hours (hrs) at a temperature of 400 °C. After 2hrs the crucible with the contents (herein referred to as fused CFA) was left to cool to room temperature (25 °C). The fused CFA samples were then ground using a mortar and pastel as the content had caked up during sintering. The fused CFA samples were then prepared for the next phase of the experiment which was acid leaching.

Figure 3. 4: Image showing the muffle furnace used for the sintering as well as the fused end product

3.3.3. Leaching Procedure

Table 3. 3 shows the materials used during the leaching phase of the experiment per sample.

Table 3. 3: Materials used during the acid leaching phase of the experiment.

Material	Use
20 g of Fused CFA	Medium to be leached
200 mℓ of 3 mol/ℓ of Hydrochloric Acid (HCL)	Solvent used to dissolve CFA
500 mℓ Silicon Oil	Maintain a constant temperature of the oil bath
500 mℓ Round Bottom Flask	Contain contents to be leached (Fused CFA + HCL)
Condenser	Reflux the contents being leached
Magnetic Stirring Hot Plate	Heats and stirs contents being leached in the round bottom flask
2 Magnetic Stir Bars	Stirs contents in the round bottom flask
2 Laboratory Utility Clamp Holders	To secure laboratory apparatus (condenser + round bottom flask)

The study adopted the experimental leaching set up of Honaker et al. (2019) and Zhang and Honaker (2020), whereby leaching took place in a reflux system. Reflux involves heating

the chemical reaction for a specific amount of time, while continually cooling the vapour produced back into liquid form, using a condenser (**Figure 3. 5**). The vapour produced above the reaction continually undergoes condensation, returning to the flask as a condensate (Teo et al., 2014).

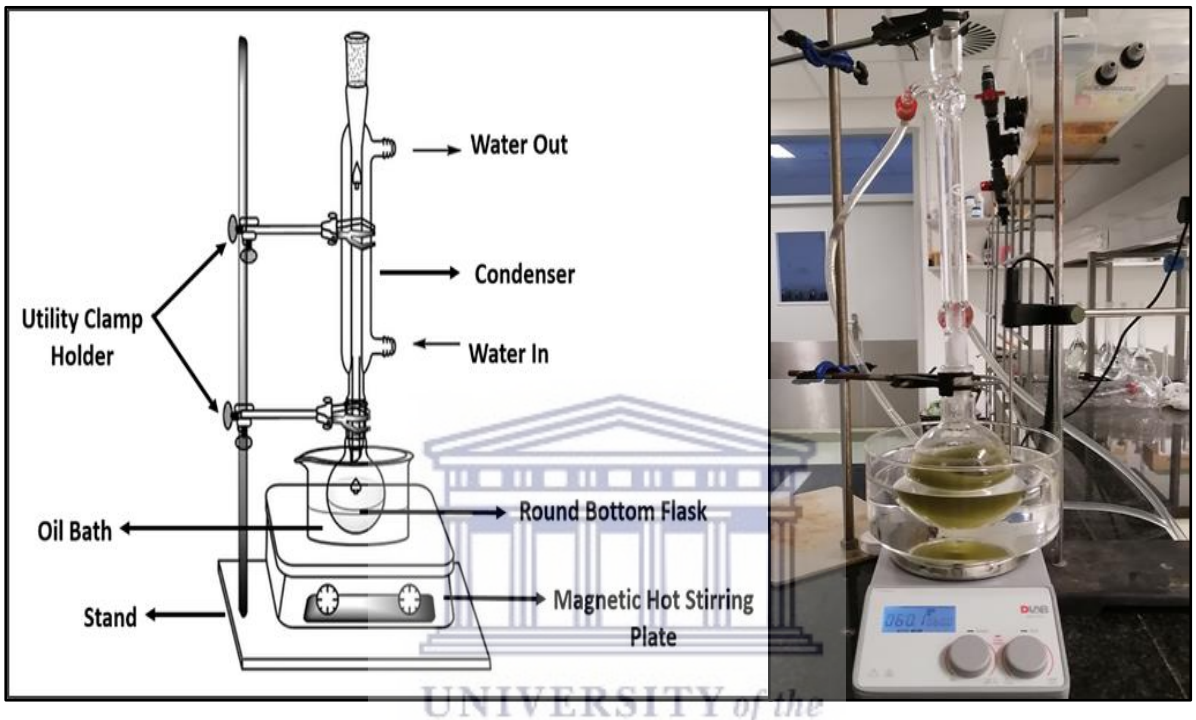

Figure 3. 5: Schematic diagram of a reflux system set up, adapted from (Teo et al., 2014)

The fused CFA was subjected to acid leaching using HCl as follows: 20 g of fused CFA was added to a round bottom flask then followed by 200 mℓ of HCl with a concentration of 3 mol/ℓ (1:10 solid-liquid ratio). The round bottom flask was then fitted onto a condenser, then placed in a silicon oil bath after the bath had reached the desired temperature. The purpose of the oil bath was to ensure that leaching occurred at a constant temperature. After fitting the round bottom flask to the condenser, water was allowed to flow into the inlet of the condenser. The temperature was set to 90 °C, while the speed was set to 400 revolutions per minute (rpm) and leaching took place for 2 hrs. Blank samples were collected during the experiment where CFA was leached with deionized water instead of HCl to understand the leaching of REEs from CFA in a natural environment (i.e., ash dump or ash dam).

It is important to note that literature recommends that a very small mass of CFA be leached such as 1 g. However, in this study, the solid residue needed to be analysed thus, 20 g of fused CFA was leached to ensure there was sufficient mass for all the analyses.

3.3.4. Filtration Procedure

Table 3. 4 shows the material used during the filtration phase of the experiment per sample.

Table 3. 4: Material used during the filtration phase of the experiment per sample

Material	Use
Büchner Funnel	Separate the liquid from the solid
250 mℓ Filter Flask (with sidearm)	Hold the filtered leachate
0.45 µm Filter Paper	Ensures that no solid filters through

After leaching, the leached contents were subjected to vacuum filtration (suction). Vacuum filtration is a technique that allows for a greater rate of filtration whereas in normal filtration gravity provides the force which draws the liquid through the filter paper. In suction filtration, a pressure gradient performs this function (**Figure 3. 6**). The mixture from the leaching phase of the experiment was separated using a 0.45 micrometre (µm) membrane filter. The filter paper was placed in a büchner funnel and damped a bit, then fitted into a filter flask. The leached contents were poured into the funnel and the vacuum source was opened. Due to the nature of the solution ("gel" like consistency), it took approximately an hour to filter approximately 100 mℓ of the leachate which was more than sufficient for what was required (ie15 mℓ) for ICP-MS analysis for each sample. For this reason, for quality control, all the samples were filtered for an hour.

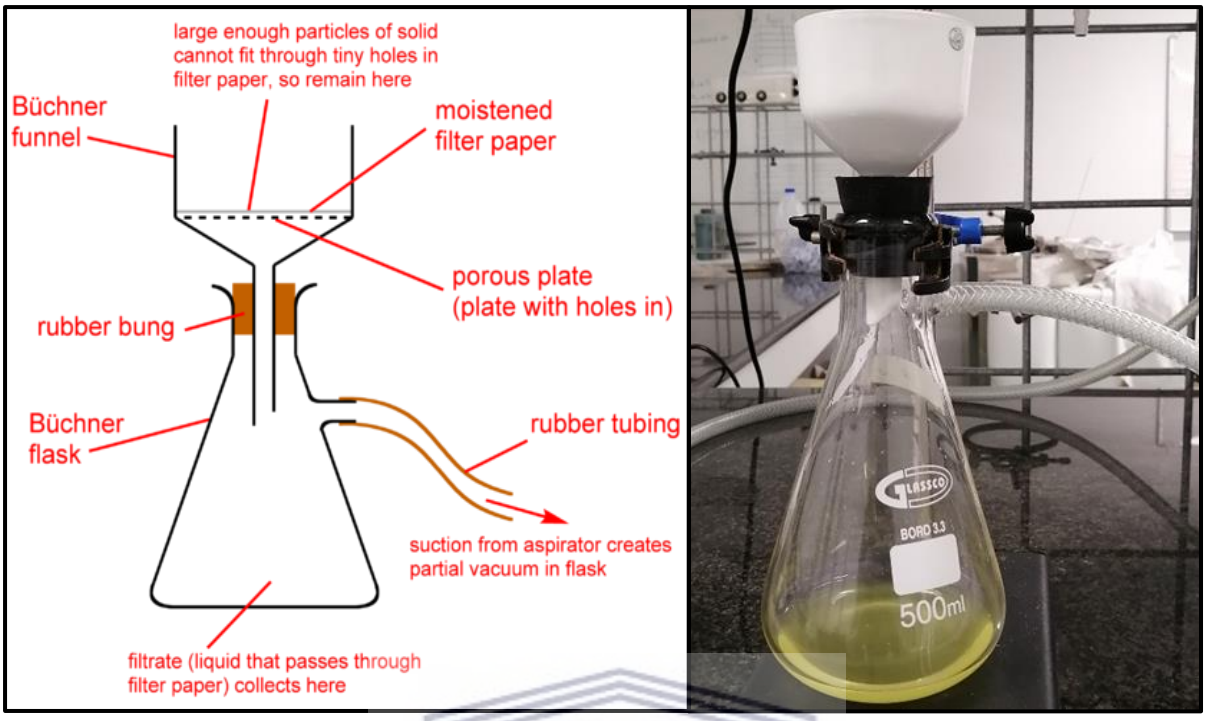

Figure 3. 6*:* Schematic diagram of a vacuum filtration system set up

The liquid samples were stored in 100 mℓ PPE sampling bottles and stored at below 4 °C until they were sent for REE analysis at an analytical lab at the University of Stellenbosch using Inductively Coupled Plasma Mass Spectrometry (ICP-MS). The solid residues were oven-dried at 50 °C for 24 hrs, then packaged in small ziploc bags, stored in a dark, cool environment. The solid residues were submitted for major oxides and REE analyses at an analytical lab at the University of Stellenbosch using X-Ray Fluorescence and Laser Ablation-Inductively Coupled Plasma Mass Spectrometry (LA: ICP-MS).

3.4. Analytical Techniques

This section describes the analytical techniques used in analysing and quantifying the fresh solid CFA, leached solid residues and liquid samples obtained after the leaching experiments. The principles involved in each technique are described. It is important to highlight that all the analytical analyses including preparation of the samples were conducted by established laboratories, one at the University of the Witwatersrand and the other at the University of Stellenbosch.

3.4.1. Scanning Electron Microscope and Energy Dispersive Spectroscopy

The Scanning Electron Microscope (SEM), is a technique that provides detailed imaging data about surface texture and morphology of a mineral substance (Kutchko and Kim, 2006). SEM images have a three-dimensional appearance and this becomes useful for judging the surface structure and morphology of the sample. SEM examines surface texture and morphology by bombarding the sample with a scanning beam of electrons and then collecting slow-moving secondary electrons that the sample generates. These are collected, amplified, and displayed on a cathode ray tube. The electron beam and the cathode ray tube scan synchronously so that an image of the surface of the specimen is formed (Fatoba, 2007). The energy dispersive spectroscopy (EDS) is attached to the SEM and is mostly used for quantitative analysis of a material, whereby specific elements are identified and their abundance is presented in atomic weight percentage. This technique is based on the collection and energy dispersion of X-rays reflected when high energy electrons are bombarded on a sample (Eze, 2011). The EDS was used for spot quantitative analysis of samples in the SEM.

The raw CFA samples were oven-dried at 105 °C for 24hrs and carbon-coated with graphite thus making them electrical conductors if they were not already. Micrographs were taken at a very slow rate to capture greater resolution. SEM-EDS allowed for the above-mentioned detail of the sampled CFAs to be determined. In addition, the SEM-EDS technique has been understood to be one of the best and most widely used techniques for the characterization and identification of the chemical and physical phases in CFA particles (Vassilev and Vassileva,2005; Surender, 2009; Eze, 2011; Alan, 2013; Yang, 2019).

3.4.2. Tescan Integrated Mineral Analyser

Tescan Integrated Mineral Analyser (TIMA) is an automated mineralogy system for fast quantitative analysis of samples such as rocks, ores, concentrates, tailings, leach residues or smelter products. TIMA combines Energy Dispersive X-Ray (EDX) and backscattered electron (BSE) signals to identify minerals and create mineral images that are analysed to determine mineral concentrations, element distributions, and mineral texture properties such as grain-size, association, liberation and locking parameters. Image analysis with TIMA is performed simultaneously with SEM backscatter electron images and a suite of X-ray images. The level

of hardware integration of the SEM and EDX allows for unprecedented acquisition speeds for fully automated data collection, resulting in fast, accurate, repeatable and reliable results.

TIMA requires the sample surface to be perfectly flat for the automated analysis. Therefore, in preparation for analysis, the samples were split into smaller representative portions of approximately 2 g to prepare the ore block. A mould of the sample was created by mixing resin and hardener at a ratio of 7:1, which was then mixed with the sample. This sample mixture was allowed to cure at room temperature for approximately 8 hours. After curing the sample ore block was subjected to grinding using a 220grit followed by a 1200grit for about a minute each. The ground sample was then polished using an MD Dur cloth and a 6 µm diamond suspension with lubricant. This was followed by polishing using an MD Mol cloth and a 3 µm diamond suspension with lubricant. Lastly, the sample block was polished using an MD Fur cloth and 1 µm diamond suspension with lubricant and each polishing step took place for approximately 10 minutes. **Figure 3. 7** depicts the polished sample ore blocks.

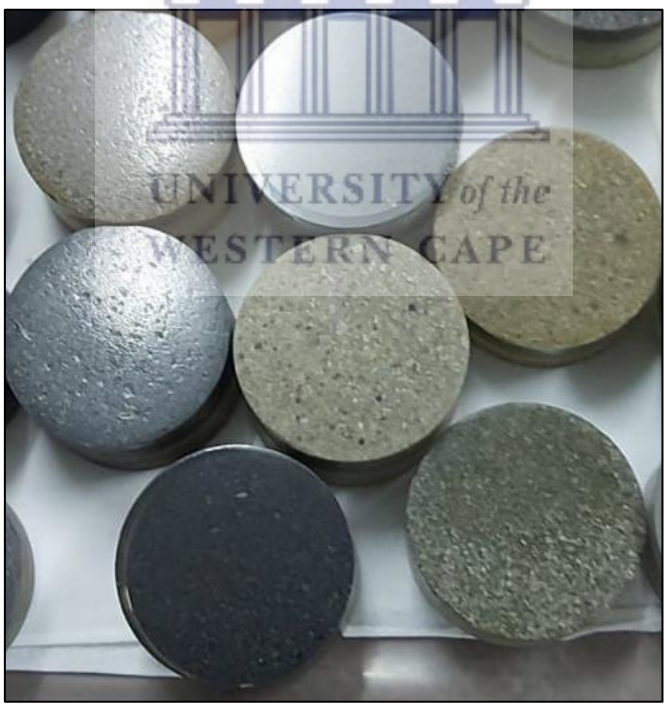

Figure 3. 7: Image illustrating the prepared sample ore blocks for TIMA analysis

3.4.3. X-Ray Diffraction Spectrometry

X-ray diffraction Spectrometry (XRD) is a very useful technique used for the identification and characterization of the physical and chemical features in solid samples (Chand et al., 2009).

The material to be analysed is finely ground, homogenised and the average bulk mineral composition is determined (Klein et al., 1975; Vassilev and Vassileva, 2005).

This technique uses the diffraction pattern produced by bombarding a single crystal with monochromatic X-rays to determine the crystal structure. The X-rays are generated by a cathode ray tube, filtered to produce monochromatic radiation, collimated to concentrate and directed toward the sample. The interaction of the incident rays with the sample produces constructive interference and a diffracted ray. The characteristic of the X-ray diffraction pattern recorded provides a unique "fingerprint" of the crystals present in the sample. This then allows for the identification of the crystal form (Fatoba, 2007; Eze, 2014).

This technique was used to analyse the mineralogical composition of the CFA collected at the two coal-fired power stations as well as the solid residue obtained from the leaching experiments. The samples were oven-dried at 105 ^{0}C for 24 hrs and ground to a fine powder by a pestle and mortar. The analysis was performed using a multi-purpose X-ray diffractometer D8-Advance from Bruker operated in a continuous ϑ-ϑ scan in locked coupled mode with Cu-K_α radiation. The sample was mounted in the centre of the sample holder on a glass slide and levelled up to the correct height.

The advantage of this technique is the detection of the occurrence and degree of crystallinity of major, and some minor crystalline phases (i.e., quartz, mullite, magnetite, hematite, feldspars, anhydrite, calcite, and others) independent from their size. Several studies investigating the extraction of REEs from CFA have proven this method to be most effective for phase identification (Oberlink et al., 2017; King et al., 2018; Taggart et al., 2018a; Taggart et al., 2018b; Mishra et al., 2019; Tang et al., 2019; Pan et al., 2020).

3.4.4. X-Ray Fluorescence Spectrometry

X-ray fluorescence spectrometry (XRF) analysis is a technique that uses X-ray fluorescence to identify the elemental composition of a sample and provides the concentration of the element (Skoog et al., 2017). An inner shell electron is excited by an incident photon in the X-ray region and during the de-excitation process, an electron moves from a higher energy level to fill the vacancy. The energy difference between the two shells appears as an X-ray, emitted by the atom. The X-ray spectrum acquired during the above process reveals several characteristic peaks. The energy of the peaks leads to the identification of the elements present in the sample

(qualitative analysis), while the peak intensity provides the relevant or absolute elemental concentration (Gitari, 2006).

In preparation for the analysis, fusion disks were prepared by an automatic Claisse M4 Gas Fusion instrument and ultrapure Claisse Flux. A sample to flux ratio of 1:10 was used and was coarsely crushed. Then after a chip of sample was mounted along with other samples in a 2.4cm round resin disk. The mount was mapped and then polished for analysis. This technique has been widely used in determining the elemental composition of CFA (Mardon and Hower, 2004; Jankowski et al., 2006; Akinyemi et al., 2011; Kashiwakura et al., 2013; Akinyemi et al., 2019; Liu et al., 2019; Tuan et al., 2019).

3.4.5. Inductively Coupled - Mass Spectrometry

Inductively Coupled Plasma (ICP) is a technique for elemental analysis of liquid samples and applies to most elements over a wide range of concentrations (Skoog et al., 2017). Inductively Coupled Plasma Mass Spectrometry (ICPS-MS), is a technique that is highly sensitive and capable of multi-element, trace and ultra-trace analysis, often at the parts per trillion level. Testing for trace elements can be performed on a large range of metals from super alloys to high purity materials.

This technique couples the use of an ICP with MS for elemental analysis by the generation of ions and operates in four main stages which are; sample introduction and aerosol generation, ionization by an argon plasma source, mass discrimination and detection. ICP-MS can accept solid as well as liquid samples, unlike an atomic emission spectrometer. Solid samples are introduced into the ICP via a laser ablation system which is usually acquired as an accessory. The ICP is involved in the generation of a high-temperature plasma source at 10 000 °C, through which the pre-treated sample is passed. The elements in the sample at such a high temperature are ionized and directed further into the MS. The MS then sorts the ions according to their mass-charge ratio followed by directing them to an electron multiplier tube detector. This detector then identifies and quantifies each ion (Muriithi, 2009; Musyoka, 2009).

This technique was used to analyse REEs from the solid CFA and the liquid samples collected after the leaching experiments. For the analyses of solid CFA samples, the LA ICP-MS instrument was set by connecting a 193 nm Excimer laser to an Agilent 7500 Q ICP-MS. Before analysis, the ICP-MS was optimized for sensitivity and low oxide ratios (< 0.2%) by tuning

both the ICP and laser parameters while ablating a line on NIST612. Ablation was performed in He gas at a flow rate of 0.35L/min, then mixed with argon (0.9L/min) and nitrogen (0.003L/min) just before introduction into the ICP plasma.

The aqueous solutions obtained from the leaching experiments were filtered through a 0.45 μm membrane to remove suspended solids and then diluted with de-mineralized. The samples were then introduced to the ICP through a high sensitivity glass, single-pass cyclone spray chamber and conical nebulizer using argon gas. Overall, this method has been proven to be quite effective for the analysis of REEs from similar studies (King et al., 2018; Taggart et al., 2018a; Taggart et al., 2018b; Tang et al., 2019; Pan et al., 2020). Also, one of the major advantages of this technique includes sensitivity and precision for its ability to quantify elements in any source.

3.5. Quality Assurance and Quality Control Measures

Quality assurance and control measures are taken to ensure that results obtained in a study are reliable and reproducible. These measures were considered during sample collection both in the field and laboratory. Duplicate samples in the laboratory were taken to estimate sampling and laboratory analysis precision. Furthermore, during CFA sample collection in the field, samples were stored in new heavy-duty bags, which were filled to the top and sealed to avoid the ingress of CO_2 and stored in 25 ℓ in HDPE buckets. The samples were stored in a dry cool place and away from any direct heat that could cause temperature fluctuations. All the equipment used for measuring and analysing the samples were calibrated before the analysis. During the leaching experiments, each leaching run was repeated twice to estimate sample and laboratory precision. In addition, blank samples were collected, where CFA that was not fused with NaOH was leached with deionized water to simulate the leaching of REEs from CFA in a natural environment. Furthermore, all the apparatus and sampling bottles used during the experiments were decontaminated before each experiment run and sample collection using deionized water. The liquid samples were stored at a cool place below 4 °C before they were sent for analysis.

3.6. Summary of Chapter Three

Chapter three describes the study site in detail as well as the methods used to achieve the objectives of the study which are outlined in chapter one. The study site, Duvha and Tutuka

Power Station are situated in Mpumalanga Province within the Witbank and Highveld Coalfield respectively.

Fresh CFA samples were collected at Tutuka and Duvha Power Stations and these samples were labelled and stored accordingly. A portion of the raw CFA samples was sent to an analytical laboratory for characterisation in terms of morphological, mineral and chemical compositions using various analytical techniques (i.e., XRF, XRD, SEM, TIMA, LA: ICP-MS and ICP-MS), while the other portion was sieved into several particle size fractions and used during the alkali-fusion acid leaching experiments. NaOH was used as the additive agent for the roasting phase of the experiment which took place before acid leaching and HCL was used as the lixiviant for the acid leaching phase of the experiment. After acid leaching, the solid and liquid phases were separated using a filter membrane. The solid residue and supernatant water were collected, labelled and stored accordingly. The samples were then sent to analytical laboratories for chemical composition analysis, using the same techniques used to characterise the raw solid CFA samples.

Quality assurance and control measures were taken to ensure that the experiment and results are reproducible. This included the storing of CFA in sealed plastic bags, preventing the ingress of CO_2 and storing the samples away from any source of heat that will cause fluctuation of temperature. Duplicate samples were collected in the field and each experiment was run twice. Also, all sampling containers were decontaminated using deionized water before sampling. All the equipment used for the analysis was calibrated accordingly before the analysis of the samples.

CHAPTER FOUR: RESULTS

4. Introduction

This chapter presents the findings of physical and chemical characterization of the whole (un-sieved) and sieved coal fly ash (CFA) samples collected from Duvha and Tutuka Power Stations. The following analytical techniques were utilised to characterize the raw CFA: X-Ray Diffraction (XRD); X-Ray Fluorescence (XRF), Scanning Electron Microscope with Energy Dispersive Spectrometry (SEM-EDS), Tescan Integrated Mineral Analyser (TIMA), Inductive Coupled-Mass Spectrometry (ICP-MS) and Laser Ablation-Mass Spectrometry (LA ICP-MS). The relationship between the particle size of CFA and rare earth elements (REEs) was assessed and the findings are presented. This was investigated before and after alkali-fusion acid leaching. Furthermore, the REE recovery efficiencies of the alkali-fusion acid leaching techniques are also presented in the chapter.

4.1. Coal Fly Ash Characterization

4.1.1. Morphology

The whole (un-sieved) CFA samples from Duvha and Tutuka Power Stations were analysed by SEM-EDS. This technique allowed for the characterization of the physical structure of the CFAs and gave the location of elements in the region being scanned, allowing the distribution of each element to be evaluated in the CFA samples.

The SEM micrographs of the two CFAs in **Figure 4. 1**and **Figure 4. 2** showed that the particles were typically spherical, with some irregular shaped structures in agglomerated form, while others appeared to be porous. The outer surfaces of Duvha CFA particles mostly displayed a smooth texture (**Figure 4. 1**), while those of Tutuka was smooth and had a rough dendritic surface texture (**Figure 4. 2B)**. Duvha CFA displayed more cenospheres (i.e., hollow microspheres), while Tutuka CFA exhibited numerous ferrospheres (i.e., spheres with a dendritic outer surface).

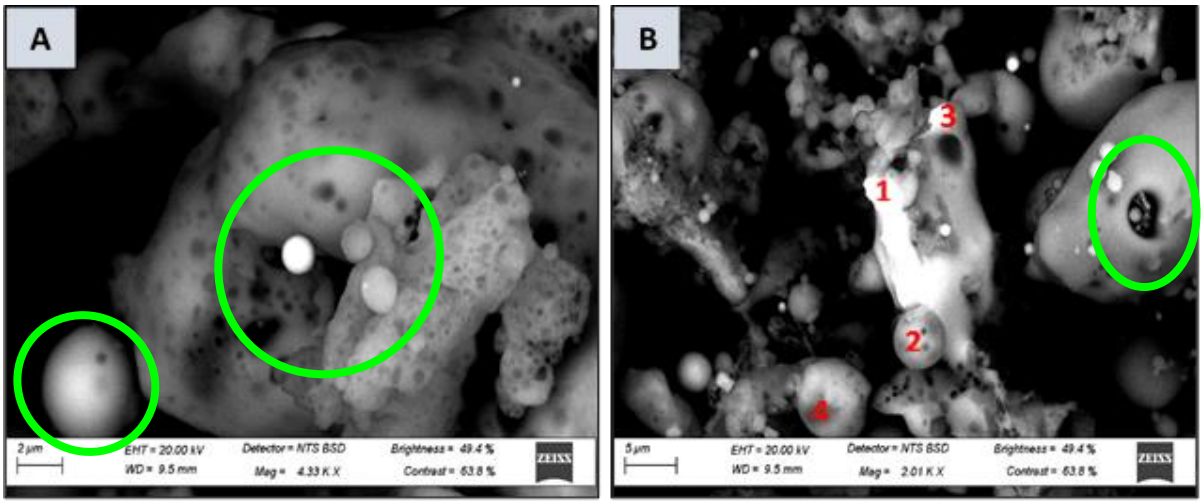

Figure 4. 1: SEM-EDS micrographs of Duvha CFA (A) overall view (B) particle spots for EDS analysis (Magnification: (A) = 4.33KX, (B) = 2.01 KX)

Figure 4. 2: SEM-EDS micrographs of Tutuka CFA (A) overall view (B) particle spots for EDS analysis (Magnification: (A) = 999 X, (B) = 4.65 KX)

The findings of the EDS spot analysis of Duvha CFA SEM micrograph **Figure 4. 1B** are shown in **Table 4. 1** and the one of Tutuka CFA SEM micrograph **Figure 4. 2B** are shown in **Table 4. 2**. The predominant elements in both CFAs were aluminium (Al), silicon (Si) as shown in the EDS analyses in **Figure 4. 3** and **Figure 4. 4**. Although these elements exhibited minor differences, they were more abundant in Duvha than in Tutuka CFA. The Al and Si content was measured to be 12.98 wt% and 26.68 wt % in Duvha CFA, whilst in Tutuka CFA it was 4.40 wt% and 6.82 wt% respectively. An association between Si and Al was evident in all the spot analyses, where the wt % of Si was found to be relatively high, Al was also relatively high. Smaller quantities of iron (Fe) potassium (K), titanium (Ti), phosphorus (P), calcium (Ca) and

sulphur (S) were observed in the spots with higher amounts of Si and Al. However, Tutuka CFA was more abundant in Fe than Duvha CFA with measured abundances of 44.47 wt% and 1.15 wt% respectively. Furthermore, Duvha CFA was less abundant in Ca compared to Tutuka CFA, with measured abundances of 1.23 wt% and 1.62 wt% respectively (**Table 4. 1** and **Table 4. 2**).

Table 4. 1: Descriptive statistics of quantitative elemental (SEM-EDS) spot analysis (weight %, n = 4) of Duvha CFA (**Figure 4. 1B**)

	Na	Mg	Al	Si	P	S	Cl	K	Ca	Ti	Fe	La	Ce
Max	0.20	0.58	21.15	43.94	5.81	0.17	0.05	0.77	1.82	2.14	1.64	9.25	16.44
Min	0.00	0.05	6.10	18.90	0.14	0.00	0.00	0.00	0.66	0.42	0.46	0.26	0.26
Mean	0.07	0.27	12.98	26.68	1.73	0.06	0.01	0.35	1.23	1.03	1.15	2.97	5.45
STDEV	0.08	0.24	6.32	9.19	2.39	0.07	0.02	0.34	0.48	0.70	0.46	3.55	6.45

Figure 4. 3*:* Graph illustrating EDS Spectrum of Spot 3 of Duvha CFA micrograph (Figure 4.1B)

Table 4. 2: Descriptive statistics of quantitative elemental (SEM-EDS) spot analysis (weight %, n = 4) of Tutuka CFA (**Figure 4. 2B**)

	Mg	Al	Si	P	S	Cl	K	Ca	Ti	Mn	Fe	Cu
Max	0.72	10.78	20.78	0.12	0.19	0.26	1.36	4.59	0.53	2.12	60.12	0.55
Min	0.17	2.08	1.52	0.00	0.00	0.00	0.05	0.56	0.14	0.06	3.66	0.04
Mean	0.32	4.40	6.82	0.06	0.10	0.09	0.38	1.62	0.31	1.28	44.47	0.31
STDEV	0.27	4.26	9.32	0.05	0.08	0.12	0.65	1.98	0.17	0.87	27.24	0.23

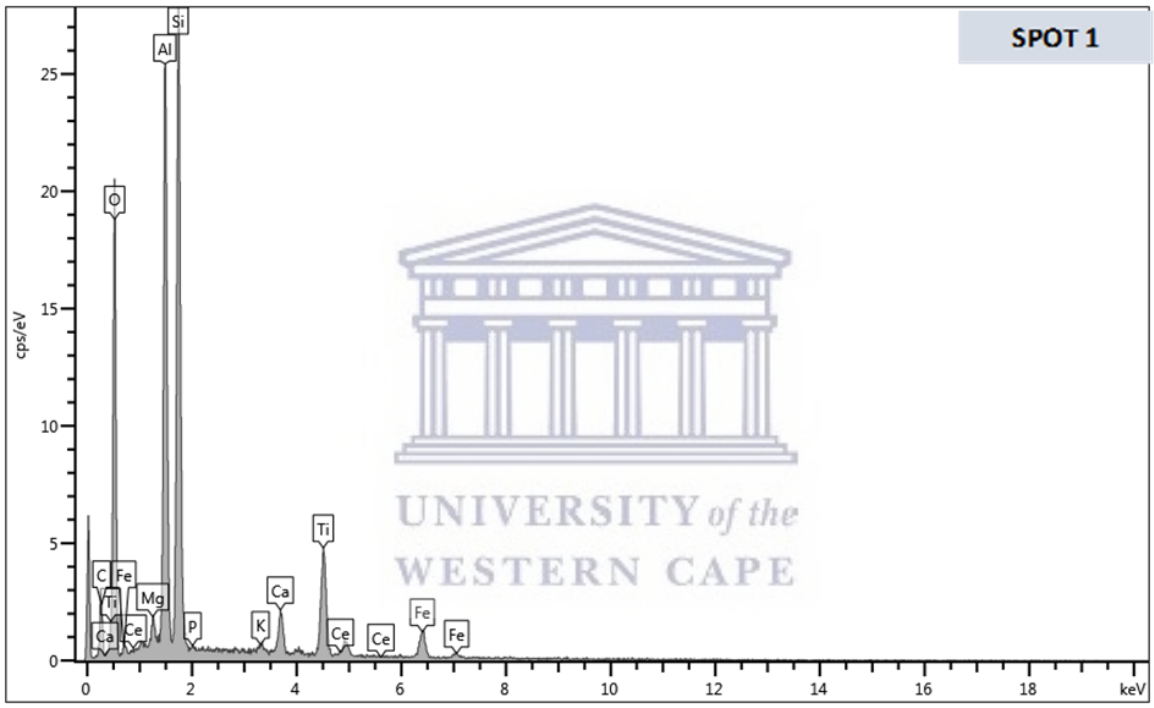

Figure 4. 4: Graph illustrating EDS spectrum of Spot 1 of Tutuka CFA micrograph (Figure 4.2B)

The REEs Lanthanum (La) and Cerium (Ce) were detected during the EDS spot analyses in both CFAs as depicted in **Figure 4. 3** and **Figure 4. 4**. In Duvha CFA the abundance of these REEs was found to be relatively high in Spot 3, whilst in Tutuka CFA it was in spot 1. Overall, Duvha CFA was found to have an abundance of La and Ce of 2.97 wt% and 5.45 wt% respectively. It is important to highlight that EDS analysis alone is an inadequate quantitative method to utilize in precisely determining elemental composition, as high variations in elemental composition within each spot for the same micrograph were observed (**Table 4. 1** and **Table 4. 2**).

4.1.2. Mineral Composition

XRD was applied to identify the mineralogical phases present in the raw whole (un-sieved) samples of Duvha and Tutuka CFA. **Figure 4. 5** depicts the XRD spectra (patterns) of these CFAs. The XRD patterns revealed minimal variation in the major crystalline mineral phases of Duvha and Tutuka CFA as they had similar patterns. The major mineral phases present in the CFAs were quartz (SiO_2), mullite ($3Al_2O_3 \cdot 2SiO_2$), while maghemite (Fe_2O_3), calcite (CaO) and microcline ($KAlSi_3O_8$) were minor. However, no calcite was identified in Duvha CFA.

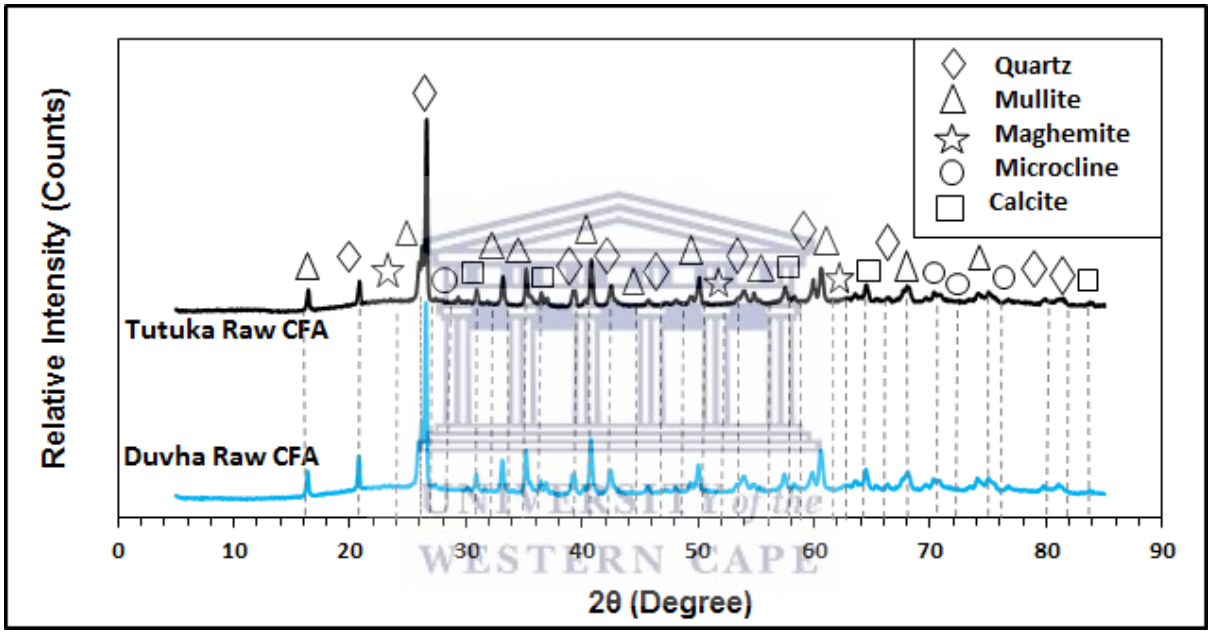

Figure 4. 5: Graph illustrating XRD patterns of Duvha and Tutuka CFA

The Tescan Integrated Mineral Analyser (TIMA) was used to provide further detail to the mineral phases present in CFA as well as their association with REEs. **Figure 4. 6** and **Figure 4. 7** depict the primary mineral phases identified in the raw whole (un-sieved) CFAs of Duvha and Tutuka power station. Overall, in Duvha CFA the mineral phases were observed to be fine and evenly distributed, while in Tutuka CFA they were rather coarser and unevenly distributed. In addition, in Duvha CFA, the primary mineral phases kaolinite and quartz were abundant (**Figure 4. 6**), whereas, in Tutuka CFA kaolinite and plagioclase were the predominant phases (**Figure 4. 7**).

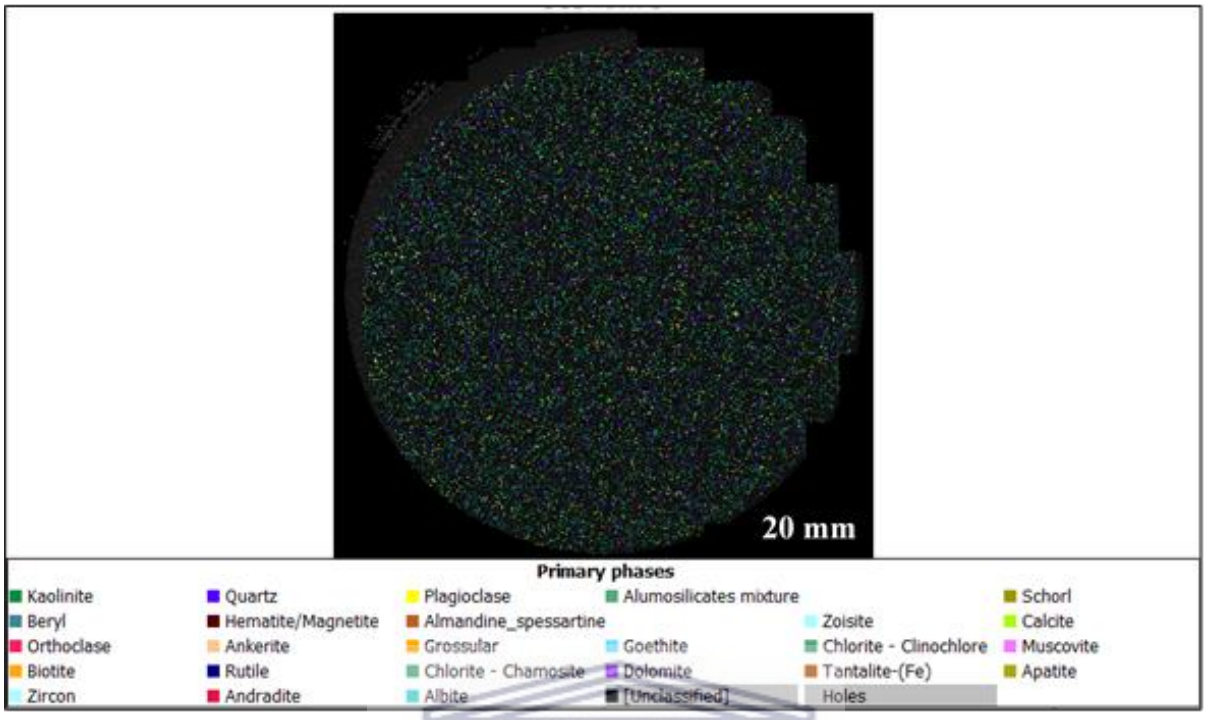

Figure 4. 6: TIMA scan illustrating the distribution of primary mineral phases in raw (un-sieved) Duvha CFA

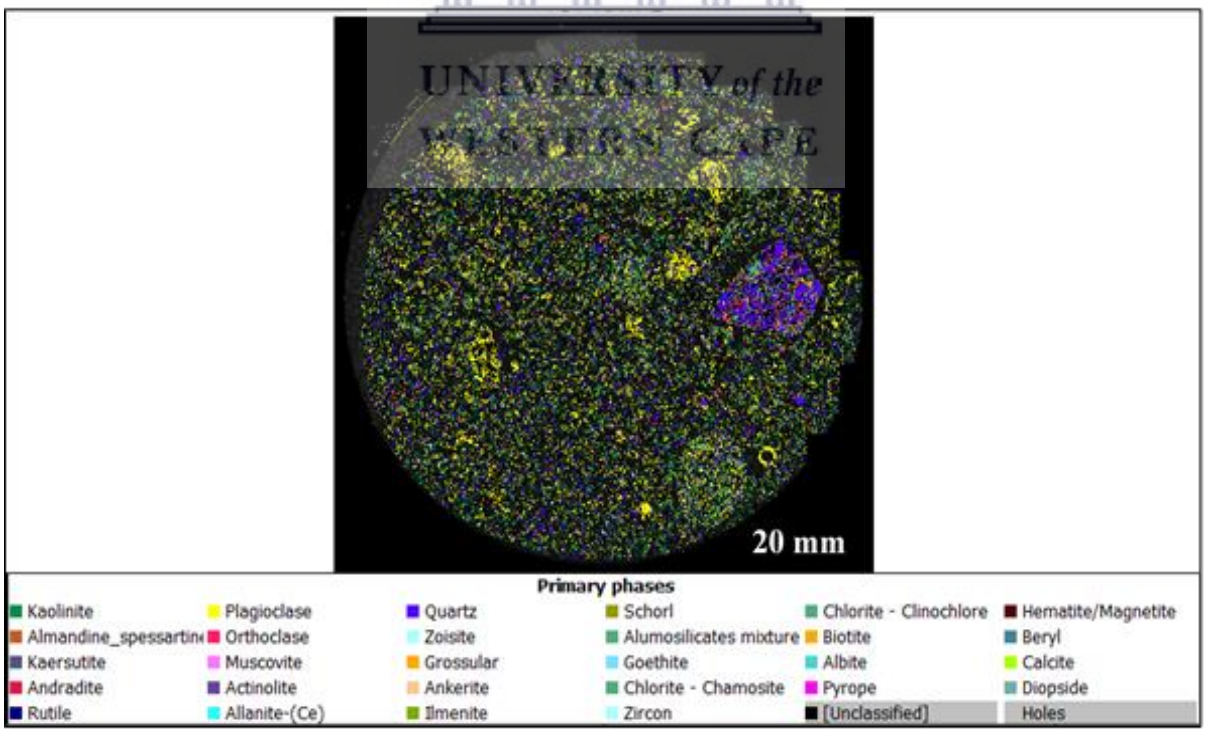

Figure 4. 7: TIMA scan illustrating the distribution of primary mineral phases in raw (un-sieved) Tutuka CFA

Furthermore, the TIMA analysis revealed that the major elements Si and Al were most abundant, while the REEs Ce, Y and La were predominant in both CFAs. In both CFAs, REEs Sc and Y were observed to be associated with the mineral zircon and calcite (**Figure 4. 8 and Figure 4. 9**). In Duvha CFA, LREEs (e.g., La, Ce, Pr and Nd) were found in rutile (**Figure 4. 10**). On the other hand, in Tutuka CFA, LREEs (e.g., La, Ce, Pr and Nd) were observed to be associated with the mineral ilmenite (**Figure 4. 11**) allanite and chlorite (**Appendix A** and **B**). MREEs (e.g., Eu and Gd) were associated with hematite (**Figure 4. 12**) and goethite, while HREEs (e.g., Ho and Lu) were mostly associated with almandine (**Figure 4. 13**).

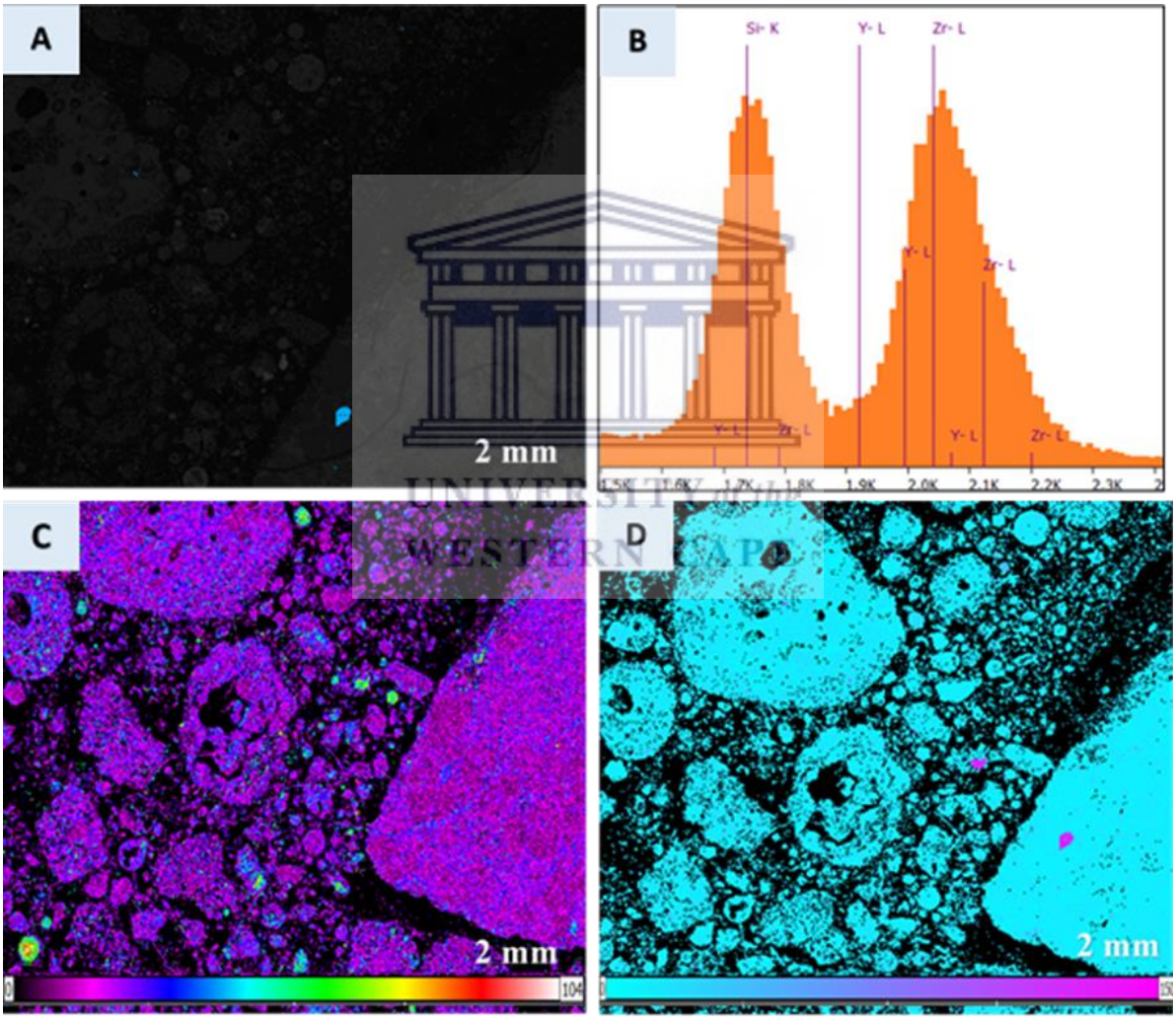

Figure 4. 8: TIMA scan illustrating the mineral zircon (**A**), EDX spectrum of zircon (**B**), elemental map of Sc (**C**) and elemental map of Y (**D**)

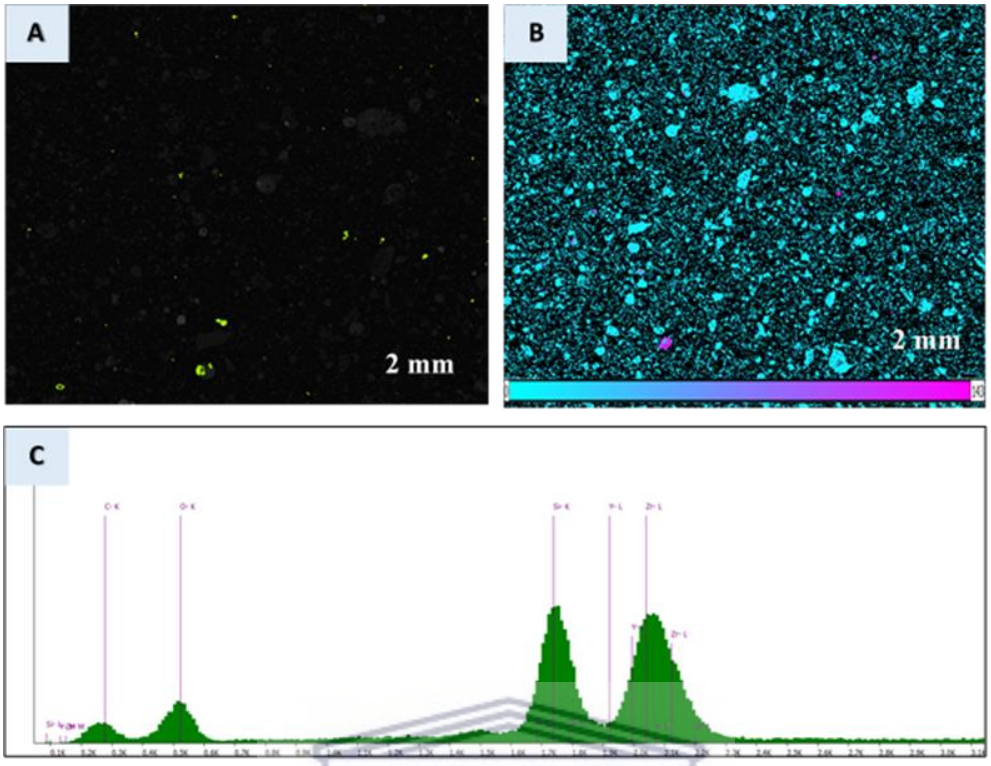

Figure 4. 9: TIMA scan illustrating the mineral calcite in Duvha CFA (**A**), elemental map of Y(**B**) and EDX spectrum of calcite (**C**)

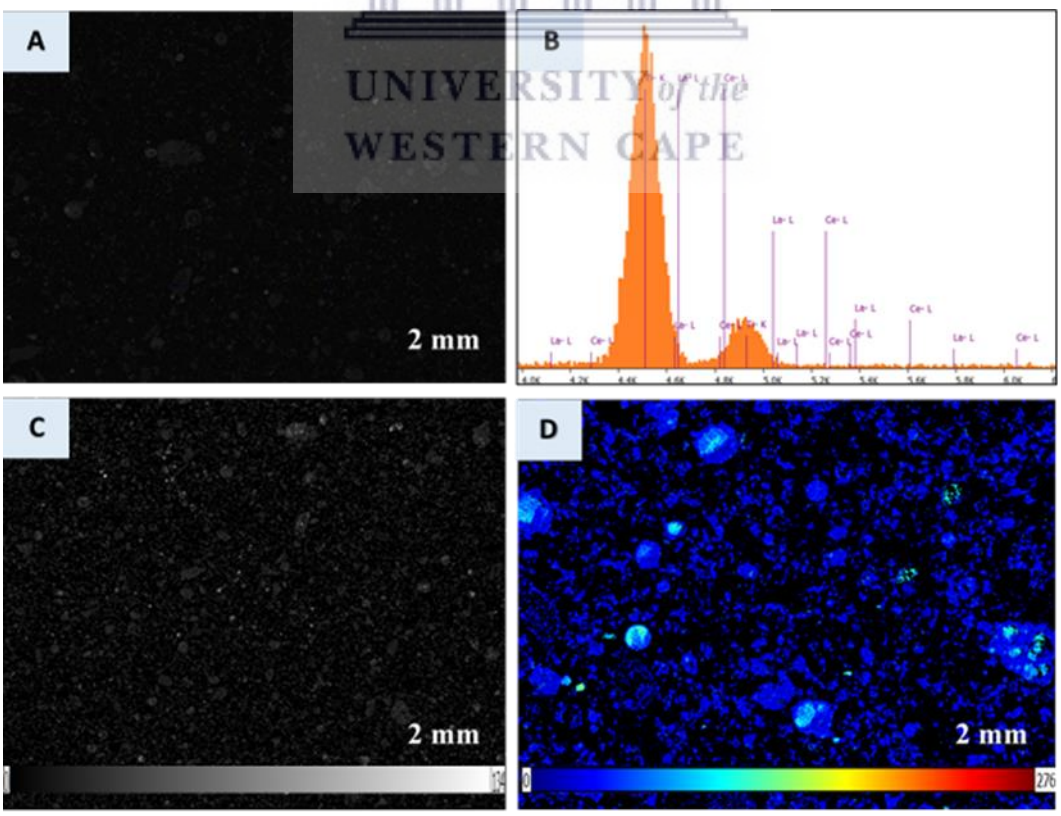

Figure 4. 10: TIMA scan illustrating the mineral rutile in Duvha CFA (**A**), EDX spectrum of rutile (**B**), elemental map of La (**C**) and elemental map of Ce (**D**)

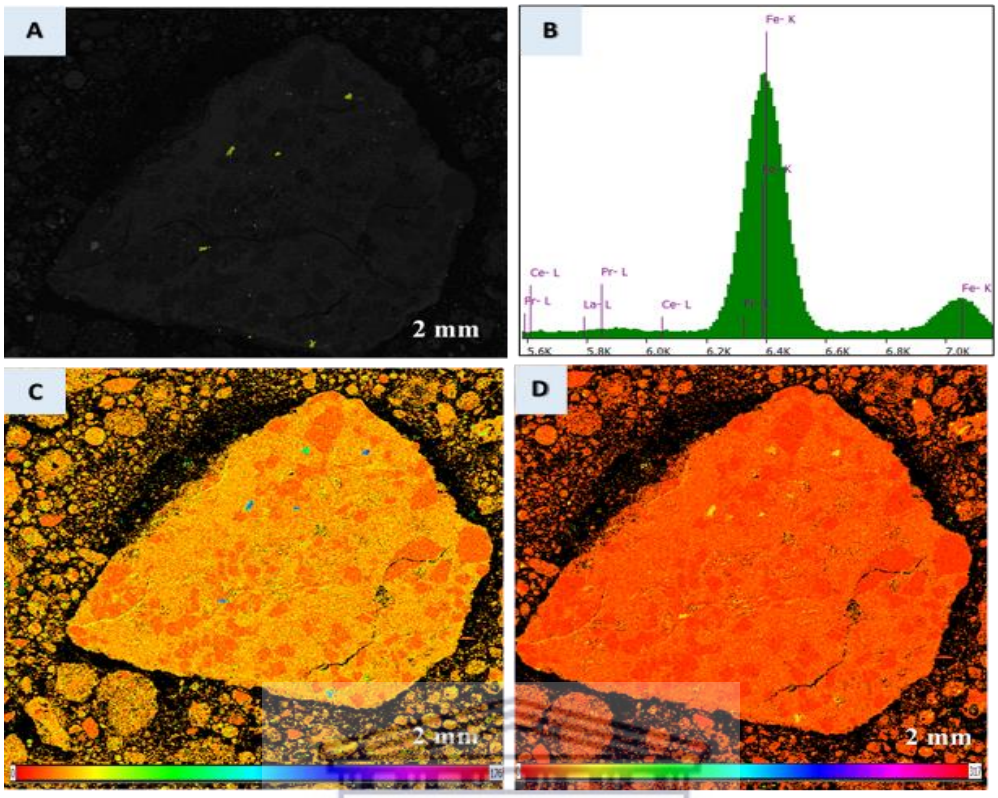

Figure 4. 11: TIMA scan illustrating the mineral ilmenite in Tutuka CFA (**A**), EDX spectrum of ilmenite (**B**), elemental map of La (**C**) and elemental map of Pr (**D**)

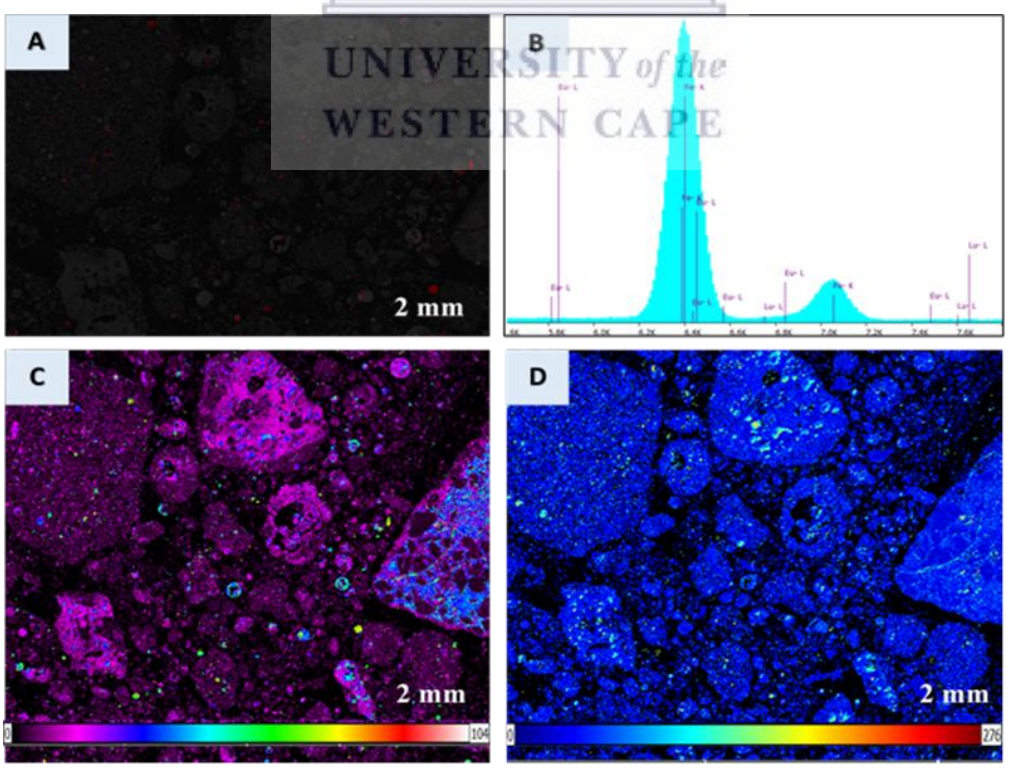

Figure 4. 12: TIMA scan illustrating the mineral hematite/magnetite in Tutuka CFA (**A**), EDX spectrum of hematite/magnetite (**B**), elemental map of Eu (**C**) and elemental map of Gd (**D**)

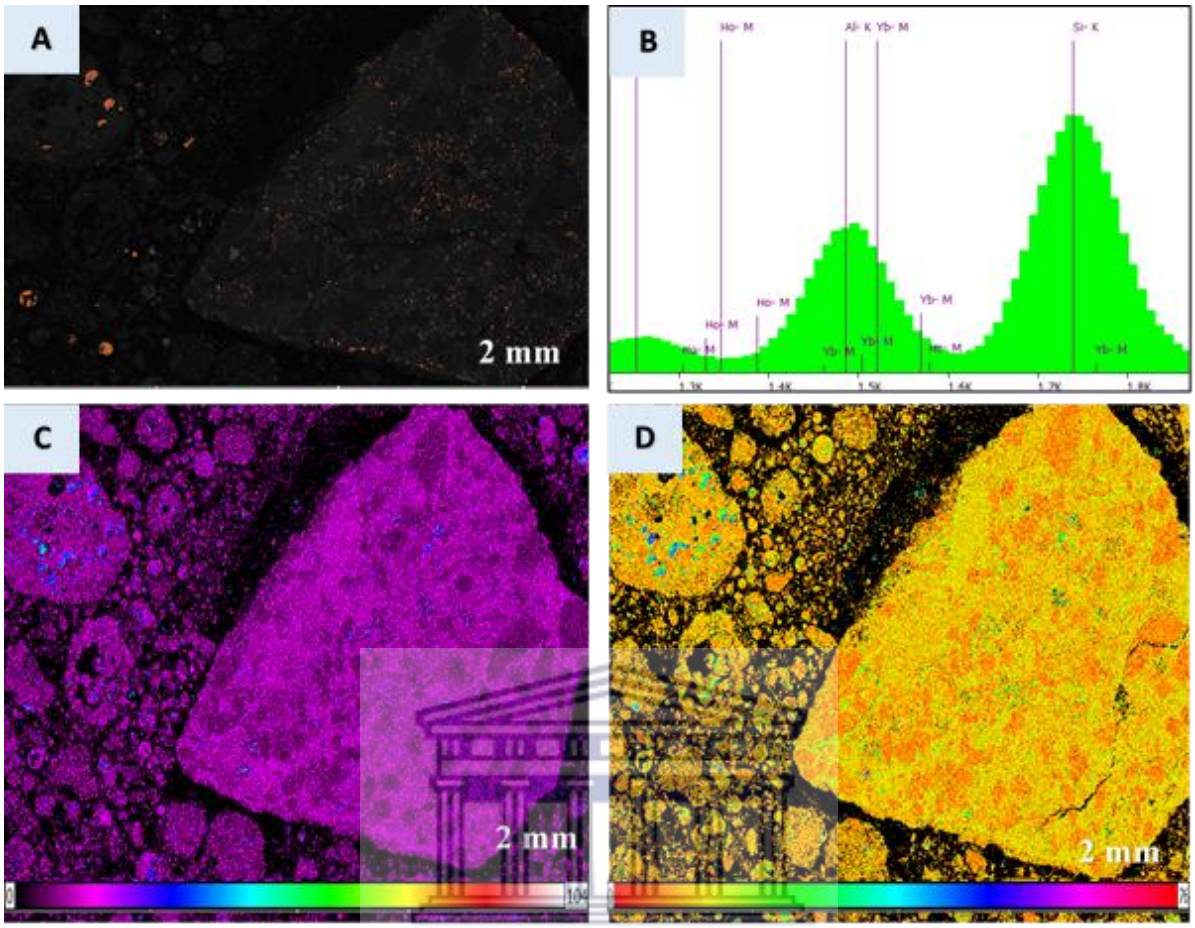

Figure 4. 13: TIMA scan illustrating the mineral almandine in Tutuka CFA (**A**), EDX spectrum of almandine(**B**), elemental map of Ho (**C**) and elemental map of Lu (**D**)

4.1.3. Elemental Composition

The elemental composition of the raw solid whole (un-sieved) samples of Duvha and Tutuka CFA were quantified using XRF for major elements and Laser Ablation Inductively Coupled Plasma - Mass Spectrometry (LA: ICP – MS) for trace elements and REEs. The major elements (as oxides in weight %) of Duvha and Tutuka CFA are shown in **Table 4. 3**. The abundance of the major elements in both CFAs were found to be in the order of $SiO2 > Al_2O_3 > Fe_2O_3 > CaO > TiO_2 > MgO > K_2O > P_2O_5 > MnO > Cr_2O_3$. In both CFAs, SiO_2 and Al_2O_3 were found to be greater than 50 % and 25 % respectively. Tutuka CFA was found to contain more Fe_2O_3 than Duvha CA with 5.18 wt% and 4.07 wt % respectively. Overall, both CFAs showed similar trends in the composition of their major elements, however, slight variations between the CFAs were observed.

Table 4. 3: Elemental composition (as oxides in weight %) of the raw samples of Duvha and Tutuka CFA determined by XRF

wt%	SiO_2	Al_2O_3	Fe_2O_3	CaO	TiO_2	MgO	K_2O	P_2O_5	Na_2O	MnO	Cr_2O_3	LOI
Duvha CFA	54.25	28.65	4.07	3.57	1.72	0.94	0.63	0.65	0.06	0.04	0.03	5.18
Tutuka CFA	52.22	27.47	5.18	4.87	1.44	1.53	0.83	0.42	0.29	0.06	0.03	5.22

Table 4. 4 shows the trace element composition of the raw whole (un-sieved) samples of Duvha and Tutuka CFA. The concentrations of trace elements such as zirconium (Zr), lead (Pb) and thorium (Th) in Duvha CFA were higher compared to Tutuka CFA, but this was different for elements like chromium (Cr) and nickel (Ni), whose concentrations were higher in Tutuka CFA. The trace element with the highest concentration in Duvha and Tutuka CFA was Zr, with concentrations of 333.76 ppm and 311.27 ppm, respectively. Cr was also found in relatively high concentrations with 166.77 ppm in Duvha CFA and 189.33 ppm in Tutuka CFA. Radionuclides thorium (Th) and uranium (U) were found in relatively significant amounts in both CFAs. Th was more abundant than U in both CFAs and Duvha CFA was most abundant in these radionuclides than Tutuka CFA (**Table 4. 4**).

Table 4. 4: Trace element composition (ppm) of raw Duvha and Tutuka CFA

Element	Cr	Co	Ni	Cu	Zn	Zr	Pb	Th	U
Duvha CFA	166.77	29.63	74.88	47.70	76.47	333.76	74.29	43.44	12.02
Tutuka CFA	189.33	24.08	71.77	44.50	63.00	311.27	53.30	36.01	11.02

Figure 4. 14 presents the REE composition of the two CFAs, in which Duvha and Tutuka CFA were found to have ΣREE content of 573.77 ppm and 546.25 ppm, respectively (**Appendix I**). The elements scandium (Sc), yttrium (Y), lanthanum (La), cerium (Ce), praseodymium (Pr), and neodymium (Nd) were most abundant in both CFAs in the order of Ce>La>Nd>Y>Sc>Pr. These elements accounted for 89.24 % in Duvha CFA and 88.72 % in Tutuka CFA of the ΣREE and fall within the light rare earth elements (LREEs) category. Lutetium (Lu) was the least abundant REE in both CFAs with measured concentrations of 0.87 ppm in Duvha CFA and 0.88 ppm in Tutuka CFA. Overall, there was minimal variation in the individual REEs between the two CFAs except for Ce, where there was a difference of 19.65 ppm.

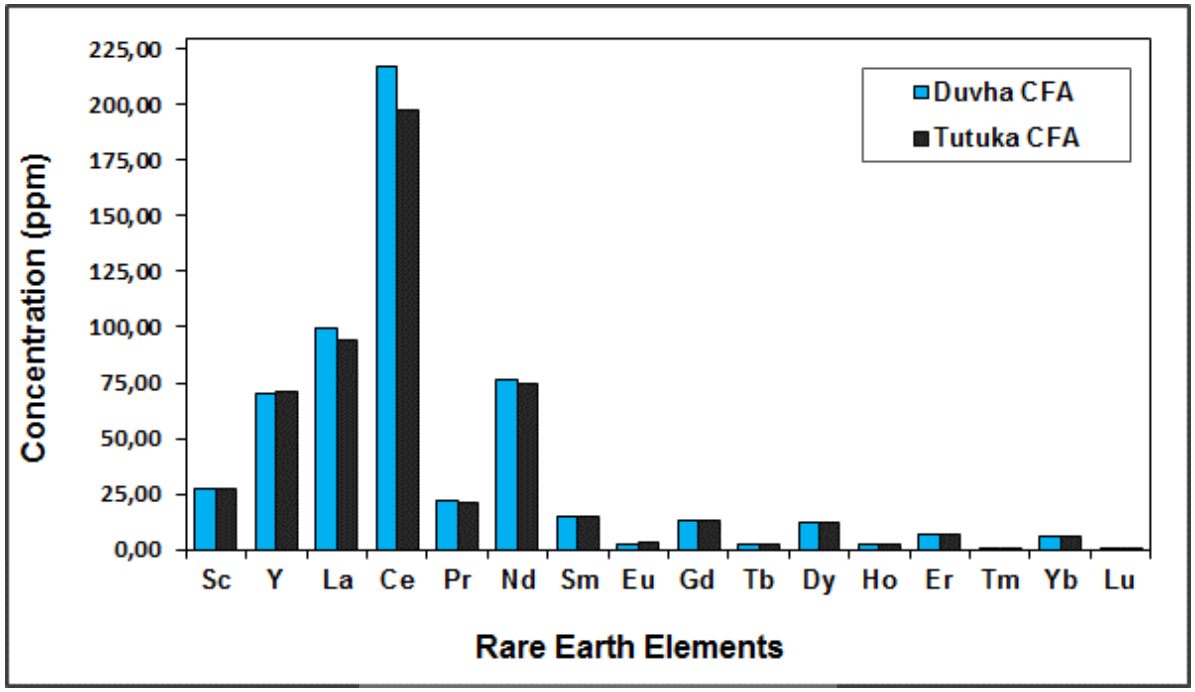

Figure 4. 14: Graph illustrating the Rare Earth Element composition (ppm) in the whole raw samples of Duvha and Tutuka CFA

4.2. Physical Separation of Coal Fly Ash

The distribution of REE as a function of the CFA physical property (particle size) was studied as an attempt to maximize the recovery of the REEs before leaching, thereby minimizing acid consumption and environmental issues of downstream purification processes. 1000 g of oven-dried Tutuka and Duvha CFA was sieved into the several particle size fractions to determine the enrichment of REEs with particle size (i.e., > 106, 106 - 75, 75 – 53, 53 - 50, 50 – 32, 32 - 25, < 25 µm). The findings are presented in the following sections below.

Figure 4. 15 illustrates the weight distribution of both CFAs in the various size fractions. Duvha and Tutuka CFA both showed a distinct peak at 50 – 32 µm, with distributions of 33.83 ± 1.39 % and 28.05 ± 1.04 %, respectively. The particle size fractions with the least weight distribution were 50 – 53 µm for Duvha CFA and < 25 µm for Tutuka with distributions of 4.86 ± 0.70 % and 1.71 ± 1.26 %, respectively (**Appendix C** and **D**). Overall, the particle size distributions of both CFAs varied significantly.

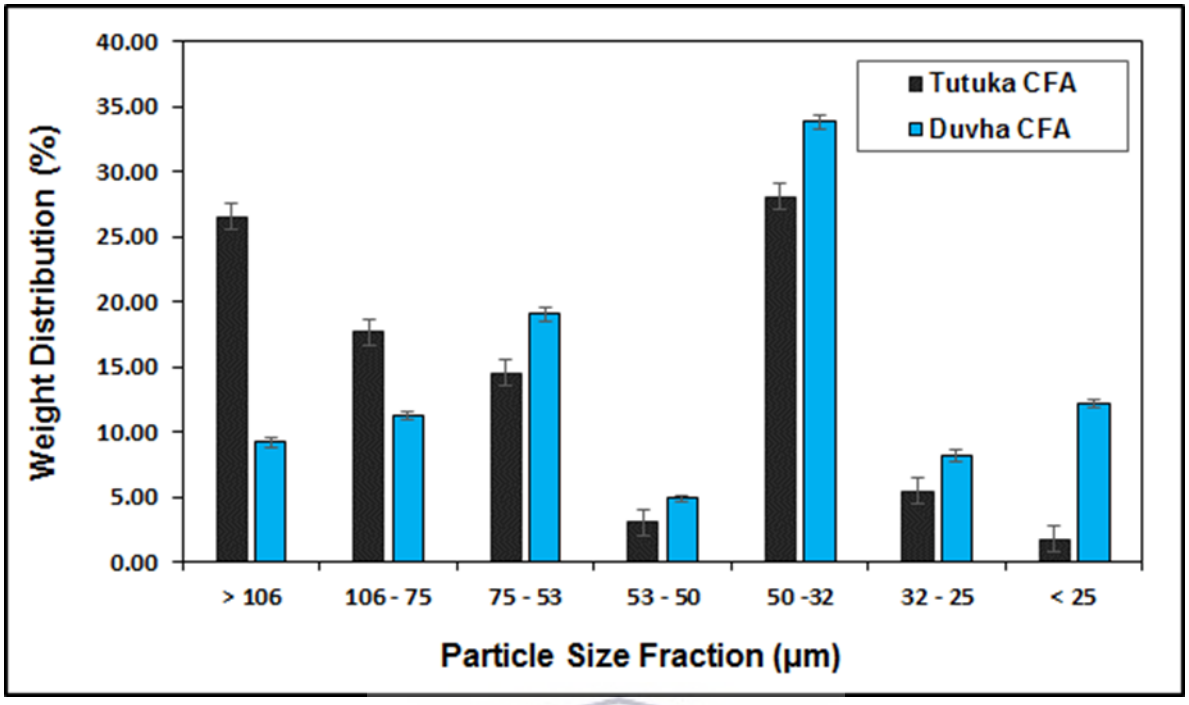

Figure 4. 15: Graph illustrating the weight distribution of Duvha and Tutuka CFA with particle Size

4.2.1. Rare Earth Element Distribution with Particle Size Fractions

The whole (un-sieved) samples of Duvha and Tutuka CFA were found to have ΣREE content of 573.77 ppm and 546.25 ppm, respectively (**Appendix I**). To better understand the distribution of REEs with the particle size of CFA, the ΣREE composition of Duvha and Tutuka CFA for each sieved particle size fraction was determined by LA-ICP-MS and the concentrations are shown in **Figure 4. 16**.

The ΣREE content varied with particle size fraction in both CFAs. Overall, there was an increase in ΣREE content with a decrease in particle size in both CFAs, showing moderate enrichment of ΣREE in the finer CFA particles as depicted in **Figure 4. 16** (**Appendix F**). In Duvha CFA, the lowest ΣREE content was found in the > 106 µm fraction (i.e., 442.43 ppm), whilst the highest was found in the < 25 µm fraction (541.07 ppm), which was lower by 32.7 ppm than that found in the whole Duvha CFA (un-sieved) (i.e., 573.77 ppm).

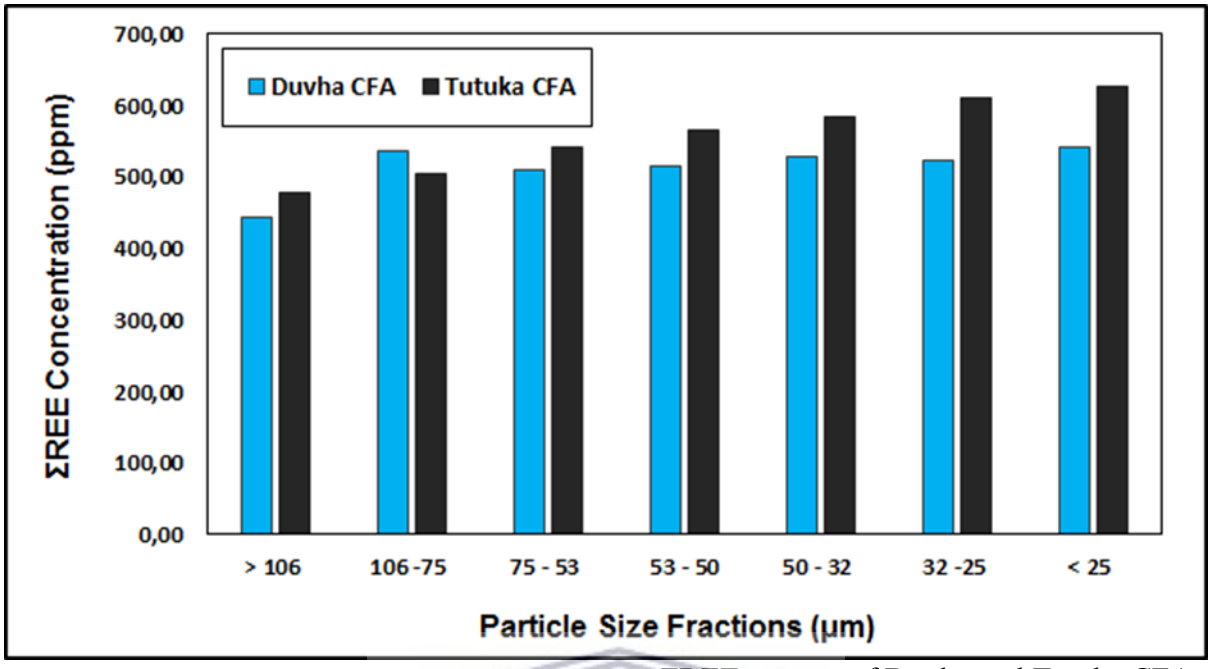

Figure 4. 16: Graph illustrating the distribution of the ΣREE content of Duvha and Tutuka CFA with particle size fraction

On the other hand, in Tutuka CFA, the finest size fraction < 25 µm was found to have the highest ΣREE content (i.e., 625.85 ppm), whilst the least was in the coarsest size fraction, > 106 µm (477.61 ppm). This was an increase of 79.6 ppm from the whole CFA (un-sieved) (i.e., 546.25 ppm). Furthermore, as the particle size fraction decreased below 75–53 µm, the ΣREE content in the CFA exceeded that in the whole Tutuka CFA.

To further understand and evaluate the relationship between REE content with particle size, regression analysis was conducted on the observations of the sieved fractions of the CFAs and the findings presented in the section below.

4.2.2. Effect of Particle Size Separation on REE Concentration

Regression analyses were conducted to evaluate the effect of the particle size of CFA on the ΣREE content in each particle size fraction. The analyses were achieved by using the Statistical Package for the Social Sciences (SPSS). The results of the analyses are presented in **Figure 4. 17A** and **B**. The findings showed a positive insignificant regression equation ($F(1,5) = 4.196$, $p = .096$, with an R^2 of 0.46, between the ΣREE content in Duvha CFA with particle size. Overall, as the particle size in Duvha CFA decreased, there was an insignificant increase (i.e., $p > .05$) in the ΣREE content (**Figure 4. 17A**). On the other hand, in Tutuka CFA, a positive

significant regression equation was found (F (1,5) = 440.738, $p < .001$, with an R^2 of 0.99, between the ΣREE content and particle size. Essentially, as the particle size in Tutuka CFA decreased, there was a significant increase (i.e., $p < .05$) in the ΣREE content (**Figure 4. 17B**).

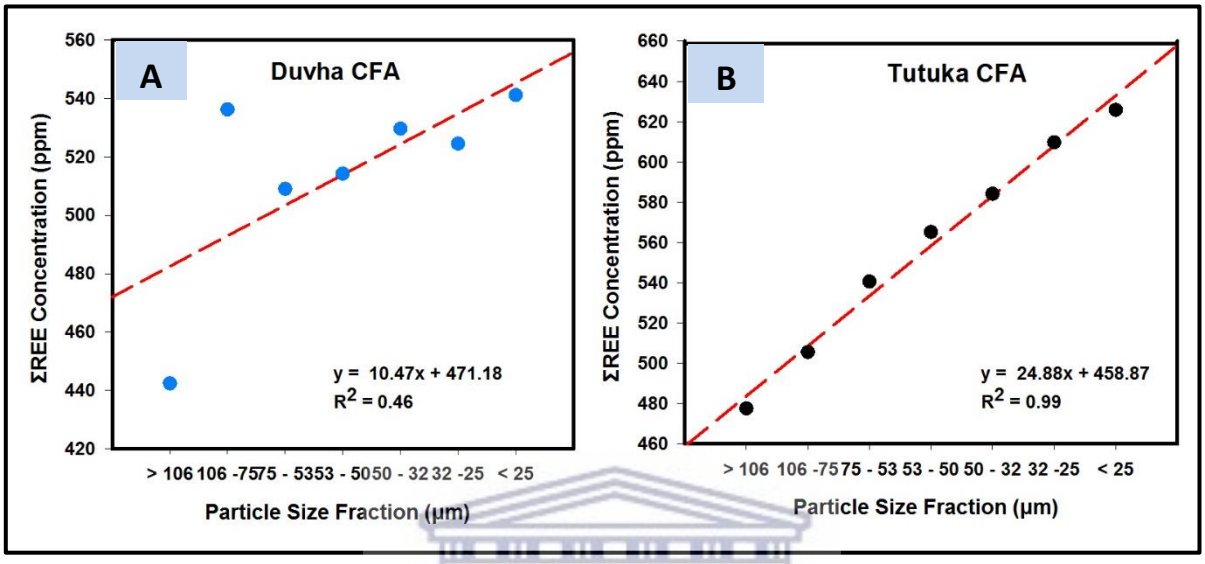

Figure 4. 17: Graph illustrating the relationship between particle size and the ΣREE content in the raw CFA (A) Duvha CFA and (B) Tutuka CFA

4.2.3. Enrichment Factors and LREE/HREE Distribution

The raw individual size fractions of both CFAs were analysed for the REE content to assess the distribution of REEs with particle size. In addition, an enrichment factor was quantified using (EF) to further quantitatively characterize REE enrichment by particle size separation, while the efficiency of the separation method was quantified using REE recovery (R_i). EF is defined by dividing the total REE concentration in the physically separated fraction by that in the whole CFA sample, as given by equation 1(Dai et al., 2010; Cao et al., 2018; Rosita et al., 2020),

$$EF = \frac{\mathrm{REE_i}}{\mathrm{REE}f} \qquad \text{(Eq 1)}$$

where REE*i* is the total REE concentration (ppm), where the subscript *i* represents the *i*th size fraction and REE*f* is the ΣREE concentration (ppm) in the feed to the sieving process.

The REE recovery (R_i) of the sieving is defined by the ratio of the amount of total REE in a given fraction to the sum amount of the total REE and weight in the feed to the sieving process, as given by equation 2 (Lin et al., 2017; Rosita et al., 2020),

$$R_i\ (\%) = \frac{REE_i W_i}{\sum_{i=1}^{n}(REE_i W_i)} \times 100 \qquad \text{(Eq 2)}$$

where REE_i is the total REE concentration (ppm) of the *i*th fraction, W*i* is the weight of the *i*th fraction (kg), and n is the total number of fractions.

The EF was observed to generally increase with a decrease in particle size in both CFAs as shown in **Table 4. 5**. In both Duvha and Tutuka CFA, the EF was lowest in the coarser size fraction (i.e., > 106 µm) and highest in the finer particle size fraction (i.e., < 25 µm) with EF of 0.77 and 0.87 in the coarser size fraction and 0.94 and 1.15 in the finer size fraction respectively.

The R_i in both CFAs was highest in the particle size fraction where most of the weight was distributed and the lowest in the particle size fraction, which had the least weight distributed in (**Table 4. 5** and **Figure 4. 15**). The lowest R_i was found in the coarsest size fraction, >106 µm with R_i of 1.15 % in Duvha CFA, while in Tutuka CFA, it was in the finest size fraction, < 25 µm with R_i of 0.28 %. Overall, Tutuka CFA was observed to have relatively higher R_i compared to Duvha CFA.

Table 4. 5: Rare Earth Element Enrichment Factors (EF) and separation efficiency (R_i %) of sieving for Duvha and Tutuka CFA

Size Fraction (µm)	Duvha CFA		Tutuka CFA	
	EF	R_i (%)	EF	Ri (%)
> 106	**0.77**	**1.15**	**0.87**	3.35
106 -75	0.93	1.70	0.93	2.36
75 - 53	0.89	2.74	0.99	2.07
53 - 50	0.90	0.71	1.03	0.46
50 - 32	0.92	**5.06**	1.07	**4.33**
32 -25	0.91	1.21	1.12	0.87
< 25	**0.94**	1.86	**1.15**	**0.28**

Often REEs are described as being light REEs (LREEs) or Heavy REEs (HREEs). Herein, LREE and HREE are defined as the groups of elements from lanthanum through gadolinium (La-Gd) and terbium through lutetium (Tb-Lu), respectively, based on the electron configuration of each REE. The LREEs and HREEs contents were observed to increase with a decrease in particle size fractions, with LREE being more abundant than HREE in both CFAs (**Appendix J and K**).

The ratio of LREE/HREE indicates the distribution of these two groups of elements within a sample. **Table 4. 6** represents the distribution of LREE/HREE with particle size. Concerning the raw whole samples (un-sieved CFAs), the ratios were higher in Duvha CFA compared to Tutuka CFA, indicating that Duvha CFA was more enriched in LREE with ratios of 14.24 and 13.34, respectively. It was found that the LREE/HREE ratios in Duvha CFA remained relatively unchanged with particle size with ratios ranging between 12.08 and 12.11, with low insignificant correlation (R = 0.43, *p* =. 332). In Tutuka CFA, there was variation in the ratios with particles size with ratios ranging between 13.77 and 14.13 with low insignificant correlation (R = 0.38, *p* = .403).

Table 4. 6: LREE/HREE ratios of Duvha and Tutuka CFA

Size Fraction (µm)	Duvha CFA	Tutuka CFA
	LREE/HREE	LREE/HREE
Whole	14.24	13.34
> 106	12.11	13.86
106 -75	12.08	14.10
75 - 53	12.09	13.77
53 - 50	12.08	**14.13**
50 - 32	12.09	13.92
32 -25	12.08	**13.70**
< 25	12.09	13.81

4.3. Alkali-Fusion Acid Leaching

4.3.1. Recovery of Major and Trace Elements

The supernatant water from the alkali-fusion acid leaching was analysed for its elemental composition (major and trace elements) to obtain a better understanding of the mobilisation of

elemental species in CFA during acid leaching. The findings presented below in **Table 4. 7**, **Table 4. 8** and **Figure 4. 18** are of the leached whole (un-sieved) samples of Duvha and Tutuka CFA and not of the sieved fractions. This is to provide a general overview of the elements that leach from CFA when REE recovery methods such as the one used in this study are applied.

Table 4. 7: Major element composition (mg/ℓ) of the whole Duvha and Tutuka CFA leachates (n =2)

Element	Duvha CFA Leachate (ppm)	Tutuka CFA Leachate (ppm)
Al	5229.00 ± 1.41	6020.00 ± 1.41
Ca	1011.15 ± 16.76	1857.00 ± 32.53
K	182.10 ± 7.92	293.30 ± 3.96
Mg	191.15 ± 3.89	392.75 ± 3.18
Na	22384.50 ± 7.78	25044.50 ± 64.35
P	84.92 ± 0.94	76.66 ± 0.41
Si	1432.25 ± 5.30	786.25 ± 13.36

The abundance of the major elements in the Duvha CFA leachate was in the order of sodium (Na) > aluminium (Al) > silicon (Si) > calcium (Ca) > magnesium (Mg) > potassium (K) > phosphorus (P), while in Tutuka CFA leachate they were in the order of Na > Al > Ca > Si > Mg > K > P. However, for all major elements, the amounts recovered were higher in the Tutuka CFA leachate compared to the Duvha CFA leachate. Na was the most leached element in Duvha and Tutuka CFA leachates, with concentrations of 22384.50 ± 7.78 ppm and 25044.50 ± 64.35 ppm, respectively as shown in **Table 4. 7**.

During the leaching of CFA, there are several heavy trace elements (i.e., iron (Fe), chromium (Cr), cobalt (Co), nickel (Ni), arsenic (As), zinc (Zn), etc.) that are of concern as they have diverse environmental impacts. The concentration of these elements in the leachates was determined and the findings are shown in **Table 4. 8** below.

Table 4. 8: Trace element composition (ppm) of the whole Duvha and Tutuka CFA leachates (n = 2)

Element	Duvha CFA Leachate (ppm)	Tutuka CFA Leachate (ppm)
Cr	5.04 ± 0.71	8.86 ± 1.63
Fe	778.92 ± 7.08	1307.52 ± 24.77
Co	6.00 ± 5.66	1.55 ± 0.77
Ni	3.35 ± 3.31	4.51 ± 2.10
Cu	2.49 ± 2.11	5.68 ± 3.43
Zn	5.66 ± 3.35	4.05 ± 1.07
As	4.56 ± 4.95	1.77 ± 1.41
Sr	44.30 ± 3.81	41.48 ± 7.47
Cd	0.72 ± 0.99	0.11 ± 0.13
Ba	25.95 ± 8.16	11.01 ± 2.83
Pb	5.45 ± 2.83	3.99 ± 2.12
Th	1.37 ± 0.42	1.70 ± 0.27
U	0.69 ± 0.35	0.36 ± 0.14

In both Duvha and Tutuka CFA leachates, Fe was found to be the most abundant trace element with concentrations of 778.92 ± 7.08 ppm and 1307.52 ± 24.77 ppm, respectively. Cr was higher in the Tutuka CFA leachate compared to Duvha CFA leachate with concentrations of 8.86 ± 1.63 and 5.04 ± 0.71 ppm, respectively. In addition, As was found to be relatively higher in Duvha CFA leachate compared to Tutuka CFA leachates, with content of 4.56 ± 4.95 and 1.77 ± 1.41 ppm respectively. Relatively high concentrations of Ba and Sr were recorded in the leachates of both CFAs from the two, Ba content in Duvha CFA leachate (i.e., 25.95 ± 8.16 ppm) was twice that in Tutuka CFA leachate (i.e.,11.01 ± 2.83 ppm).

Radionuclides Th and U are two elements that are often observed to be co-recovered during the recovery of REEs (Taggart, 2015; Tang et al., 2019). These radionuclides were present in both leachates in small amounts and there was minimal variation in the recovery of these elements. Th content was higher than that of U in both CFAs as shown in **Table 4. 8**. In Duvha and Tutuka CFA, Th was measured to be 1.37 ± 0.42 ppm and 1.70 ± 0.27 ppm respectively, while U was 0.69 ± 0.35 ppm and 0.36 ± 0.14 ppm respectively.

4.3.2. Recovery of Rare Earth Elements

The REE content recovered in the whole (un-sieved) samples of Duvha and Tutuka CFA was analysed and the findings are presented in **Figure 4. 18** below. The ΣREE recovered in the leachates of Duvha and Tutuka CFA s were 15.67 ppm and 17.20 ppm, respectively (**Appendix L** and **M**). In order of abundance the following REEs were well recovered in comparison to the rest, Ce > La > Nd > Y in the Duvha CFA leachate, while in Tutuka CFA, it was Ce > Y > La > Nd. In Duvha and Tutuka CFA leachates, Ce the most abundant REE was recorded to have content of 4.45 ppm and 4.32 ppm respectively (**Appendix L** and **M**).

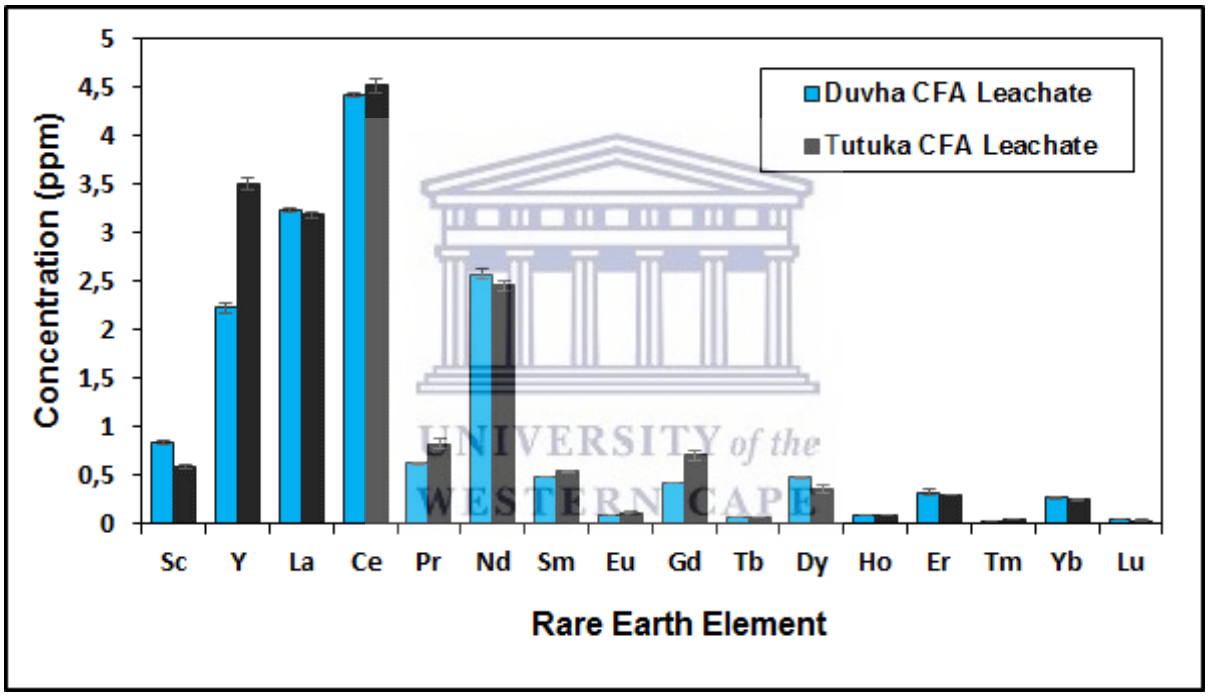

Figure 4. 18: REE composition (ppm) of the whole sample leachates of Duvha and Tutuka CFA

On the other hand, the leachates of Duvha and Tutuka CFA were measured to have equal contents of Lu and Tm. In addition, Tm and Lu had the lowest content measured in both CFAs with concentrations of 0.04 ppm and 0.03 ppm, respectively (**Appendix L** and **M**). Minimal variation between the LREEs and HREEs of the two CFA leachates was observed. Herein, LREEs and HREEs are defined as the groups of elements from lanthanum through gadolinium (La-Gd) and terbium through lutetium (Tb-Lu), respectively. The leachate of Duvha CFA had LREE and HREE content of 11.66 ppm and 1.14 ppm respectively, while the leachate of Tutuka CFA had LREE and HREE content of 11.98 ppm and 1.23 ppm respectively.

4.3.3. The Effect of Particle Size on the Recovery of Rare Earth Elements

The relationship between REEs recovered from alkali-fusion acid leaching with particle size was investigated. This was done to assess whether the relationship between particle size and REE content from the physical separation existed in the recovery. The whole (un-sieved) leached samples of Duvha and Tutuka CFA had ΣREE content recovered of 15.66 ppm and 17.12 ppm respectively (**Figure 4. 18**) (**Appendix L** and **M**).

Figure 4. 19 presents the ΣREE recovered in each particle size fraction of both CFAs. The ΣREE content varied with particle size in both CFAs. Overall, there was an increase in ΣREE content recovered with a decrease in particle size, displaying moderate enrichment of ΣREE in the finer CFA particles as depicted in **Figure 4. 11** (**Appendix L** and **M**). In both CFA leachates, the finest (i.e., < 25 µm) and coarsest (i.e., > 106 µm) particle size fractions had the highest and lowest ΣREE content recovered respectively. In the Duvha CFA leachate, the lowest and highest ΣREE recovered was 12.45 ppm and 20.73 ppm respectively, whilst in the leachate of Tutuka CFA, it was 14.96 ppm and 22.77 ppm respectively.

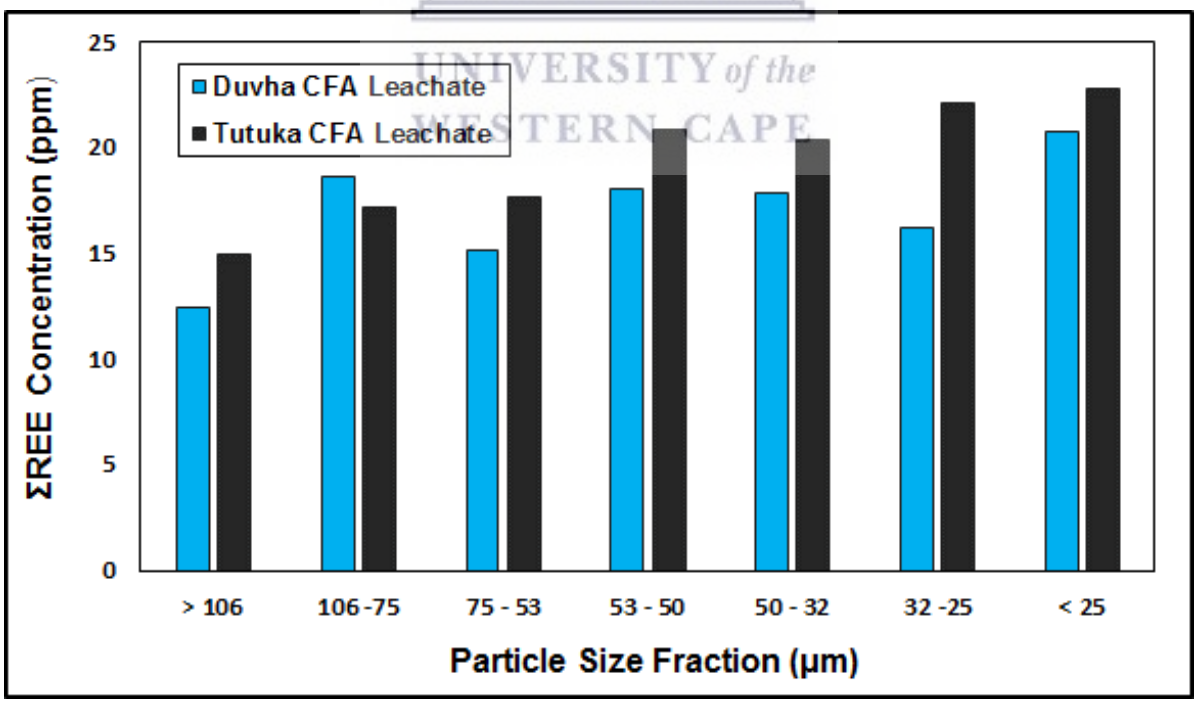

Figure 4. 19: Graph illustrating the ΣREE recovered during alkali-fusion acid leaching of Duvha and Tutuka CFA

To further understand and evaluate the relationship between REE content recovered from alkali-fusion acid leaching with particle size, regression analyses were conducted on the observations of the leached sieved fractions of the CFAs and the findings presented in **Figure 4. 20**. The findings showed a positive insignificant regression equation (F (1,5) = 3.835, p = .108, with an R^2 of 0.43, between the ΣREE content recovered in the leachates of Duvha CFA with particle size. Overall, as the particle size of Duvha CFA decreased, there was an insignificant increase (i.e., $p > .05$) in the ΣREE recovered in the leachate as depicted in **Figure 4. 20A**. On the other hand, a positive significant regression equation was found (F (1,5) = 37.974, p = .002, with an R^2 of 0.88, between the ΣREE content recovered in the leachates of Tutuka CFA with the particle size. Essentially, as the particle size of Tutuka CFA decreased, there was a significant increase (i.e., $p < .05$) in the ΣREE recovered in the leachate as shown in **Figure 4. 20B**.

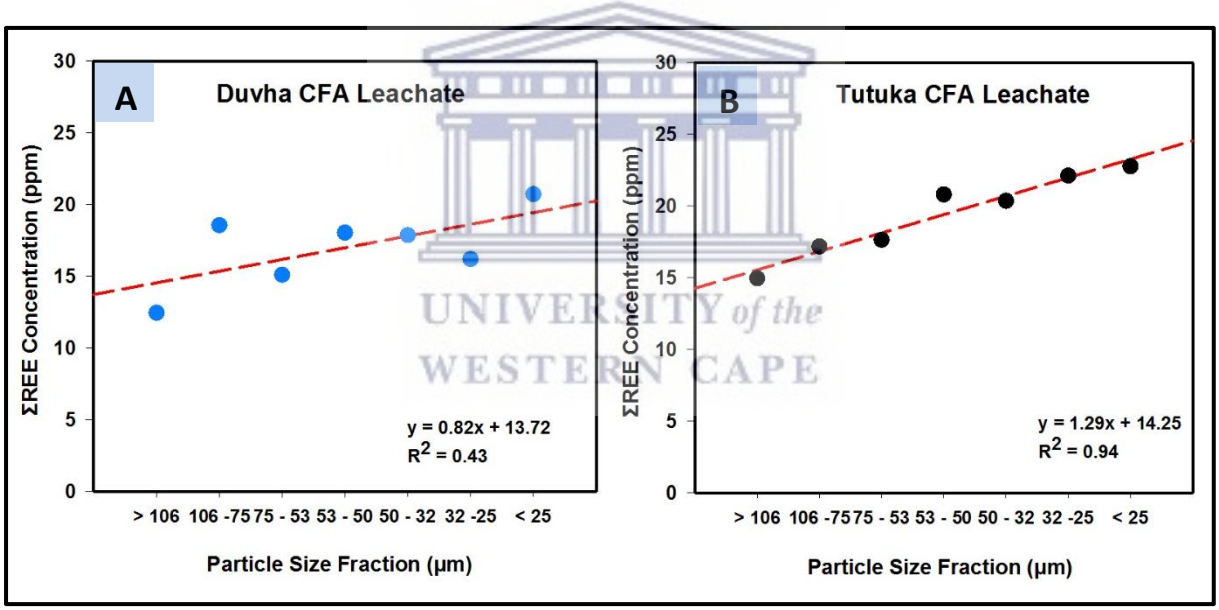

Figure 4. 20: Graph illustrating the relationship between particle size and the REE content in the leachates (A = Duvha CFA and B = Tutuka CFA)

4.3.4. Recovery Efficiencies of Rare Earth Elements

During the alkali-fusion acid leaching, the acid leaching process of the experiments was performed in a sealed environment (reflux system) to prevent the volatilization of acids. Furthermore, to better understand the recovery of REEs from CFA and the feasibility of applying the alkali-fusion acid leaching technique in South African CFA, the recovery leaching

efficiency was determined. The leaching efficiency (α) was calculated by the following equation 3 (Cao et al., 2018; Pan et al., 2019; Pan et al., 2020; Wen et al., 2020),

$$\alpha = \frac{VC_2}{MC_1} \times 100 \qquad \text{(Eq 3)}$$

where V is the volume of leachate (mℓ); M is the mass of the CFA sample (g); C_1 is the element content in the CFA sample (ppm) and C_2 is the element concentration in leachate (ppm).

The leaching efficiencies (α) of the whole and sieved fractions of Duvha and Tutuka CFA are presented in **Table 4. 9** below. Overall, in both CFAs α increased with a decrease in particle size, showing relatively greater leachability of ΣREE in the finer fractions. However, the trend was more defined in Tutuka CFA compared to Duvha CFA. It is important to note that total α included the elements Sc and Y, whilst the LREEs and HREEs represented the elements from La to Gd and Tb to Lu, respectively. In both the particle size fraction leachates of Duvha and Tutuka CFA, the lowest α for ΣREE was observed in the coarsest particle size fraction (i.e., > 106 µm).

The lowest α for ΣREE was determined to be 28.13 % and 31.32 % for Duvha and Tutuka CFA leachates respectively. In Duvha CFA, this was relatively greater than the α determined in the whole (un-sieved) leachate with α of 27.30 %, whilst in Tutuka CFA there was minimal variation (i.e., 39.42 % and 31.32 %). The finest particle size fraction, < 25 µm in Duvha CFA was found to have the highest α for ΣREE (i.e., 38.31 %). Contrarily, in Tutuka CFA, it was found to be in the 53 - 50 µm particle size fraction with α for ΣREE of 36.82 %. However, it must be noted that there was minimal variation between the determined α in the 53 - 50 µm (i.e., 36.82 %) and < 25 µm (i.e., 36.39 %) particle size fraction in the leachates of Tutuka CFA. The highest α in the particle size fractions in both CFA leachates were relatively greater than that determined in the whole (un-sieved) CFAs.

Table 4. 9: REE recovery efficiencies (%) of the alkali-fusion acid leaching of Duvha and Tutuka CFA

	Duvha CFA Leachate			Tutuka CFA Leachate		
	LREE (%)	HREE (%)	Total (%)	LREE (%)	HREE (%)	Total (%)
Whole	26.21	36.46	27.30	28.76	39.45	31.49
> 106 µm	27.95	30.33	28.13	29.18	39.49	31.32
106 -75 µm	34.02	38.69	34.62	30.89	44.47	33.97
75 - 53 µm	30.05	35.18	29.68	29.91	41.87	32.63
53 - 50 µm	35.40	35.89	35.09	34.62	44.94	36.82
50 – 32 µm	33.97	41.79	33.75	32.50	45.59	34.86
32 -25 µm	29.71	39.77	30.90	33.29	47.44	36.28
< 25 µm	39.29	48.38	38.31	33.75	47.16	36.39

Generally, the α of HREEs was higher in both CFAs compared to that of LREEs, with the highest α observed in the finest size fraction (<25 µm) in Duvha CFA with α of 48.38 % and the 32 -25 µm size fraction in Tutuka CFA with α of 47.44 %. In Duvha CFA, the α of HREEs in whole (un-sieved) leachate was greater than that in the > 106 µm size fraction, with α of 36.46 % and 30.33 % respectively, whereas in Tutuka CFA the α of these fractions were relatively the same (i.e., 39.45 % and 39.49 %). Overall, the range of α observed in Duvha and Tutuka CFA leachates of the whole (un-sieved) and various particle size fractions were low.

4.4. Solid Residue Characterization

4.4.1. Morphology

In an attempt to obtain a better understanding of the changes that occur to CFA during alkali-fusion acid leaching, the leached solid residues of both CFAs were characterized in terms of their morphological structure, mineral and elemental compositions. It is important to note that the characterization of the leached solid residues was conducted on the whole (un-sieved) samples and not the sieved size fractions. The same analytical techniques that were used to characterize the raw CFAs were used to characterize the leached solid residues. The findings are presented below.

The SEM micrographs of the leached solid residues of Duvha and Tutuka CFA are presented in **Figure 4. 21** and **Figure 4. 22**. The particles of these leached solid residues appeared to be

less agglomerated and moderately disintegrated compared to the raw CFAs. In addition, they were irregular and appeared to have been crusted, etched and corroded. Despite the irregular shape of the leached solid residues, some particles exhibited smooth surfaces (**Figure 4. 22B)**. In **Figure 4. 21**, the particles of the leached solid residue of Duvha CFA appeared shattered, with fewer spheres and agglomeration. Contrarily, in **Figure 4. 22**, in the leached Tutuka CFA solid residue the particles did not appear shattered but rather disintegrated (eroded) in irregular but agglomerated form.

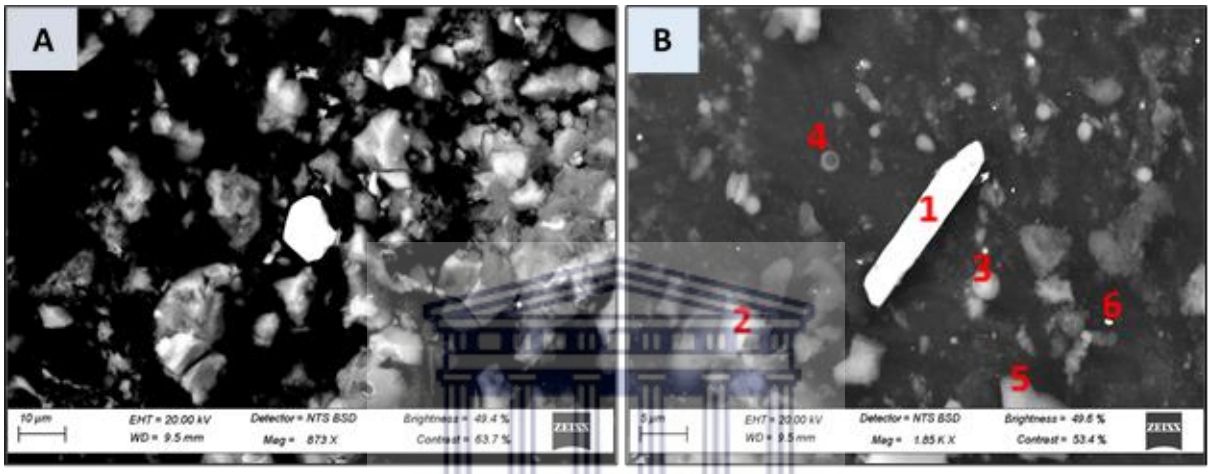

Figure 4. 21: SEM-EDS micrographs of Duvha CFA (A) overall view (B) particle spots for EDS analysis (Magnification: (A) = 873 X, (B) = 1.85 KX)

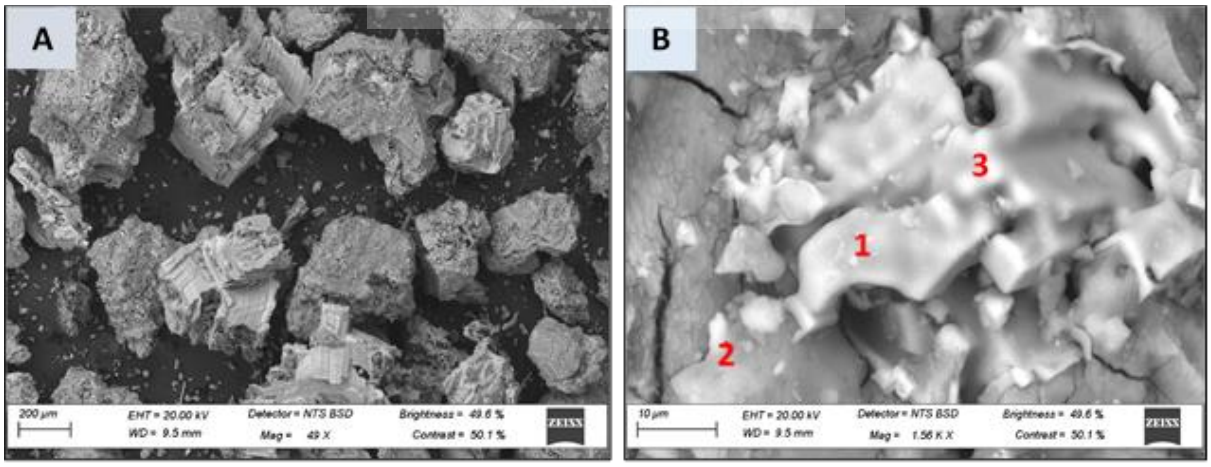

Figure 4. 22: SEM-EDS micrographs of Tutuka CFA (A) overall view (B) particle spots for EDS analysis (Magnification: (A) = 49 X, (B) = 1.56 KX)

Table 4. 10 and **Table 4. 11** presents the EDS analyses of the SEM micrographs of the leached solid residues of Duvha and Tutuka CFA. In both leached solid residues of Duvha and Tutuka

CFA, Cl was the most abundant major element with recorded contents of 15.35 wt% and 42.04 wt% respectively. An association between Na and Cl was observed, where Na was found in high contents, Cl was also relatively high. The leached solid residue of Tutuka CFA was more abundant in Na and Cl compared to the leached solid residue of Duvha CFA. Al and Si were detected to be relatively abundant in both CFAs, however, was greater in the leached solid residue of Duvha CFA, with abundances of 7.77 wt% and 13.40 wt% respectively.

Table 4. 10: Descriptive statistics of SEM-EDS spot analysis (weight %, n = 6) of Duvha CFA acid leached residue (**Figure 4. 21B**)

	Na	Mg	Al	Si	P	S	Cl	K	Ca	Ti	Fe	Cu	Au
Max	34.14	2.66	19.82	26.98	0.28	1.66	49.07	0.99	3.06	1.23	4.67	94.41	60.72
Min	0.00	0.00	2.40	2.47	0.00	0.00	1.43	0.00	0.47	0.00	0.00	0.00	0.00
Mean	6.56	0.63	7.77	13.40	0.09	0.41	15.35	0.23	1.97	0.51	1.91	15.74	10.12
STDEV	13.55	1.03	6.32	10.07	0.10	0.63	17.54	0.39	1.19	0.59	1.89	38.54	24.79

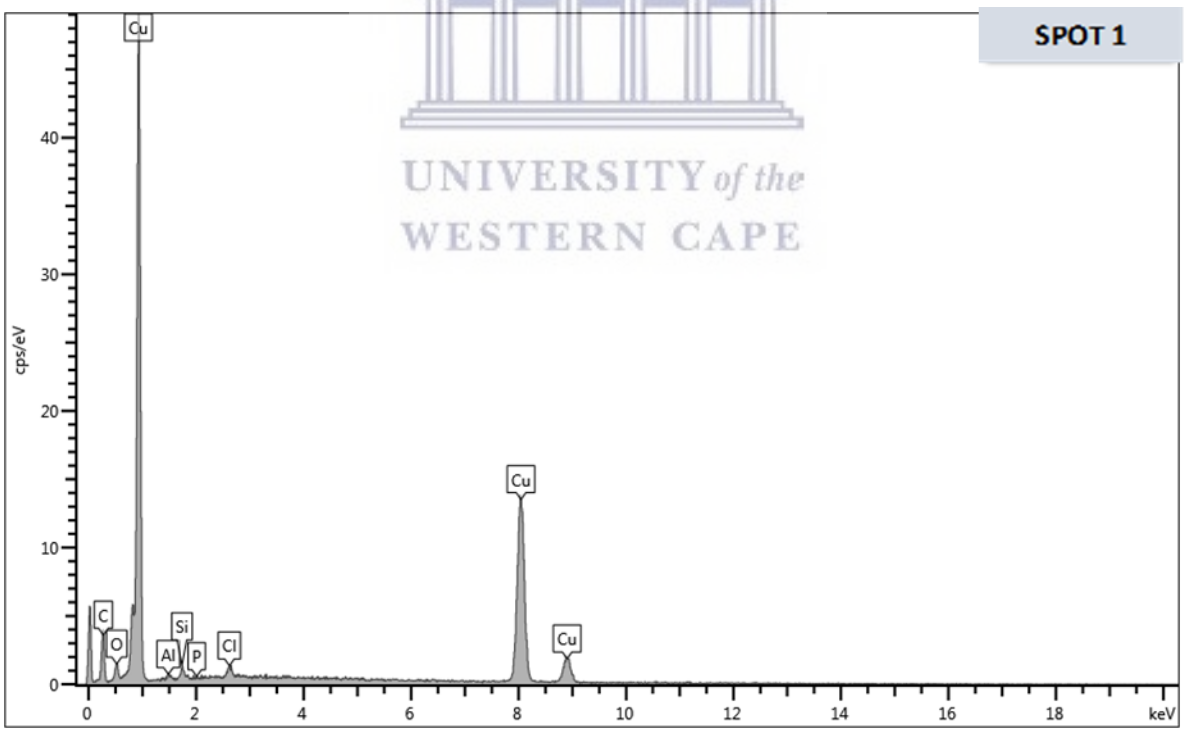

Figure 4. 23: Graph illustrating EDS Spectrum of Spot 1 of Duvha CFA micrograph (**Figure 4. 21B**)

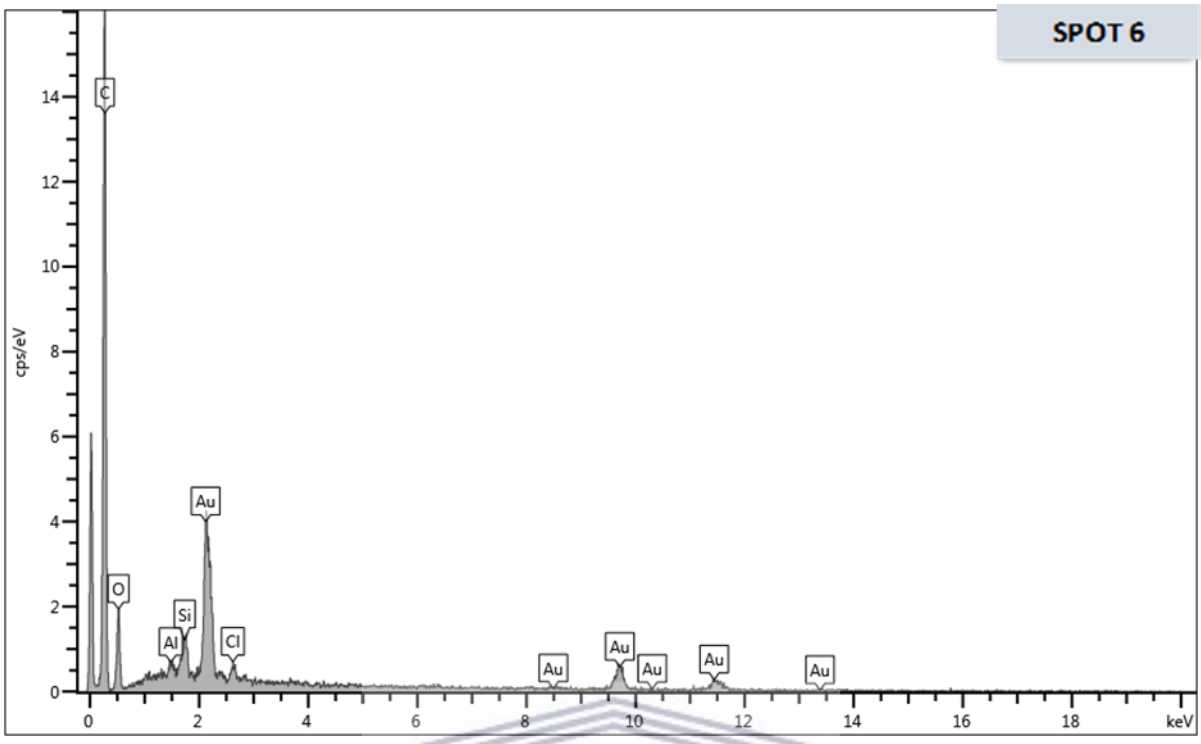

Figure 4. 24: Graph illustrating EDS Spectrum of Spot 6 of Duvha CFA micrograph (**Figure 4. 21B**)

In the leached solid residues of Duvha CFA, the trace elements copper (Cu) and gold (Au) were present in high amounts, with recorded abundances of 15.74 wt% in spot B1 and 10.12 wt% in spot B6 (**Figure 4. 23** and **Figure 4. 24**). Fe was found to be present in relatively low quantities in both CFAs, with measured abundances of 1.91 wt% in the leached solid residue of Duvha CFA, while in the leached solid residue of Tutuka CFA it was 1.08 wt%. REEs were not detected in the leached solid residue of Duvha CFA with the SEM-EDS technique, however, were observed in the leached solid residue of Tutuka CFA. The REE Ce was detected in the leached solid residue of Tutuka CFA with an abundance of 0.23 wt % (**Table 4. 11** and **Figure 4. 25**).

Table 4. 11: Descriptive statistics of SEM-EDS spot analysis (weight %, n = 3) of Tutuka CFA acid leached residue (**Figure 4. 22B**)

	Na	Mg	Al	Si	P	S	Cl	K	Ca	Ti	Fe	Ba	Ce
Max	39.74	0.51	19.30	16.89	0.15	0.08	55.89	0.36	1.42	0.31	2.94	0.21	0.41
Min	0.92	0.00	0.50	0.44	0.00	0.03	15.79	0.00	0.17	0.01	0.13	0.00	0.09
Mean	26.76	0.17	6.86	6.05	0.05	0.05	42.04	0.15	0.61	0.12	1.08	0.07	0.23
STDEV	22.38	0.29	10.77	9.38	0.08	0.03	22.75	0.19	0.70	0.17	1.61	0.12	0.16

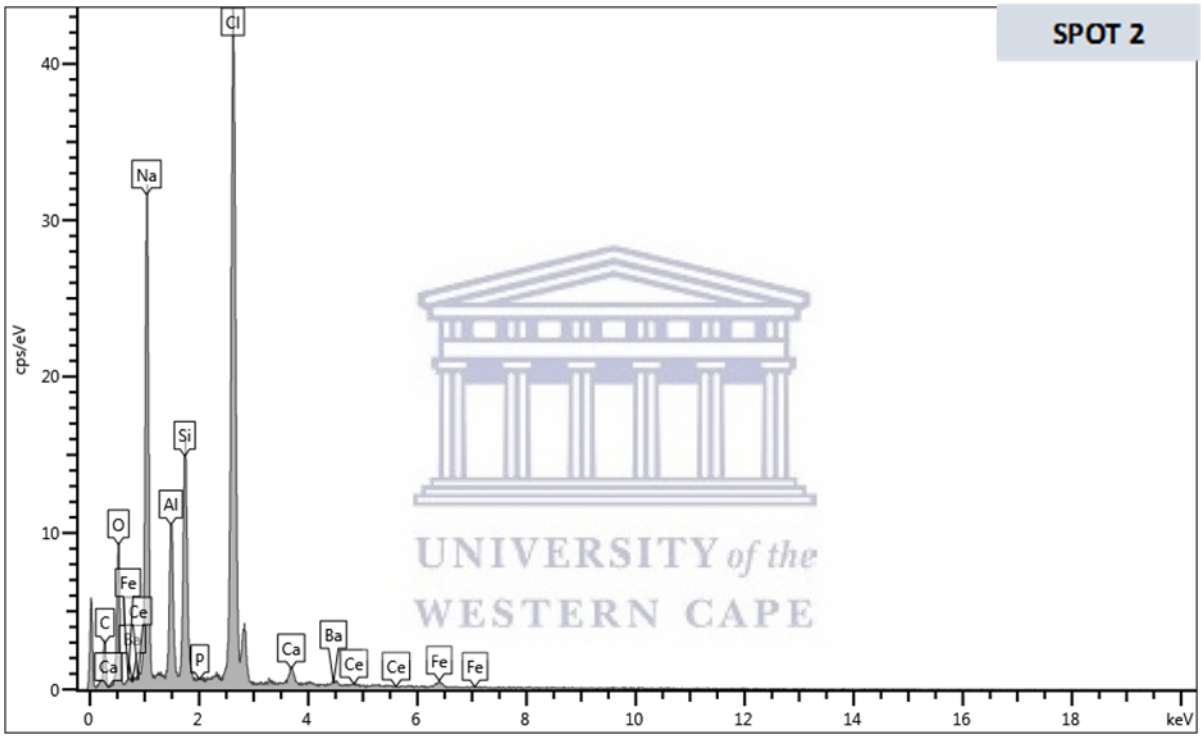

Figure 4. 25: Graph illustrating EDS Spectrum of Spot 2 of Tutuka CFA micrograph (**Figure 4. 22B**)

4.4.2. Mineral Composition

The leached residues of Duvha and Tutuka CFA displayed quite similar XRD spectra as depicted in **Figure 4. 26**. Three minerals were identified in both residues and order of abundance were as follows: halite (NaCl), chloraluminite ($AlCl_3 \cdot 6H_2O$) and quartz (SiO_2). The most significant difference between the spectra of these residues is the peak of halite at 32 °, the peak is higher for the leached solid residue Tutuka CFA.

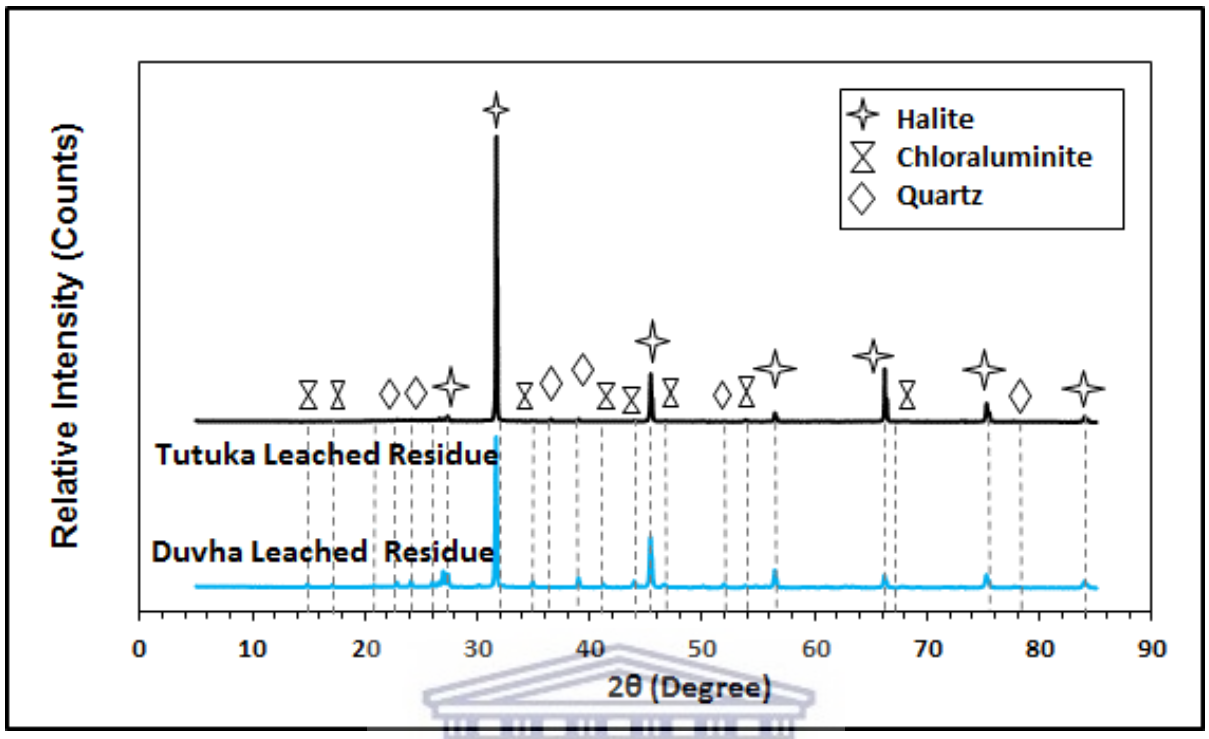

Figure 4. 26: Graph illustrating XRD patterns of the leached solid residues of Duvha and Tutuka CFA

4.4.3. Elemental Composition

Table 4. 12 presents the composition of the major components as oxides in weight % that remained in the solid residue after acid leaching of the whole samples of Duvha and Tutuka CFA. There was variation in the elemental composition between the two residues. The findings revealed that SiO_2 and Al_2O_3 remained the dominant oxides in both residues, with abundances of 21.47 wt % and 8.68 wt% respectively in the leached solid residue of Duvha CFA, while in the leached solid residue of Tutuka CFA it was 29.94 wt% and 8.62 wt% respectively. Fe_2O_3 was recorded to be present in relatively low quantities in the leached solid residues of Duvha and Tutuka CFA with abundances of 1.24 wt% and 1.85 wt%. MgO and MnO were below the detection limit in both leached solid residues.

Table 4. 12: Table: Elemental composition (as oxides in weight %) of the solid residues of Duvha and Tutuka CFA determined by XRF

	SiO_2	Al_2O_3	Na_2O	Fe_2O_3	CaO	Cr_2O_3	K_2O	P_2O_5	MgO	MnO	TiO_2	LOI
Duvha Residue	21.47	8.68	7.42	1.24	0.98	BDL	0.06	0.20	BDL	BDL	0.57	58.59
Tutuka Residue	29.94	8.62	8.55	1.85	1.37	0.01	0.10	0.13	BDL	BDL	0.55	47.91

* BDL means element was below the detection limit

Table 4. 13 shows the trace element composition of the whole (un-sieved) leached solid residues of Duvha and Tutuka CFA. The concentrations of Cr, Ni, Cu, Zn Zr and Pb in the leached solid residue of Tutuka CFA were higher compared to that of the leached solid residue of Duvha CFA. The trace element with the highest concentration in the leached solid residues Duvha and Tutuka CFA was Zr, with concentrations of 198.12 ppm and 235.72 ppm, respectively. Cr was also found in relatively high concentrations with 46.75 ppm in the leached solid residue of Duvha CFA and 60.33 ppm in Tutuka CFA. Radionuclides Th and U were found in significant quantities in both CFAs. Th was found in greater quantities in both leached solid residues compared to U. In addition, there were insignificant differences in the content of these radionuclides between the two leached solid residues.

Table 4. 13: Trace element composition (ppm) of leached solid residues of Duvha and Tutuka CFA

Element	Cr	Co	Ni	Cu	Zn	Zr	Pb	Th	U
Duvha CFA	46.75	7.37	21.90	25.87	13,78	198.12	0.66	16.40	3.92
Tutuka CFA	60.33	7.28	23,66	61.87	27,48	235.72	2.55	16.46	3.41

Figure 4. 27 depicts the REE composition of the leached solid residues of Duvha and Tutuka CFA. The leached solid residues of Duvha and Tutuka CFA were found to have ΣREE content of 192.81 ppm and 206.82 respectively. There was minimal variation in the amounts of REE retained between the two leached solid residues except for Ce. The REE Ce was retained more in Tutuka compared to Duvha CFA leached residue with 88.42 ppm (44.81%) and 75.40 (34.75%) ppm retained, respectively. The elements Tm and Lu were the least abundant in the leached solid residues.

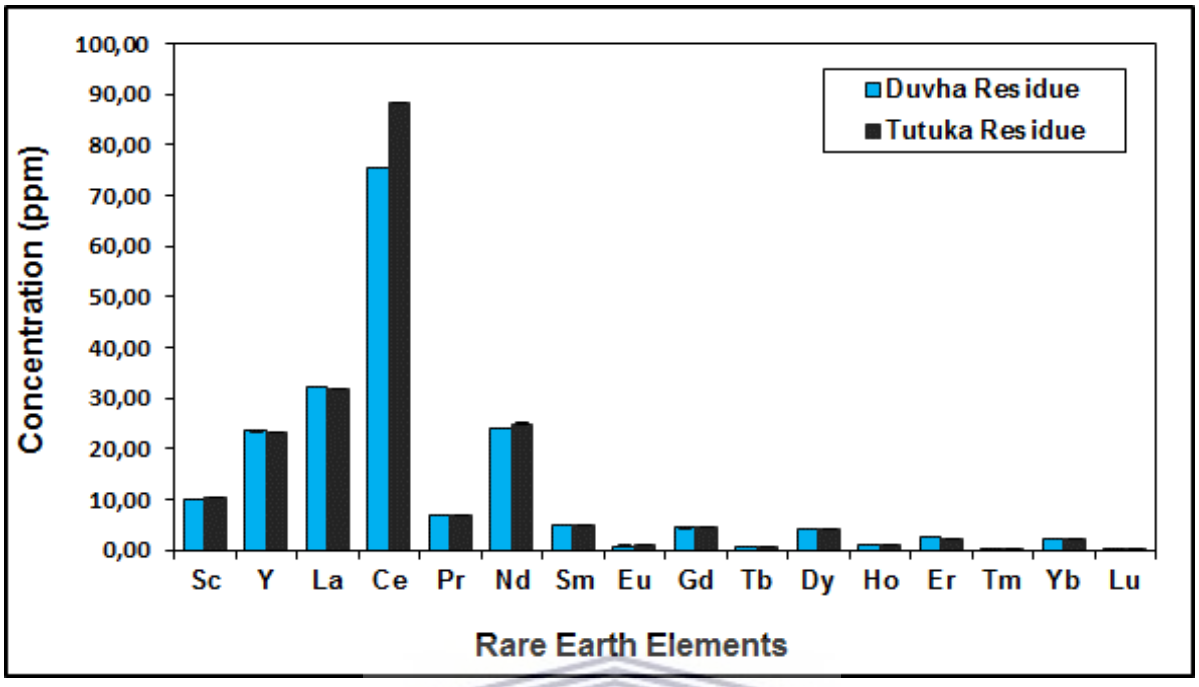

Figure 4. 27: REE composition (ppm) in the whole leached solid residues of Duvha and Tutuka CFA

4.5. Summary of Chapter Four

This chapter presented the findings of physical and chemical characterization of the raw CFA, sieved CFA, leachates and leached solid residue samples of Duvha and Tutuka CFA. The morphological analyses of Duvha and Tutuka CFA revealed that the majority of the particles were typically spherical with some irregular shaped structures in agglomerated form. Tutuka CFA exhibited numerous ferrospheres. Quartz and mullite were identified as the major mineral phases in both CFAs, while maghemite, microcline and calcite were present in low quantities. The abundance of the major elements in both CFAs was found to be in the order of SiO2 > Al_2O_3 > Fe_2O_3 > CaO > TiO_2 > MgO > K_2O >P_2O_5 > MnO > Cr_2O_3. Tutuka CFA was found to contain more Fe than Duvha CFA with 5.18 wt% and 4.07 wt % respectively. Zr and Cr were found to be the most abundant trace elements in both CFAs. Radionuclides Th and U were found in relatively significant amounts in both CFAs and Th was more abundant than U. The ΣREE content in the raw whole (un-sieved) Duvha and Tutuka CFA was measured to be 573.77 ppm and 546.25 ppm, respectively. An increase in ΣREE content with a decrease in particle size in both raw CFAs was observed, showing moderate enrichment of ΣREE in the finer particle size fractions.

Overall, the leachability of major and trace elements were determined from the whole (un-sieved) samples of Duvha and Tutka CFA. The abundance of the major elements in Duvha CFA leachate was in the order of Na > Al > Si > Ca > Mg > K > P, while in Tutuka CFA leachate, they were in the order of Na > Al > Ca > Si > Mg > K > P. Tutuka CFA leachate was most abundant in all the major elements. In both Duvha and Tutuka CFA leachates, Fe was found to be the trace element that was most abundant with concentrations of 778.92 ± 7.08 ppm and 1307.52 ± 24.77 ppm, respectively. In Duvha CFA, the abundance of ΣREE recovered in the leachates of the whole (un-sieved) samples was in the order of Ce > La > Nd > Y in Duvha CFA, while in Tutuka CFA it was Ce > Y > La > Nd.

REEs in the leachates of the sieved particle size fractions of Duvha and Tutuka CFA revealed an increase in the recovery of ΣREE with a decrease in particle size. Similarly, the leaching efficiencies revealed the same trend where the efficiencies increased with a decrease in particle size. In both Duvha and Tutuka CFA, the highest α for total REEs was observed in the smallest size fraction (< 25 μm) with α of 38.31 % and 36.39 % respectively. HREEs were found to be easily leached in both CFAs compared to the LREEs with the highest α observed in the smallest size fraction (<25 μm) in Duvha CFA (48.38 %) and the 32 -25 μm size fraction in Tutuka CFA (47.44 %).

The morphology of the particles of the leached solid residues of both CFAs was different in shape and structure compared to the raw CFAs. The particles of the leached solid residues appeared to have been crusted, etched and corroded. Also, ferrospheres that were observed in the raw Tutuka CFA were not found in the leached CFA. The leached solid residues of Duvha and Tutuka CFA displayed quite similar XRD spectra and in order of abundance halite, chloraluminite and quartz were identified as the dominant mineral phases. SiO_2 and Al_2O_3 remained the major elements retained in the leached solid residues. The analyses of the REEs retained in the leached solid residues showed minimal variation in the amounts of REEs retained between the two leached solid residues, except for the REE Ce. The REE Ce was retained more in Tutuka compared to the Duvha CFA leached solid residue with 88.42 ppm (44.81%) and 75.40 (34.75%) ppm retained, respectively. In order of abundance, the following REEs were most retained in the leached solid residues of both CFAs: Ce > La > Nd > Y > Sc > Pr.

CHAPTER FIVE: DISCUSSION

5. Introduction

The content of REEs has been found to increase with a decrease in the particle size of CFA, particularly for separates between 100 and 30 micrometres (µm)(Lin et al., 2018; Rosita et al., 2020) However, Scott et al. (2015) showed disagreements in experimental results, which indicates that different CFAs might have different responses to these separation techniques. This study aimed to assess this relationship on South African CFA as well as determine whether particle separation improves REE recovery efficiencies. This chapter discusses the findings of the study that are presented in the previous chapter.

5.1. Characteristics of Duvha and Tutuka Coal Fly Ash

5.1.1. Morphological Structures

Duvha and Tutuka CFA consisted of spherical particles, with some irregular shaped structures in an agglomerated form. In addition, the surface texture of the particles was mostly smooth in the case of Duvha CFA (**Figure 5. 1A**) and dendritic in Tutuka CFA (**Figure 5. 2B**). The spherical shapes and the agglomeration observed on both CFAs are a result of the combustion conditions. Spherical shapes are an indication that the CFA particles were formed under uncrowded freefall conditions with sudden cooling. This aids in maintaining the spherical shape of CFA particles, while the agglomerated particles indicate that the particles were produced at high temperatures during combustion (Seames, 2003; Saikia et al., 2006). Seames (2003) suggested that the smooth outer surfaces on CFA particles are predominantly aluminosilicate structures.

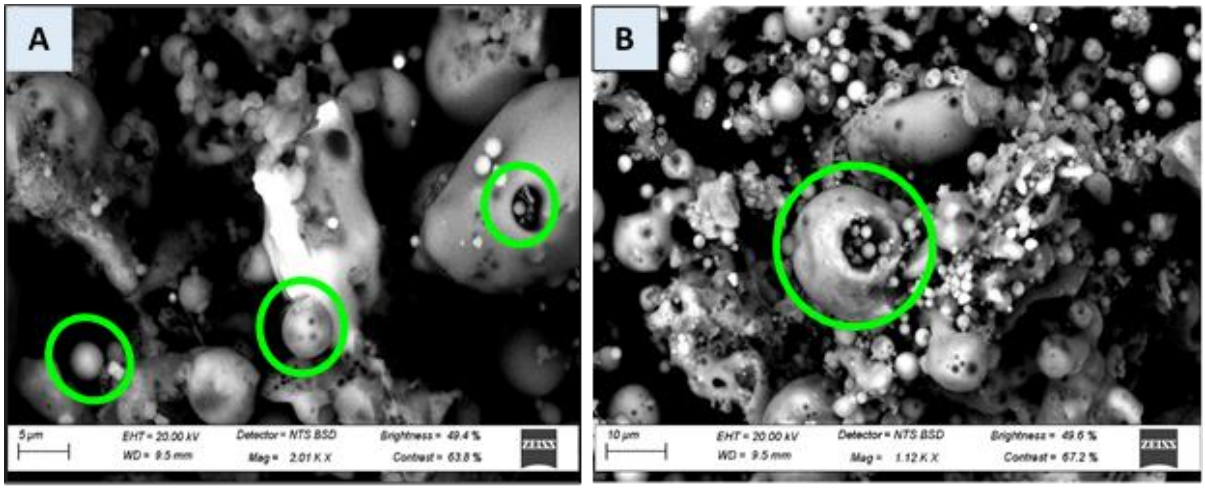

Figure 5. 1: SEM micrographs illustrating Duvha CFA particles (A) smooth spherical particles (B) pleronospheres (Magnification: (A) = 2.01 KX, (B) = 1.12 KX)

Duvha CFA was more porous than Tutuka CFA as shown in **Figure 5. 1A**. The presence of pores increases the specific surface area and enhances the adsorption ability (Liu et al., 2016) and this plays an important role during weathering of CFA, particularly the leaching process. In addition, Duvha CFA displayed cenospheres (hollow microspheres) and plerospheres (larger hollow spherical particles, encapsulating smaller spheres) as depicted in **Figure 5. 1B**. Cenospheres are associated with high Al and Si content and this agreed with the EDS and XRF analyses where higher content of Si and Al was recorded in Duvha compared to Tutuka CFA. Cenospheres generally have better mechanical properties and a higher chemical reactivity than plerospheres (Liu et al., 2016; Etale et al., 2018) and this plays a role during acid leaching.

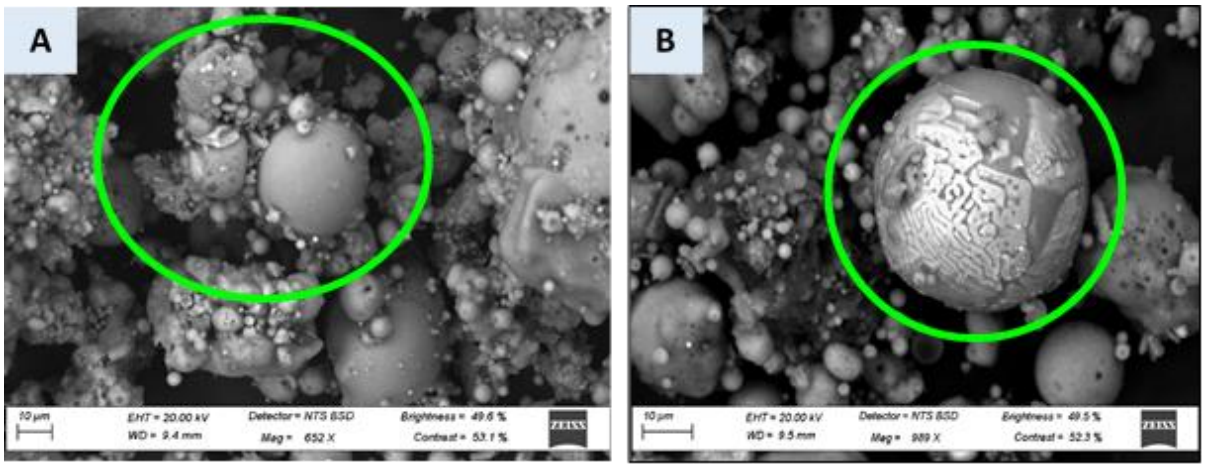

Figure 5. 2: SEM micrographs illustrating Tutuka CFA particles (A) agglomeration CFA (B) ferrospheres (Magnification: (A) = 652 X, (B) = 999 X)

On the other hand, Tutuka CFA exhibited numerous ferrospheres, spheres with a rough and dendritic surface as shown in **Figure 5. 2B** and these spheres are associated with high iron oxide (Fe_2O_3) (Saikia et al., 2006). This observation coincided with the XRF analyses where Tutuka CFA was recorded to have Fe_2O_3 content of 5.18 wt% while Duvha CFA had 4.07 wt %. In support of this, the EDS analysis also showed a relatively high abundance of Fe in Tutuka CFA in comparison to Duvha CFA with an abundance of 44.47 ± 27.24 wt %, 1.15 ± 0.46 wt % respectively.

REEs are often encased within the Fe-rich aluminosilicate glass phases (Cao et al., 2018). Thus the presence of Fe_2O_3 was indicative of the presence of REEs, and the SEMD-EDS revealed REEs La and Ce to be relatively abundant in both CFAs. This observation was to be expected as naturally, La and Ce are most abundant (Franus et al., 2015; Balaram, 2019). However, these were the only REEs detected during the SEM-EDS analysis. A possible explanation for this is that the particles and spots chosen for EDS analyses were not abundant in REEs. In addition, the observation also suggests that SEM-EDS may be ineffective at determining the abundances of REEs in relatively small quantities such HREEs.

5.1.2. Mineralogical Phases

The major mineral phases identified by XRD in Duvha and Tutuka CFAs were quartz (SiO_2), mullite ($3Al_2O_3{\cdot}2SiO_2$). Maghemite (Fe_2O_3), calcite (CaO) and microcline ($KAlSi_3O_8$) were present in lower quantities. These findings agreed with those reported by Gitari et al. (2009), Akinyemi et al. (2011), Eze (2011), Alegbe et al. (2018) and van der Merwe et al. (2014) for some South African CFAs. Quartz is a primary mineral and is considered non-reactive during the combustion processes of coal due to its high melting temperature (i.e., > 1100 ° C) (Ward, 2002; Vassilev and Menendez, 2005). Therefore, relatively large quantities of quartz are expected to be present in CFA and any trace elements remain embedded within its matrix. Secondary minerals (newly-formed) mullite, maghemite, calcite, microcline and perhaps a portion of the quartz were formed by recrystallization as the molten mass cooled down during combustion (Liu et al., 2016).

In CFA, mullite is formed during the thermal decomposition of kaolinite ($Si_2Al_2O_5(OH)_4$), an aluminosilicate mineral in coal that crystallizes from the melt forming a spherical network of crystals under a surface of glassy material (Koukouzas et al., 2009). Calcite is formed by the contact of lime (CaO) with ingressed carbon dioxide (CO_2) (Vassilev and Menendez, 2005),

and in the TIMA analyses, this mineral was observed to be associated with the REEs Sc and Y.

On the other hand, maghemite is a Fe bearing mineral typically formed through oxidation of magnetite (Fe_3O_4) and in CFA, this happens during coal combustion. Fe_3O_4 is often associated with REEs (Saikia et al., 2006), this was observed in the EDS analyses of both CFAs, where a relatively high wt % of Fe was detected, and the REEs La and Ce were identified. In addition, Tutuka CFA displayed numerous ferrospheres, indicating that the CFA was abundant in Fe. Moreover, the TIMA analyses revealed the MREEs (e.g., Eu and Gd) to exist in the mineral hematite (Fe_2O_3) and goethite (FeO(OH)) in both CFAs.

5.1.3. Chemical Composition

The major elements in both CFAs were found to be abundant in the order of $SiO2 > Al_2O_3 > Fe_2O_3 > CaO > TiO_2 > MgO > K_2O > P_2O_5 > MnO > Cr_2O_3$. The XRD and XRF analyses of both CFAs agree with respect to the major elements Si, Al, Fe, and Ca reported, which exist in the form of quartz (SiO_2), mullite ($3Al_2O_3{\cdot}2SiO_2$), maghemite (Fe_2O_3) and calcite (CaO). Tutuka CFA was found to contain more Fe_2O_3 than Duvha CFA with 5.18 wt% and 4.07 wt % respectively. This coincided with the SEM-EDS analyses where higher Fe content was observed on the particles of Tutuka CFA as well the presence of ferrospheres. Overall, both CFAs showed similar trends in the composition of their major elements, however, variations between the CFAs were observed. The variations observed can be attributed to the difference in the geological composition of the mined coal sources. Duvha Power Station is situated in the Witbank Coalfield, whilst Tutuka Power Station is in the Highveld Coalfield. Therefore, there is a likelihood of the power stations burning coal sourced from different coalfields, which would lead to different chemical compositions of the CFAs produced. In addition, the XRD spectra of both CFAs concur with the results of the XRF analysis, which showed high percentages of the oxides of Si, Ca, Fe and Al as these elements were the major components of the mineral phases observed in the XRD analyses. XRD findings are significant when accompanied by XRF findings as XRD is ineffective in inferring the amounts present for each element.

According to the American society for testing and materials (ASTM) classification method, the two CFAs can be classified as Class F fly ash (ASTM C618, 2005). This was indicated by the sum of the weight percent composition of the major mineral phases: SiO_2, Al_2O_3 and Fe_2O_3

present in the CFAs which was found to be > 70 %. The findings obtained for the elemental analyses of these CFAs agree with those reported in previous studies particularly those of the same CFA and those where the coal was sourced from the same coalfield (Fatoba, 2010; Eze, 2014; van der Merwe et al., 2014; Alegbe et al., 2018).

Loss on ignition (LOI), is usually taken as a measure of the amount of the unburned carbon remaining in the CFA (Koukouzas et al., 2009). Minimal variation in the LOI was observed between the CFAs, however, the LOI of Tutuka CFA (i.e., 5.22) was slightly greater than that of Duhva CFA (i.e., 5.18). Variation in the LOI can be attributed to the different combustion temperatures of the power stations and the incomplete oxidation of combustible constituents of coal (Gitari et al., 2009).

The content of the trace element zircon (Zr) was highest in Duvha and Tutuka CFA with concentrations of 333.76 and 311.27 ppm. The abundance of Zr in these CFAs indicates the presence of Zr bearing minerals such as zircon ($ZrSiO_4$) and this was in agreement with the TIMA analyses. Zr bearing minerals have been reported to be associated with significant amounts of REEs (Huang et al., 2020). In addition, the TIMA analyses revealed the REEs Y and Sc to be associated with the mineral zircon. Overall, Duvha CFA had relatively higher concentrations of trace elements and this can be explained in terms of its sulphur content which was higher than that of Tutuka CFA, which was recorded from the EDS analysis. Ainsworth and Rai (1987) explained that often the concentrations of some trace elements are higher in CFA from bituminous coal, as these are associated with the sulphide contents of the coal.

The source and type of coal burnt contributed to the variations in the oxides and trace element content in the CFA from the two power stations, resulting in variation in the mineralogical and chemical composition of the CFAs. In addition, the ΣREE concentrations of Duvha and Tutuka CFA were quantified to be 573.77 ppm and 546.25 ppm, respectively and these concentrations were similar to those reported in previous studies of South African CFA (Fatoba, 2010; Wagner and Matiane, 2018). In order of abundance, Ce>La>Nd>Y>Sc>Pr were found to be the most abundant REEs in both CFAs. These REEs are categorised as Light Rare Earth Elements (LREEs), and their predominance in CFAs than the Heavy Rare Earth Elements (HREEs) can be explained by the fact that LREEs are naturally relatively more abundant compared to HREEs (Franus et al., 2015; Balaram, 2019). The observed order of abundance of these elements was similar to that reported by Eze (2014) and Fatoba (2010), who investigated REEs in some South African CFAs (i.e. Tutuka and Matla CFA).

5.2. Particle Size Separation of Coal Fly Ash

5.2.1. Rare Earth Element Distribution in Various Particle Size Fractions

The weight distribution of Duvha and Tutuka CFA in the various size fractions revealed a peak at 50 – 32 µm in both CFAs, while the least weight distribution was found at 50 – 53 µm for Duvha CFA and < 25 µm for Tutuka CFA. Overall, the particle size distributions of both CFAs varied significantly. This indicated that the CFAs were of different sources and possibly imply different CFA formation mechanisms during coal combustion (Lin et al., 2017b).

It is important to note that despite variations in the weight distribution of the CFAs with particles size, the size fractions also varied visually in colour (**Figure 5. 3**). However, when comparing the two CFAs, there was no variation. The fraction of the largest diameter (>106 µm) contained more dark and black particles; while the smaller fractions were almost entirely grey, especially the smallest fraction (<25 µm). According to the particle size diameter from the biggest to smallest, the colour gradually became light grey. Stoch (2015) explained that this resulted from a higher content of unburnt carbon in the larger fractions than in the smaller fractions. Furthermore, Stoch (2015) observed a similar trend with the colour of 5 particle size fractions (> 320 to < 63 µm). Moreover, by comparing the separated fractions with the whole CFA samples (non-sieved), it is noticeable that the light grey colour is more dominant than the black, indicating that the CFAs are dominated by smaller particle size fractions (**Figure 5. 3**).

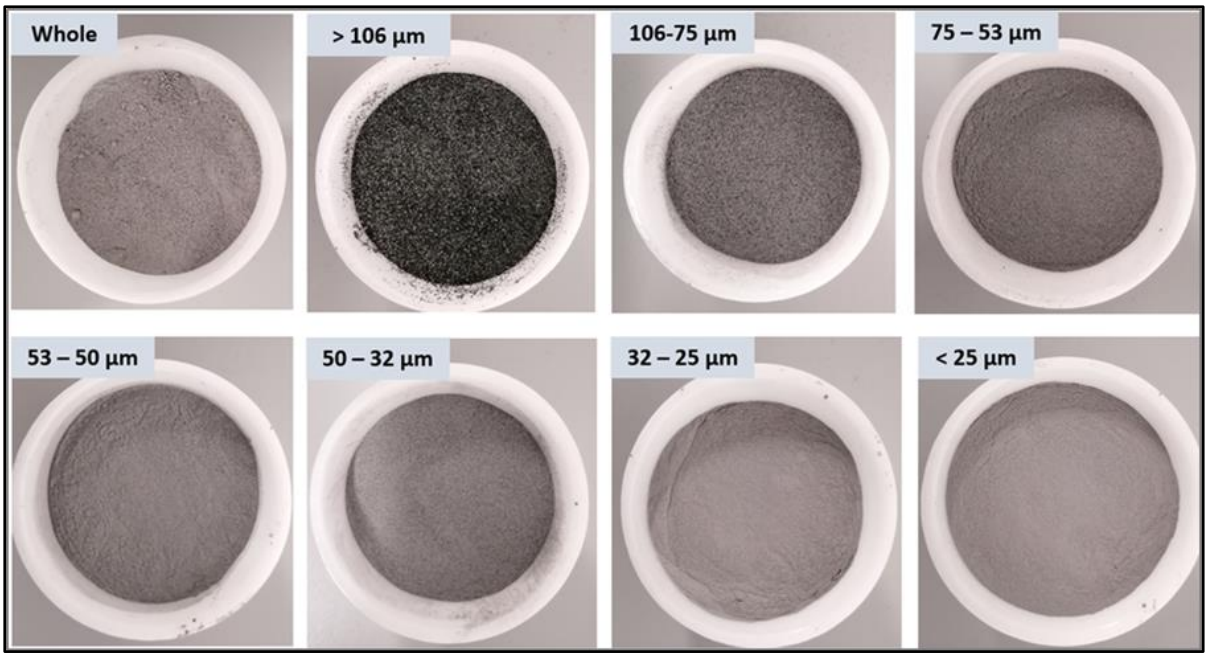

Figure 5. 3: Image displaying the variation in the colour of coal fly ash with particle size

Duvha and Tutuka CFA were found to have ΣREE content of 573.77 ppm and 546.25 ppm, respectively (**Appendix I**). The distribution of REEs with the particle size of CFA was investigated and overall, there was an increase in ΣREE content with a decrease in particle size in both CFAs, showing moderate enrichment of ΣREE in the finer particle size fractions (**Appendix F**). In both CFAs the lowest and the highest ΣREE content were measured in the > 106 µm and < 25 µm particle size fractions respectively. Pan et al., (2020) observed a similar trend when investigating the distribution of REEs in various sizes of CFA (i.e., 150-100, 100-74, 74-55, 55- 35, 38-25 and < 25 µm). The author reported the ΣREE content to increase from 608 ppm to 896 ppm with decreasing particle size, and the highest ΣREE content was measured at the < 25 µm particle size fraction.

In Duvha CFA, the finest size fraction (i.e., < 25 µm) had the highest ΣREE content of 541.07 ppm, however, this was lower by 32.7 ppm than that found in the whole (un-sieved) Duvha CFA (i.e., 573.77 ppm). This indicated that the finest size fraction in Duvha CFA was rather depleted in REEs than the whole (un-sieved) CFA. Contrarily, in Tutuka CFA, the finest size fraction was found to have the highest ΣREE content of 625.85 ppm and this was higher than that measured in the whole (un-sieved) CFA (i.e., 546.25 ppm). This indicated that the finest size fraction of Tutuka CFA was more enriched in REE than the whole (un-sieved) CFA. In

addition, as the particle size fraction decreased below 75–53 μm, the ΣREE content in the CFA exceeded that in the whole (un-sieved) Tutuka CFA.

The findings of both Duvha and Tutuka CFA were in good agreement with findings of previous studies (Dai et al., 2010; Hower et al., 2013; Dai et al., 2014; Taggart et al., 2016; Lin et al., 2017; Rosita et al., 2020), which confirmed that there is an increase in REE content with a decrease in particle size of CFA. Moreover, these observations also corroborate that REEs are depleted in the coarse fraction (i.e., > 100 μm) relative to the whole (un-sieved) CFA. Blissett et al. (2014) explained that the possible reason for REEs to be more concentrated in the finer particle size fractions is that coarser particle size fractions of CFA tend to have a higher carbon content. LOI can be used as a simple indicator to detect the existence of unburned carbon, although there are many factors that can effect this value. Rosita et al. (2020) observed the LOI to decrease with particle size. This coincides with the LOI of the size fractions Duvha and Tutuka CFA, where lower LOI values were observed in the finer particle size fractions (**Appendix E**). Furthermore, variation in the colour of the particle size fractions agreed with that observed by Blissett et al. (2014) and Rosita et al. (2020) as the colour of the particle size fractions became light grey (from black to light grey) as the particle size fractions decreased.

5.2.2. Effect of Particle Size Separation on REE Concentration

The effect of the particle size of CFA on ΣREE content was evaluated by regression analyses and the findings revealed a positive insignificant regression equation ($F(1,5) = 4.196$, $p = .096$, with an R^2 of 0.46, between the ΣREE content in Duvha CFA with the particle size. Overall, as the particle size of Duvha CFA decreased, there was an insignificant increase (i.e., $p > .05$) in the ΣREE content. This indicated that higher ΣREE content was present in the finer size fractions than in the coarser size fractions. Moreover, the paired samples t-tests of the sieved fractions of Duvha CFA showed that significant differences (i.e., $p < .05$) between the means of the ΣREE content with a decrease in particle size fractions existed in only the 1st and 2nd sample pair as shown in **Table 5. 1**. This showed that with the rest of the sample pairs, whether the ΣREE content increased or not with a decrease in particle size, the difference was insignificant.

Table 5. 1: Summary of the paired t-tests of the REE composition of Duvha CFA sieved particle size fractions

Duvha Sieved CFA Paired Samples t-Test							
	Pair	Mean	STDEV	SE	t	df	Sig. (2-tailed)
1	DUV-Whole - > 106 µm	8.209	15.273	3.818	2.150	15	**.048**
2	> 106 µm - 106 -75 µm	5.860	8.915	2.229	2.629	15	**.019**
3	106 -75 µm - 75 - 53 µm	1.701	5.293	1.323	1.285	15	.218
4	75 - 53 µm - 53 - 50 µm	-.328	3.764	.941	-.349	15	.732
5	53 - 50 µm - 50 - 32 µm	-.961	4.898	1.225	-.784	15	.445
6	50 - 32 µm - 32 -25 µm	.319	2.077	.519	.615	15	.548
7	32 -25 µm - < 25 µm	1.036	3.645	.911	1.137	15	.273

On the other hand, a positive significant regression equation was found ($F(1,5) = 440.738$, $p < .001$, with an R^2 of 0.99, between the ΣREE in Tutuka CFA with the particle size. This indicated that as the particle size of Tutuka CFA decreased, there was a significant increase (i.e., $p < .05$) in the ΣREE content. In support of this, the paired samples t-tests of the sieved fractions of Tutuka CFA revealed that there were significant differences (i.e., $p < .05$) between the means of the ΣREE in all the sample pairs as shown in **Table 5. 2**, except for the 4th pair.

Pretorius (2007) suggested 5 categories for interpreting the strength of a relationship between two variables, the correlation coefficient (R). The categories are as follows; ≤ 0.2 (slight, almost negligible relationship), 0.2 – 0.4 (low correlation, definite but small relationship), 0.4 – 0.7 (moderate correlation, substantial relationship), 0.7 – 0.9 (high correlation) and ≥ 0.9 (very high correlation, very dependable relationship). Therefore, a moderate positive correlation and substantial relationship existed between the particle size of Duvha CFA with the ΣREE content (R = 0.68), while there was a very high positive correlation and dependable relationship (R = 0.99) between the particle size of Tutuka CFA with the ΣREE content. Contrarily, Scott et al. (2015) did not observe a relationship between the REE content with particle size. The author suggested that the reason for that observation was the different size ranges (1000, 100, 10, 5 and < 5 µm) used compared to other studies and the possibility of there being a limit to REE enrichment with decreasing grain size or for that particular study a finer increment of sampling was needed. Regardless, the study did confirm that REEs are depleted in the coarse fraction (> 100 µm) relative to the whole CFA, which is what was observed in Duvha and Tutuka CFA.

Table 5. 2: Summary of the paired t-tests of the REE composition of Tutuka CFA sieved particle size fractions

Tutuka Sieved Paired Samples t-Test							
	Pair	Mean	STDEV	SE	t	df	Sig. (2-tailed)
1	TUT-Whole - > 106 µm	4.289	6.619	1.654	2.592	15	**.020**
2	> 106 µm - 106 -75 µm	-1.751	2.925	.731	-2.394	15	**.030**
3	106 -75 µm - 75 - 53 µm	-2.183	3.204	.801	-2.726	15	**.016**
4	75 - 53 µm - 53 - 50 µm	-1.536	2.894	.723	-2.124	15	.051
5	53 - 50 µm - 50 - 32 µm	-1.187	1.642	.410	-2.893	15	**.011**
6	50 - 32 µm - 32 -25 µm	-1.599	2.245	.561	-2.851	15	**.012**
7	32 -25 µm - < 25 µm	-1.008	1.775	.444	-2.271	15	**.038**

Effect size is a quantitative measure of the magnitude of the experimental effect and in this study, it is the physical separation of CFA. Cohen's ***d*** is an effect size used to indicate the standardised difference between two means. Cohen suggested that a *d* of 0.2 can be considered a 'small' effect size, 0.5 represents 'medium' effect size and 0.8 'large' effect size. Therefore, if two groups' means do not differ by 0.2 standard deviations or more, the difference is insignificant, even if it is statistically significant (McLeod, 2019) and the larger the effect size the stronger the relationship between the two variables.

The effect sizes of the sample pairs in **Table 5. 1** and **Table 5. 2** were determined and the results are presented in **Table 5. 3.** The effect sizes revealed that the ΣREE content in the sieved fractions in Duvha CFA was 'medium' for the 1st and 2nd pair ($0.2 \geq d \leq 0.5$), insignificant for the remaining pairs ($d \leq 0.2$). Furthermore, only the pairs with a 'medium' effect size were found to be statistically significant ($p < .05$) in Duvha CFA. In Tutuka CFA, the effect sizes were 'medium' throughout all the particle size fraction pairs ($0.2 \geq d \leq 0.5$). This indicated that the sieving of the CFA into various size fractions had a medium effect on the increase in the ΣREE content in each size fraction. This suggested a much stronger relationship between particle size and REE content in Tutuka CFA compared to Duvha CFA (**Table 5. 3**).

Furthermore, this suggested that there was a significant increase in the ΣREE content recovered between the particle size fractions of the 1st and 2nd of Duvha CFA as well as all the pairs in Tutuka CFA that were determined to have a median effect size. Therefore, particle size separation of these pairs had a medium effect on the increase in ΣREE content recovered. The

pairs that Cohens *d* was found to be small suggest that the decrease in the particle size fractions had an insignificant impact on the increase in the ΣREE content, indicating a weak relationship between the two variables.

Table 5. 3: Summary of the paired sample effect sizes of the REE composition of the sieved particle size fractions of Duvha and Tutuka CFA

		Duvha CFA	Tutuka CFA
Pair		*d*	*d*
1	Whole CFA - > 106 µm	.537	.648
2	> 106 µm - 106 -75 µm	-.657	-.598
3	106 -75 µm - 75 - 53 µm	.321	-.681
4	75 - 53 µm - 53 - 50 µm	-.087	-.531
5	53 - 50 µm - 50 - 32 µm	-.196	-.723
6	50 - 32 µm - 32 -25 µm	.154	-.713
7	32 -25 µm - < 25 µm	-.284	-.568

Overall, the relationships observed between ΣREE content with particle size in Duvha and Tutuka CFA confirms and supports previous studies that as the particle size of CFA decreases, there is an increase in the ΣREE content (Dai et al., 2010; Hower et al., 2013; Dai et al., 2014; Taggart et al., 2016; Lin et al., 2017; Rosita et al., 2020). A stronger relationship was found in Tutuka CFA (R = 0.99, p = .096) compared to Duvha CFA (R = 0.68, p < .001). In addition, both CFAs confirmed that REEs are depleted in the coarse fraction (> 100 µm) relative to the whole (un-sieved) CFA.

5.2.3. Enrichment Factors and LREE/HREE Distribution

Enrichment factors (EF) were determined to quantitatively characterize REE enrichment by particle size separation, while the efficiency of the separation method was quantified using REE recovery (R_i). Overall, in both CFAs the EF increased with a decrease in particle size, indicating that REEs were enriched in the finer particle size fractions, thus leaving the coarser fractions depleted in REEs. These findings supported the regression analyses which showed an increase in ΣREE content with a decrease in particle size. In both Duvha and Tutuka CFA, the EF was lowest in the coarser size fraction (> 106 µm) and highest in the finer particle size fraction (< 25 µm). Consequently, the sieving of both CFAs into various particle size fractions resulted in Tutuka CFA being more enriched in REEs in each size fraction compared to Duvha CFA. Generally, Tutuka CFA was observed to have relatively higher R_i compared to Duvha

CFA. The R_i in both CFAs was highest in the particle size fraction where most of the weight was distributed and the lowest in the particle size fraction, which had the least weight distributed. Thus, in Duvha and Tutuka CFA, the R_i was highest in the 50 – 32 µm with R_i of 5.06 % and 4.33 %, respectively. The lowest R_i was found in the >106 µm with R_i of 1.15 % in Duvha CFA, while in Tutuka CFA, it was in the > 35 µm with R_i of 0.28 %.

The ratio of LHREE/HREE indicates the distribution of these two groups of elements within a sample. The LREE/HREE ratios in Duvha CFA remained relatively unchanged with low insignificant correlation (R = 0.43, p = .332), while in Tutuka CFA, there was variation in the ratios with particles with low insignificant correlation (R = 0.38, p = .403). In contrast to these findings, Lin et al. (2017) found that the LREE/HREE of two CFAs collected from a power station in Kentucky and Ohio States in the USA decreased significantly as the particle size decreased. This observation disagreed with the findings of Hower et al. (2013), where the highest LREE/HREE ratio was found in the finest fraction. During physical separation of CFA by particle size separation, LREEs and HREEs do not equally contribute to the enrichment of REEs. Thus, in Duvha and Tutuka CFA, LREEs contributed more than the HREE towards the enrichment, which was similar to the findings of Dai et al. (2010). A possible explanation for the unequal contribution of LREEs and HREEs is the variation in the chemical composition of individual REE containing minerals, although REEs typically occur in the same minerals. Consequently, this leads to unequal distributions of LREEs and HREEs across REE-bearing minerals (Lin et al., 2017b).

5.3. Alkali-Fusion Acid Leaching

5.3.1. Recovery of Major and Trace Elements

The leachates of the whole (un-sieved) samples of Duvha and Tutuka CFA were analysed for their major and trace elemental composition. This was done to provide a general overview of the elements that leach from CFA when REE recovery methods such as the one used in this study are applied. Overall, the leachate of Tutuka CFA was more abundant in all the major elements compared to the Duvha CFA leachate. Na was the most leached major element in Duvha and Tutuka CFA leachates with concentrations of 22384.50 ± 7.78 ppm and 25044.50 ± 64.35 ppm respectively. However, in raw Duvha and Tutuka CFA Na in the form of Na_2O was present in relatively small quantities with compositions of 0.06 wt% and 0.29 wt% respectively. In addition, the elemental composition of the leached blanks samples, which were

not fused with NaOH and were leached with water showed that relatively small quantities of Na were leached (**Table 5. 4**) compared to the content in the alkali-fused acid leached samples. The blank leachates of Duvha and Tutuka CFA had Na content of 1.40 ± 0.04 ppm and 63.22 ± 2.06 ppm respectively. Based on this and the elemental as well as the mineralogical composition of the raw CFAs, the high content of Na quantified in the alkali-fused acid leached samples suggest an additional source of Na was introduced. A plausible explanation for this is the addition of NaOH to the CFA during alkali-fusion.

Table 5. 4: Elemental composition (ppm) of the blank samples of Duvha and Tutuka CFA

	Al	Ca	K	Mg	Na	P	Si
Duvha CFA	7,23	227,65	1,67	0,04	1,40	BDL	117,44
Tutuka CFA	14,15	179,30	15,05	0,38	63,22	BDL	1,14

* BDL means element was below the detection limit

In CFA, most heavy trace metals exist in the internal glass matrix of the aluminosilicate phases of the CFA particles and are not readily solubilized (Izquierdo and Querol, 2012). However, depending on the leaching conditions to which the CFA is subjected they become more soluble. Trace elements such as Fe, Cr, Co, Ni, As and Zn have diverse environmental impacts, therefore, during CFA leaching they become of concern. In both Duvha and Tutuka CFA acid leachates, Fe was found to be the most abundant trace element in the leachates with concentrations of 7779.92 ±7.08 ppm and 1307.52 ± 24.77 ppm respectively. This coincided with the morphological (SEM-EDS) and mineralogical (XRD and TIMA) findings of the raw CFAs, where the mineral maghemite (Fe_2O_3) was found in both raw CFAs, indicating that both CFAs contained a substantial amount of Fe and Fe-oxides (Kolker et al., 2017). The SEM-EDS of several spot analyses of both CFAs revealed that raw Tutuka CFA (57.79 ± 37.93 wt %) was more abundant in Fe than Duvha CFA. In addition, the raw Tutuka CFA exhibited numerous ferrospheres (**Figure 4. 2**), which are spheres with a rough and dendritic surface and are considered to be s rich in Fe (Sharonova et al., 2015).

The mobilization and speciation of trace elements like Cr in CFA is a major concern as their different oxidation states pose different threats to the environment. Depending on the oxidation state, Cr can be carcinogenic and highly soluble in aqueous media (e.g., Cr^{+6}) or is less soluble and of much less concern to human health (e.g., Cr^{+5}). Cr was higher in the Tutuka CFA leachate compared to Duvha CFA leachate. The leaching of a substantial amount of Cr is often

associated with a yellow to orange colour of the leachate and this was observed with leachates of both CFAs as depicted in **Figure 5. 4**.

In CFA barium (Ba) often forms soluble compounds with carbonates and sulphates and is associated with strontium (Sr) (Izquierdo and Querol, 2012). Relatively high concentrations of Ba and Sr were recorded in the leachates of both CFAs from the two, Ba content in Duvha CFA leachate (25.95 ± 8.16 ppm) was twice than that in Tutuka CFA leachate (11.01 ± 2.83 ppm). Ba exists as soluble salts on the surface of CFA and the aluminosilicate glass associated fractions. Gitari et al. (2009), reported Ba contents of 10.81 ppm and 5.42 ppm in the leachates of Secunda and Tutuka CFA, respectively. The author suggested that the dissolution of Ba was of the soluble salts on the surface of the CFA particles rather than the aluminosilicate glass fractions because of the short duration of the leaching test and the use of demineralised water as the leaching medium. The dissolution of Ba in Duvha and Tutuka CFA could have possibly been of the aluminosilicate glass fractions of the CFAs as the Ba contents in the leachates observed in this study were significantly higher than those reported by Gitari et al. (2009). Furthermore, the leaching conditions used in this study were more aggressive than the former.

Radionuclides Th and U were observed to be co-recovered during the recovery of REEs. These radionuclides were present in both leachates in small amounts and there was not much variation in the recovery of these elements just like in the raw CFA, Th content was higher than that of U in both CFAs. U in CFA is mostly associated with the particle surfaces while Th is associated with the aluminosilicate matrix (Taggart et al., 2018a; Tang et al., 2019). The recovery of these elements in the leachates of both CFAs suggests that the alumina-silicate matrix in both CFAs was decomposed to some extent with the leaching conditions applied in the study.

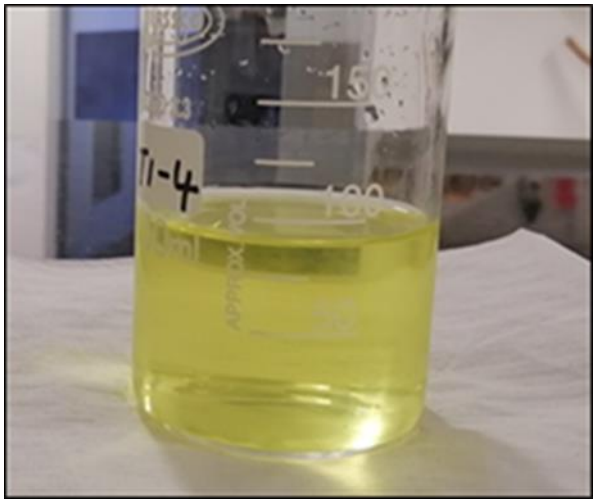

Figure 5. 4: Image showing the colour of the leachate observed from the fused samples of Duvha and Tutuka CFA

5.3.2. Recovery of Rare Earth Elements

The ΣREE recovered in the whole (un-sieved) samples of Duvha and Tutuka CFA leachates were 15.67 ppm and 17.20 ppm, respectively as shown in **Table 5. 5** (**Appendix L** and **M**). These values were quite lower than those reported by Eze (2014) (i.e., 91.74 ppm), who recovered REEs from Matla CFA, which came from a coal-fired power station in Mpumalanga Province in South Africa. Perhaps a major contributor to the observed differences in the recovered ΣREE content is the application of a different leaching method as well as that the CFA is from a different power station. In order of abundance the following REEs were well recovered in comparison to the rest, Ce > La > Nd > Y in the Duvha CFA leachate, while in Tutuka CFA leachate, it was Ce > Y > La > Nd. These elements were most abundant in the raw CFAs in the order of Ce > L a> Nd > Y >Sc. The order of REE abundance in Duvha CFA leachate was similar to that observed by Eze (2014). Contrarily, Cao et al. (2018) found La to be more readily leached from CFA than the other elements in the leachate (La > Ce > Nd) when leaching Chinese Class F CFA.

The alkali-fused acid leachates of Duvha and Tutuka CFA recovered more REEs than the respective blank samples which were not fused with NaOH and were leached with deionized water. In the blank leachate of Tutuka CFA 4.93 ppm of ΣREE were recovered while in Duvha CFA the recovered ΣREE were below the detection limit as shown in **Table 5. 5** (**Appendix R** and **S**). This observation indicates that the fusion of CFA with NaOH using HCl as a lixiviant improved the recovery of REEs.

Table 5. 5: Total REE composition (ppm) in leachates of Duvha and Tutuka CFA

	Blank Leachate	Acid Leachate
Duvha CFA	BDL	15.67
Tutuka CFA	4.93	17.20

* BDL means element was below the detection limit

Overall, the leaching conditions used in this study favoured Tutuka CFA over Duvha CFA as more REEs were leached in Tutuka CFA (Σ17.51 ± 0.40 ppm) than in Duvha CFA (Σ16.16 ± 0.66 ppm), although the difference between the means of the ΣREE recovered from the two CFA leachates was insignificant (i.e., $p > .05$) (**Appendix L** and **M**). The above findings of the recovery of REEs from these two CFAs suggest that the leaching conditions applied in the study mostly targeted the first few REEs (Sc, Y, La, Ce, Pr, Nd, Sm) which can be categorised as LREEs. It can be deduced from this that the difference in leachability of different REEs may be due to their association with different minerals as well as the difference in their ionic radius. Furthermore, previous studies reported that REEs are concentrated in Fe and Ca-enriched fractions, as well as in minerals and nanoparticles that are outside the aluminosilicate glass matrices (Hower et al., 2016; Hood et al., 2017; Kolker et al., 2017). The TIMA analyses revealed Ca (e.g., calcite) and Fe (e.g., maghemite, goethite, allanite, ilmenite etc.) bearing minerals to be associated with a range of REEs. Tutuka CFA was found to contain more Fe and Ca than Duvha CFA, therefore, it is possible that during acid leaching the presence of greater Ca and Fe bearing minerals in Tutuka CFA improved the recovery of REEs.

5.3.3. The Effect of Particle Size on the Recovery of Rare Earth Elements

The effect of particle size of CFA on the ΣREE content recovered from the alkali-fusion acid leaching was evaluated by regression analyses and the findings showed a positive insignificant regression equation ($F(1,5) = 3.835$, $p = .108$, with an R^2 of 0.43, between the ΣREE content recovered in the leachates of Duvha CFA with particle size. Overall, as the particle size of Duvha CFA decreased, there was an insignificant increase (i.e., $p > .05$) in the ΣREE content recovered in the leachate, indicating that relatively more REEs were recovered in the finer size fractions. In addition, the paired samples t-tests of the leachates of the particle size fractions of Duvha CFA revealed that significant differences (i.e., $p < .05$) between the means of the ΣREE content recovered in the leachates with an increase in particle size only existed in the 1st, 2nd,3rd and 7th sample pair (**Table 5. 6**).

Table 5. 6: Summary of the paired t-tests of the ΣREE composition in the leachate of the sieved particle size fractions of Duvha CFA

Duvha CFA Leachate Paired Samples t-Test							
	Pair	Mean	STDEV	SE	t	df	Sig. (2-tailed)
1	**DUV-Whole - > 106 µm**	.201	.242	.061	3.319	15	**.005**
2	**> 106 µm - 106 -75 µm**	-.382	.506	.127	-3.020	15	**.009**
3	**106 -75 µm - 75 - 53 µm**	.216	.311	.078	2.781	15	**.014**
4	**75 - 53 µm - 53 - 50 µm**	-.184	.546	.137	-1.344	15	.199
5	**53 - 50 µm - 50 - 32 µm**	.011	.590	.148	.072	15	.944
6	**50 - 32 µm - 32 - 25 µm**	.104	.218	.054	1.918	15	.074
7	**32 - 25 µm - < 25 µm**	-.283	.466	.117	-2.425	15	**.028**

On the other hand, a positive significant regression equation was found (F (1,5) = 37.974, p = .002, with an R^2 of 0.88, between the ΣREE content recovered in the leachates of Tutuka CFA with the particle size. Thus, as the particle size of Tutuka CFAs decreased, there was a significant increase (i.e., $p < .05$) in the ΣREE content recovered in the leachates. This showed that relatively more REEs were leached in the finer size fractions compared to the coarser size fractions. Furthermore, the paired samples t-tests of the leachates of the sieved fractions of Tutuka CFA revealed that significant differences (i.e., $p < .05$) between the means of the ΣREE content recovered in the leachates with a decrease in particle size only existed in the 2nd, 3rd and 6th pair (**Table 5. 7**).

According to the category of the strength of a relationship by Pretorius (2007), there was a positive moderate correlation and substantial relationship between the particle size of Duvha CFA with the ΣREE recovered in the leachates (R = 0.66), while there was a very high positive correlation and dependable relationship (R = 0.94) between the particle size of Tutuka CFA with the ΣREE content recovered in the leachate.

Table 5. 7: Summary of the paired t-tests of the ΣREE composition in the leachate of the sieved particle size fractions of Tutuka CFA

Tutuka CFA Paired Samples t-Test							
	Pair	Mean	STDEV	SE	t	df	Sig. (2-tailed)
1	TUT-Whole - > 106 µm	.140	.286	.072	1.959	15	.069
2	> 106 µm - 106 -75 µm	-.139	.168	.042	-3.306	15	**.005**
3	106 -75 µm - 75 - 53 µm	-.029	.036	.009	-3.241	15	**.005**
4	75 - 53 µm - 53 - 50 µm	-.198	.414	.104	-1.913	15	.075
5	53 - 50 µm - 50 - 32 µm	.028	.207	.052	.535	15	.600
6	50 - 32 µm - 32 -25 µm	-.110	.141	.035	-3.126	15	**.007**
7	32 -25 µm - < 25 µm	-.041	.145	.036	-1.120	15	.280

The effect sizes of the samples pairs in **Table 5. 6** and **Table 5. 7**were determined and the results are presented in **Table 5. 8**. The effect sizes revealed that for the ΣREE content recovered in the leachates of the sieved size fractions in Duvha CFA were 'large' for the 1st pair ($d \geq 0.8$), 'medium' for the 2nd, 3rd and 7th pair ($0.2 \geq d \leq 0.5$) 'small' for the 4th , 5th and 6th pair ($d \leq 0.2$). The 'large' and 'medium' effect sizes found in the leachates of Duvha CFA were significant ($p < 0.5$), while those that were 'small' were found to be insignificant ($p > 0.5$) (**Table 5. 7**). This suggests that there was a significant increase in the ΣREE content recovered with a decrease in particle size between size fractions of the 1st pair. Thus, rendering the particle size separation of those fractions to have a large effect on the increase in ΣREE content recovered. For the pairs that Cohens *d* was found to be small, the decrease in the particle size fractions had an insignificant impact on the increase in the ΣREE.

Table 5. 8: Summary of the paired sample effect sizes of the ΣREE recovered in the leachates of the sieved particle size fractions of Duvha and Tutuka CFA

		Duvha CFA	Tutuka CFA
	Pair	*d*	*d*
1	DUV-Whole - > 106 µm	.830	.490
2	> 106 µm - 106 -75 µm	-.755	-.827
3	106 -75 µm - 75 - 53 µm	.695	-.810
4	75 - 53 µm - 53 - 50 µm	-.336	-.478
5	53 - 50 µm - 50 - 32 µm	.018	.134
6	50 - 32 µm - 32 -25 µm	.480	-.781
7	32 -25 µm - < 25 µm	-.606	-.280

In Tutuka CFA, the effect sizes were 'large' for the 2nd and 3rd pair ($d \geq 0.8$), 'medium' for the 6th pair ($0.2 \geq d \leq 0.5$), 'small' for the 1st, 4th , 5th and 7th pair and ($d \leq 0.2$). The 'large' and 'medium' effect sizes found in the leachates of Tutuka CFA were significant ($p < 0.5$), while those that were 'small' were found to be insignificant ($p > 0.5$) (**Table 5. 7**). This suggests that there was a significant increase in the ΣREE content recovered between the particle size fractions of the 2nd, 3rd and 6th pair. Therefore, the particle size separation of these pairs had a large effect on the increase in ΣREE content recovered. For the pairs that Cohens *d* was found to be small indicates that the decrease in the particle size fractions had an insignificant impact on the increase in the ΣREE.

5.3.4. Recovery Efficiencies of Rare Earth Elements

The leaching efficiencies (α) of the whole and sieved fractions of Duvha and Tutuka were determined and overall, in both CFAs α was low and increased with a decrease in particle size, showing relatively greater leachability of ΣREE in the finer fractions. However, the trend was defined in the leachate of Tutuka CFA compared to the leachate of Duvha CFA. In both the leachates of Duvha and Tutuka CFA, the highest α for ΣREE was observed in the finest size fraction (< 25 µm) with α of 38.31 % and 36.39 %, respectively. The lowest α was observed in the un-sieved (whole sample) in Duvha CFA (27.30 %) and the > 106 µm in Tutuka CFA (31.32 %). Although in the raw sieved fractions of both CFAs it was observed that the >106 µm fractions were depleted in REEs relative to the whole, the α were slightly greater in this fraction in Duvha CFA and lower in Tutuka CFA than the whole. Furthermore, an insignificant positive moderate correlation was found between α of the ΣREE with particle size in Duvha CFA (R = 0.59, p = .16), while in Tutuka CFA very high significant positive correlation (R = 0.81, p = .025) was found. Similarly to the recovery of REEs from sieving of the raw CFAs, α of the ΣREE in Tutuka CFA displayed a much stronger relationship with particle size compared to Duvha CFA.

The range of α observed in the leachates of the whole (un-sieved) and particle size fractions of Duvha and Tutuka CFA were generally low. In addition, the observed α were lower than those reported in previous studies, more specifically studies whose suggested optimum fusion and acid leaching conditions were adopted in this study **(Section 2.7**)(Guo et al., 2013; Taggart et al., 2016; Taggart et al., 2018a; Cao et al., 2018; Tang et al., 2019). Tang et al. (2019) used an S/L ratio of 1:20 and reported REE α to increase from below 50 % to 60 - 92 % and Cao et al.

(2018) reported similar α. King et al. (2018), reported REE α ranging between 40 - 60 % when conducting a similar study with CFA of similar properties to Duvha and Tutuka CFA.

The α of HREEs was higher in both CFAs compared to that of LREEs with the highest α observed in the finest size fraction (<25 μm) in Duvha CFA (48.38 %) and the 32 -25 μm size fraction in Tutuka CFA (47.44 %). Anand et al. (2020) observed a similar trend where approximately 88% of HREEs were leached, while 42% of the LREEs were leached, although sulphuric acid (H_2SO_4) was used as the lixiviant in this study. Often, HREEs are associated with organic matter in coal and are released from the matrix during combustion, this leaves the potential of HREEs being absorbed onto other solid phases acting as exchangeable type ions, thus making HREEs more easily leachable than LREEs (Meor, 2013). Contrarily, Meor (2013) observed the leachability of HREEs (i.e., 28 %) to be rather poor than LREEs (i.e., 95 %) when leaching with HCl. The leaching behaviour of LREEs in Duvha and Tutuka CFA may suggest that LREEs were encapsulated in mineral phases that may not have been effectively leached under the conditions applied in this study, hence, partially responsible for their low recovery in the whole (un-sieved) and particle size fractions.

5.4. Solid Residue Characterization

5.4.1. Morphology

In an attempt to obtain a better understanding of the changes that occur to CFA during acid leaching, the leached solid residues of both CFAs were characterized in terms of their morphological structure, mineral and elemental compositions. It is important to note that the characterization of the solid residues was conducted on the whole samples and not the sieved size fractions. The same analytical techniques that were used to characterize the raw CFAs were used to characterize the residues. The findings are presented in the following sections below.

The morphology of the particles of the leached solid residues of Duvha and Tutuka CFA were quite different in shape and structure in comparison to the raw and fused CFAs as depicted in **Figure 5. 5** and **Figure 5. 6**. In the raw CFAs, the particles were mostly spherical, with some irregular shaped structures in an agglomerated form. In addition, the surface texture of the particles was mostly smooth in the case of Duvha CFA (**Figure 5. 5B**) and dendritic in Tutuka CFA (**Figure 5. 6B**). The fused CFAs appeared to have lost most of the structures that were

observed in the raw CFA such as the ferrospheres and the spherical shapes of most particles (**Figure 5. 5C** and **Figure 5. 6C**). In addition, the fused samples had features of disintegration in the form of melting as depicted in **Figure 5. 5C** and **Figure 5. 6C**. The absence of the original morphology in the sintered CFA indicates that the inherent mineral composition was destroyed and localized melting between particles occurred to break bonds and form new compounds (Shemi, 2013; Bai et al., 2018).

On the other hand, the leached solid residues were irregular in shape and appeared to have been crusted, etched and disintegrated. In addition, the ferrospheres observed on the raw Tutuka CFA were not observed on the leached solid residue as depicted in **Figure 5. 6E**. This agreed with the EDS and XRF analyses as Fe and Fe_2O_3 were not abundant in the leached CFA residue compared to the raw, suggesting that most of the Fe present in the CFA had been leached. The observed changes in the morphology including the absence of ferrospheres and predominance of irregular disintegrated particles rather than spherical (**Figure 5. 5F** and **Figure 5. 6F**) indicate physical decomposition. This is a result of alkali fusion with NaOH as well as leaching with HCl.

The EDS analyses of the leached solid residues of Duvha and Tutuka CFA revealed that Al and Si were relatively abundant in both CFAs, however, less abundant compared to the raw (un-leached) samples. This was expected as the alkali fusion of CFA with NaOH decomposed (activated) the aluminosilicate glass and the CFA metal oxides, thus rendering the compounds soluble when the CFA was reacted with HCl (Wen et al., 2020). The leached solid residue of Duvha CFA was observed to have a relatively high abundance of Au (10.12 ± 24.79 wt %). Au is often found on the surface of the glass spherules in CFAs, with similar leaching behaviour to several trace elements (i.e., As, Sb, W, F, Pb, Ag) (Seredin and Dai, 2014) and is represented by the white spots on the SEM micrographs (**Figure 5. 5F** and **Figure 5. 6F**). This element was not detected in the raw Duvha and Tutuka CFA EDS analyses however, this does not mean Au was not present in the raw CFAs. The possible explanation for this is that the particle spots analysed in the raw CFAs were not abundant in Au or that the alkali-fusion acid leaching of the CFAs resulted in easier detection of Au in the residues.

REEs were not detected in the EDS analyses of the fused CFAs of Duvha and Tutuka as well as in the leached residue of Duvha CFA. However, REEs were observed in the leached solid residue of Tutuka CFA, and Ce was the only REE detected, with an abundance of 0.23 ± 0.16 wt %. The inability to identify REEs during SEM-EDS analysis of the leached solid residues

may imply that majority of REEs were recovered in the leachate. However, considering the low REEs recoveries obtained in this study the observation in the latter suggests that the particle spots selected for EDS analyses in the fused and leached solid residues of both CFAs were not abundant in REEs. Furthermore, SEM-EDS may be an ineffective technique in quantifying REEs, particularly those that are embedded within the matrix and not associated with the surface of the particle.

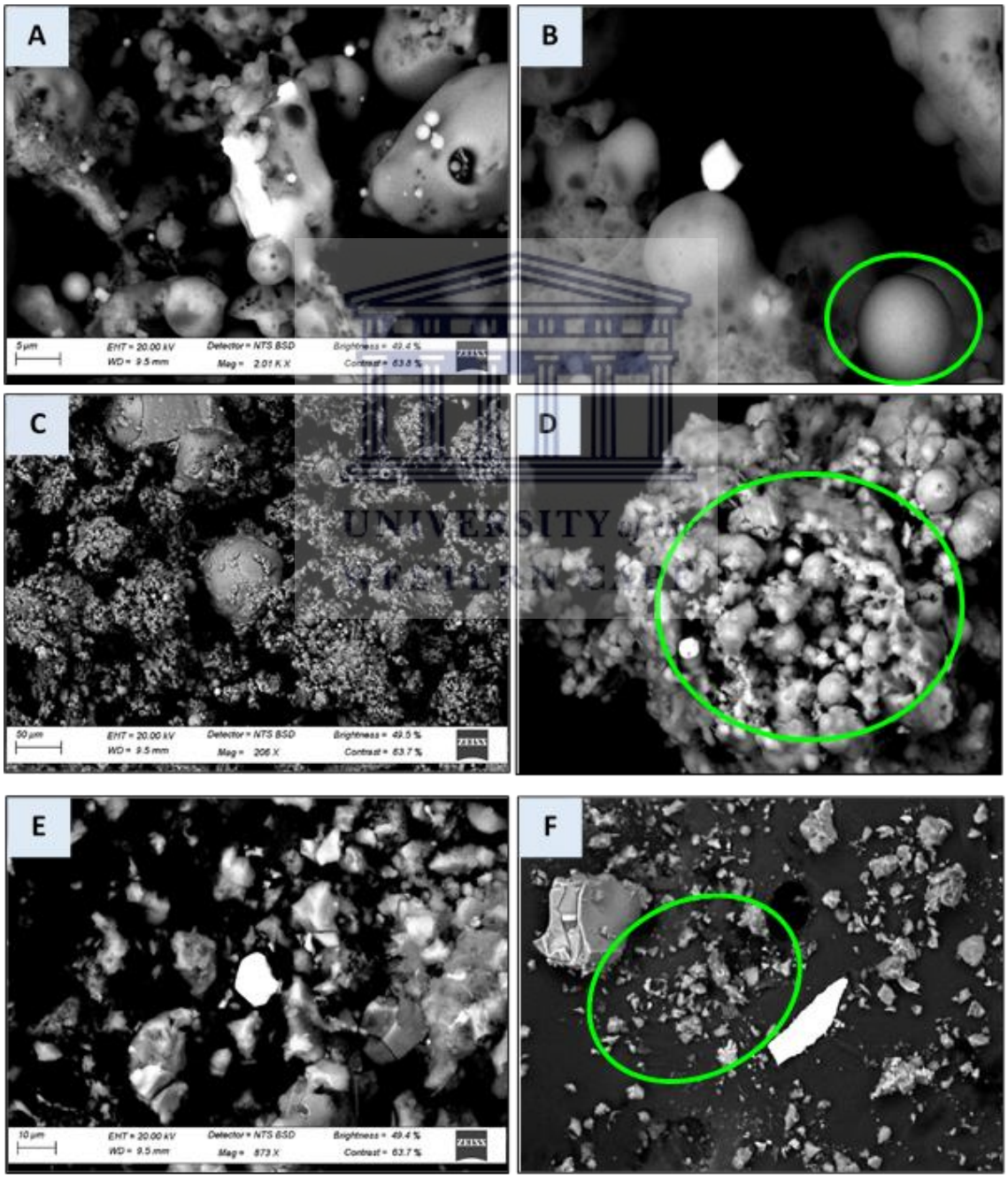

Figure 5. 5: SEM micrographs of Duvha CFA (A & B) raw CFA, (C & D) Fused CFA and (E & F) acid leached CFA

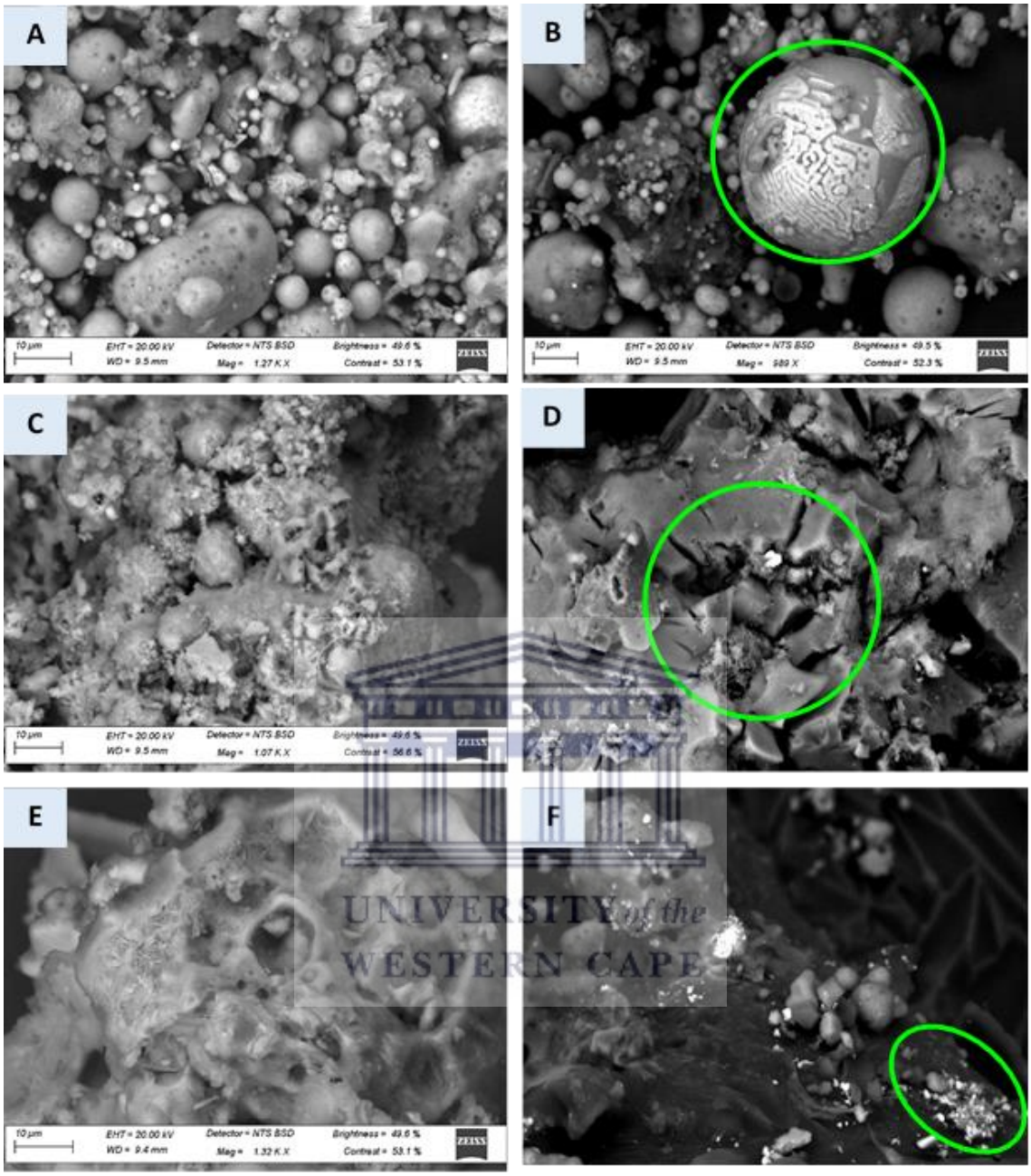

Figure 5. 6: SEM micrographs of Tutuka CFA (A & B) raw CFA, (C & D) Fused CFA and (E & F) acid leached CFA

5.4.2. Mineral Composition

The leached solid residues of Duvha and Tutuka CFA displayed quite similar XRD spectra. In order of abundance halite (NaCl), chloraluminite ($AlCl_3 \cdot 6H_2O$) and quartz (SiO_2) were the only mineral phases identified. Halite and chloraluminite are the two mineral phases formed during and possibly after the leaching of the CFA as these minerals were not identified in the raw CFAs. The abundance of halite in the residue is due to the fusion of the CFAs with NaOH and

the leaching of the fused CFA with HCl, whereby high amounts of Na^+ and Cl^- were made available in solution. Furthermore, as the residues dried crystallization of some minerals, possibly of halite and chloraluminite took place on the top surface of the residue as shown in **Figure 5. 7.**

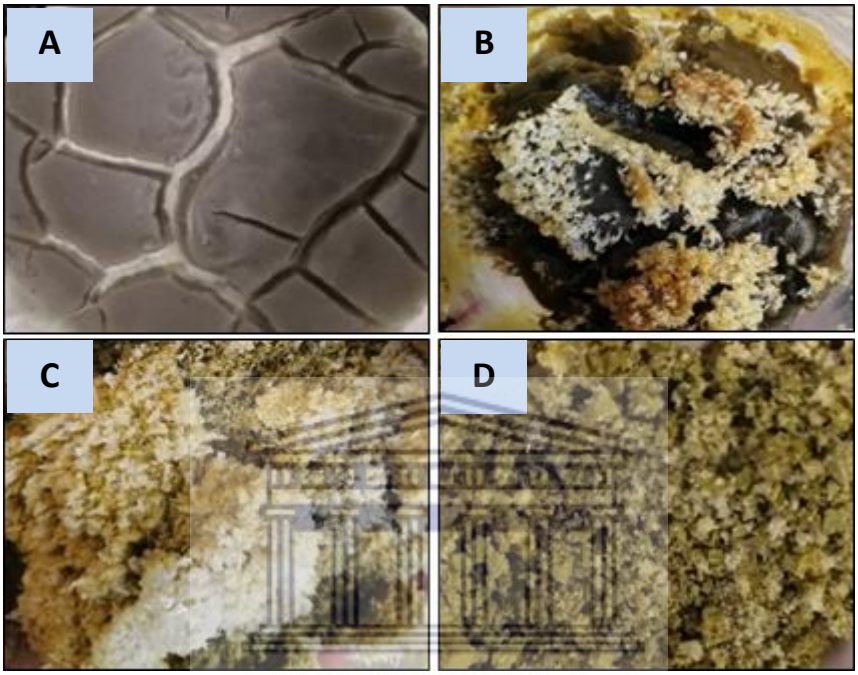

Figure 5. 7: Images showing the progression of the drying of the leached solid residues with time (A) after filtering, (B) after 12hrs of drying in the oven, (C) after 24hrs of drying and (D) post drying and grinding

The quartz peaks that were observed in the raw CFAs appear to have disappeared in the leached solid residues of both CFAs, however, they appeared so due to the extremely high peak of halite in the solid residues (**Figure 5. 8** and **Figure 5. 9**). Thus, there was minimal variation in the relative intensity of quartz in the XRD spectra of the leached solid residues compared to that of the raw CFAs. This suggests that relatively small amounts of quartz were decomposed during alkali fusion with NaOH and leaching with HCl. There are several possible explanations for this observation. Firstly, the use of NaOH as a sintering agent and the conditions used during the fusion of CFA may have been ineffective at transforming and decomposing the quartz in both of the CFAs. Thus, not effectively assisting in the solubilisation of REE-bearing phases during acid leaching. Secondly, as much as HCl has proved to be one of the acids that yield relatively high REE recovering efficiencies, meaning HCl can effectively dissolve the aluminosilicate phases in CFA. It is possible that the leaching conditions applied including the

use of HCl as a lixiviant did not favour the aluminosilicate phases in the selected CFAs used in this study. Therefore, quartz remained relatively unchanged in the acid leached solid residue of both CFAs, meaning the mineral was not effectively transformed into soluble compounds.

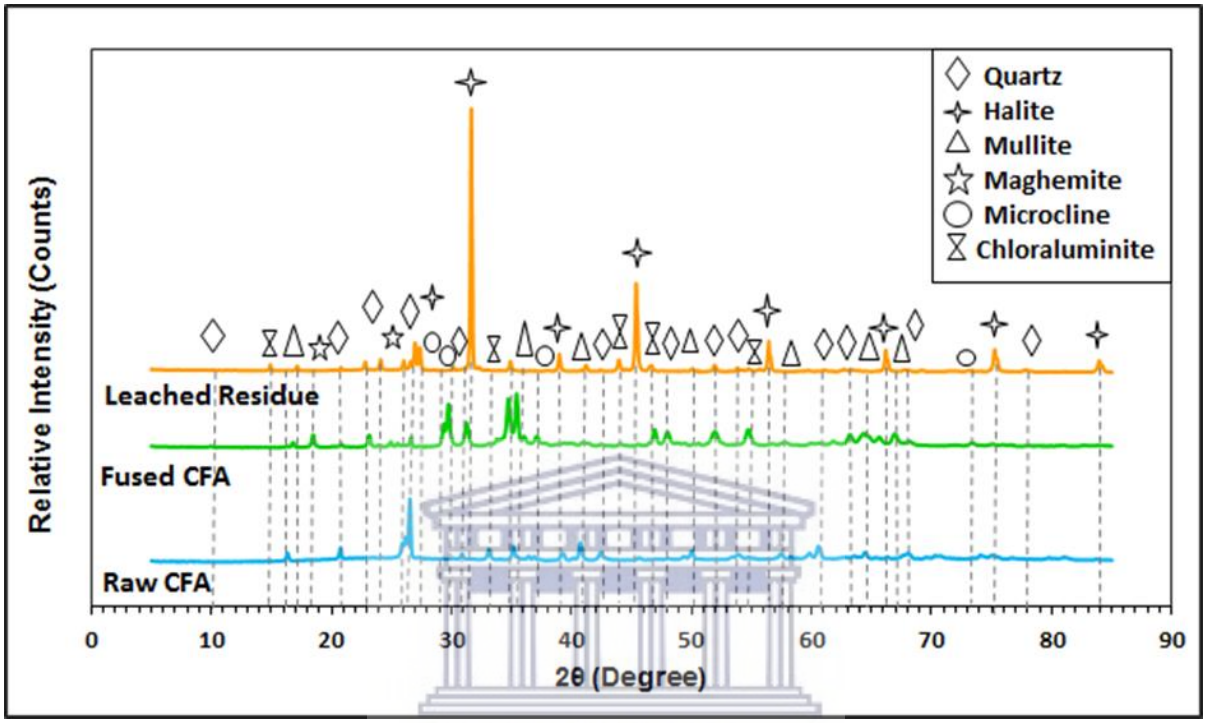

Figure 5. 8: Graph illustrating the XRD patterns of the raw, fused and leached solid residues of Duvha CFA

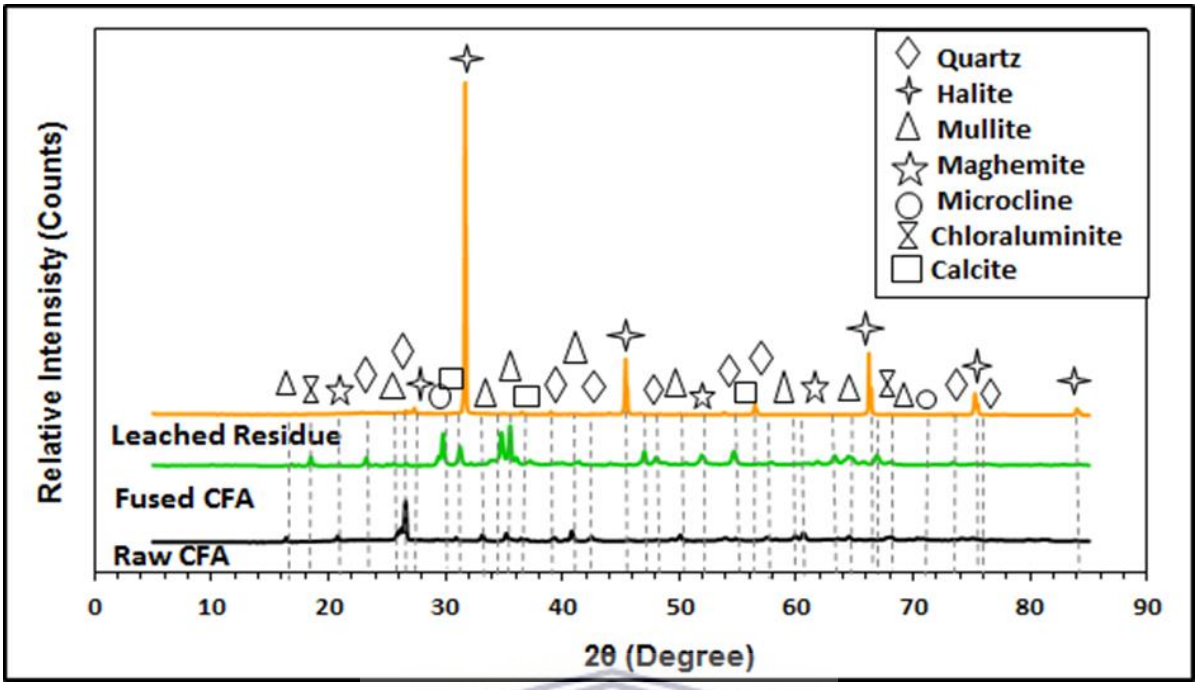

Figure 5. 9: Graph illustrating the XRD patterns of the raw, fused and leached solid residues of Tutuka CFA

The leached solid residues of both CFAs were observed to have a "gel" like consistency after filtering and this was most likely silica as it was one of the major elements leached. Tang et al. (2019) also observed this "gel" like substance and suggested that its abundance could hinder the recovery of REEs. Taking into account the shrinking core model which describes the leaching process of CFA with HCl (Shemi, 2013; Wanta et al., 2020) and that relatively low REEs were recovered during the alkali-fusion acid leaching in this study, the possibility of the 'gel' like inhibiting the recovery of REEs can be explained as follows. The mineral quartz (SiO_2) and mullite ($3Al_2O_3 \cdot 2SiO_2$) were the two major mineral sources of silica in the leachates of both CFAs. Therefore, during CFA leaching with HCl, it is expected for silica to be one of the major products, most likely be in a form of a gel and this was observed. Over time, this silica gel in solution can potentially act as the product layer in the shrinking core model, thereby limiting the reaction as the surface area is reduced. Thus, reducing the transport of reactants to the surface of the CFA particles. For this reason, further dissolution of quartz, mullite and other aluminosilicate phases was limited, thereby limiting the liberation of REEs. Therefore, the product layer (silica gel) acts as the rate-determining step.

Based on the XRD data of the raw CFAs and the acid leached solid residues, it is possible to conclude that the following chemical reactions took place in the presence of the CFA with HCl and can be summarised as shown below (Cao et al., 2018; Valeev et al., 2018). Furthermore, REEs tend to be encased in Fe, Ca-rich aluminosilicate glass phases. Therefore, the HCl or any other acid is often preferentially reacted with the oxides of the major metal elements (as shown in eqs 1, 2 and 3) and then the chemical reaction shown in equation 4 proceeds.

$$Fe_2O_{3\,(s)} + 6HCl_{\,(l)} = 2FeCl_{3\,(aq)} + 3H_2O_{\,(l)} \quad (1)$$

$$CaO_{\,(s)} + 2HCl_{\,(l)} = CaCl_{2\,(aq)} + H_2O_{\,(l)} \quad (2)$$

$$3Al_2O_3 \cdot 2SiO_{2\,(s)} + 18HCl_{\,(l)} = 6AlCl_{3\,(aq)} + 2SiO_{2\,(s)} + 9H_2O_{\,(l)} \quad (3)$$

Using RE_2O_3 as an example, the following reaction could occur between oxides of REEs and HCl:

$$RE_2O_{3\,(s)} + 6HCl_{\,(l)} = 2RECl_{3\,(aq)} + 3H_2O_{\,(l)} \quad (4)$$

5.4.3. Elemental Composition

The composition of the major elements as oxides in weight % that remained in the leached solid residue whole (un-sieved) samples of Duvha and Tutuka CFA were determined. SiO_2 and Al_2O_3 remained the dominant oxides in both leached solid residues, indicating that these elements were strongly retained in the leached solid residues. However, the content was lower compared to that in the raw CFAs and this was to be expected as substantial amounts of these elements were leached during the recovery of REEs. The decrease in SiO_2 and Al_2O_3 reflects the dissolution of the aluminosilicate matrix of the CFAs to a certain degree, while the decrease in CaO content in the leached solid residues reflects the dissolution of free lime which exists on the outermost surface of the CFA particles (Eze et al., 2013; Akinyemi et al., 2019). MgO and MnO were below the detection limit for both leached solid residues, suggesting that the majority of these elements entered into solution during leaching. Fe_2O_3 was recorded to be present in relatively low quantities in the leached solid residues of Duvha and Tutuka CFA and this coincided with the absence of ferrospheres from the SEM micrographs of the leached solid residues. Overall, there was a decrease in wt % of the major oxides in the leached solid residues of both CFAs compared to that of the raw CFA.

The leached solid residues of Duvha and Tutuka CFA were observed to have ΣREE content of 192.81 ppm and 206.82 ppm. There was minimal variation in the individual REE content retained between the two leached solid residues except for Ce (**Appendix Q**). This observation can be attributed to the two CFAs having similar coal sources and coal combustion techniques, thus they behaved similarly during leaching. In the leached solid residue of Tutuka CFA, more Ce was retained compared to the leached solid residue of Duvha CFA with concentrations 88.42 ppm (44.81%) and 75.40 (34.75%) ppm retained, respectively. However, Duvha CFA contained more Ce than Tutuka CFA before leaching, with Ce concentrations of 216.98 ppm and 197.33 ppm, respectively. This showed that the recovery of Ce was better in Duvha CFA compared to Tutuka CFA

Interestingly, the blank leached solid residues of both CFAs contained higher ΣREE content than that measured in the raw CFAs as shown in **Table 5. 9** (**Appendix R and S**). This observation was not expected as 4.93 ppm were recovered from the Duvha CFA blank leachate. The observation could indicate potential errors with the REE analyses; the acid digestions from which the total REE values are based might have incompletely extracted the target elements from the CFAs. Similary, King et al. (2018) leached several CFAs and obtained REE recovery efficiencies >100%. The author argued that the observation indicated measurement errors, such as polyatomic interferences of REEs. However, it is also important to note that variations in the measured ΣREE can also be a function of sampling, where certain particles within the same sample contained relatively more REEs. Nevertheless, the findings of the blank leached solid residues compared to that of the acid leached solid residues depict the ineffectiveness of recovering REEs from CFA using deionized water. In addition, this supports the need for more aggressive leaching conditions such as alkali fusion and acid leaching.

Table 5. 9: Total REE composition (ppm) in the solid residues of Duvha and Tutuka CFA

	Raw CFA	Blank Leached Residue	Acid Leached Residue
Duvha CFA	573.77	614.50	192.81
Tutuka CFA	546.25	555.30	206.82

It is also important to note that Duvha CFA contained ΣREE before leaching of 573.77 ppm, while Tutuka CFA contained 546.25 ppm, this indicated that Duvha CFA performed better under the leaching conditions outlined in this study compared to Tukuka CFA as it had the least

retained ΣREE (**Table 5. 9**). The REEs Sc, Y, La, Ce, Pr and Nd were strongly retained in the acid leached solid residues of both CFAs, indicating that a relatively small amount of these REEs entered into solution during the leaching process relative to their abundance in the raw CFA (**Appendix Q**). These elements were retained in the order of Ce > La > Nd > Y > Sc > Pr, and this was in the same order of abundance for the raw CFA of both these CFAs.

The comparison of the dominant minerals and major element composition (i.e., Fe, Ca, Al, Mg, and Si) in the raw CFAs and leached solid residues of both CFAs showed that the properties which are associated with REEs and the ones that contribute to the pozzolanic character of both CFA were not unduly changed. This suggests further possible leaching of the leached solid residues, perhaps with a different lixiviant in an attempt to liberate more REEs. However, this was not conducted as it was not within the scope of this study. Due to the pozzolanic properties of the CFA that remained in the leached solid residues, it renders the residue useful and qualifies as geo-polymeric material to be used in fly ash brick and as a binding material in the cement industry (Anand et al., 2020) which are the large-volume consumers of the fly ash waste as the untreated fly ash. In addition, it has also been investigated that the liquid effluent from acid leaching could be used to obtain gypsum by the addition of lime (CaO) and the acid recovered by distillation or membrane evaporation (Dhawan and Sharma, 2019; Anand et al., 2020). Although the acid leaching of CFA has environmental concerns due to the waste products produced, the leached residues, as well as the liquid effluent, have a potential industrial value.

5.5. Summary of Chapter Five

The study aimed to assess the effect of particle size separation on the enrichment and recovery of REEs from South African CFA. The findings of the study contribute to the understanding of the distribution of REEs with particle size and evaluating the efficiency of the alkali-fusion acid leaching technique in recovering REEs from South African CFA. This chapter discussed the findings of physical and chemical characterization of the raw CFA, sieved CFA, leachates and residue samples of Duvha and Tutuka CFA.

Duvha CFA was more porous than Tutuka CFA and the presence of pores in CFA particles increases the specific surface area and enhances the adsorption ability which plays a vital role during the leaching of CFA. Tutuka CFA exhibited numerous ferrospheres, which are considered to be rich in Fe and this agreed with the EDS analysis, which revealed high Fe

content Tutuka CFA. The presence of a relatively high content of Fe_2O_3 was indicative of the presence of REEs as they are often encased within the Fe-rich aluminosilicate glass phases and the SEMD-EDS revealed REEs La and Ce to be relatively abundant in both CFAs. This observation was to be expected as naturally, La and Ce are most abundant. However, these were the only REEs detected during the SEM-EDS analysis. Nonetheless, a broader range of REEs were detected by the TIMA analyses and REEs were found to be associated with minerals such as but not limited to maghemite, allanite, ilmenite, calcite. The abundance of REEs in both CFAs were found in the order of Ce>La>Nd>Y>Sc>Pr. Based on the American society for testing and materials (ASTM) classification method, the two CFAs can be classified as Class F fly ash (ASTM C618, 2005). This was indicated by the sum of the weight percent composition of the major mineral phases: SiO_2, Al_2O_3 and Fe_2O_3 present in the CFAs which was found to be > 70 %.

To better understand the distribution of REEs with the particle size of CFA, the ΣREE composition of Duvha and Tutuka CFA for each sieved particle size fraction was determined. Overall, there was an increase in ΣREE content with a decrease in particle size in both CFAs, showing moderate enrichment of ΣREE in the finer particle size fractions. Moreover, statistical analyses revealed that an insignificant negative moderate correlation and substantial relationship existed between the particle size of Duvha CFA with the ΣREE recovered ($R = 0.68$, $p = .096$,). At the same time, there was a very high negative correlation and dependable relationship ($R = 0.99$, $p < .001$) between the particle size of Tutuka CFA with the ΣREE recovered. It was found that LREEs and HREEs did not contribute equally to the enrichment of REEs. The unequal contribution of LREEs and HREEs is attributed to the variation in the chemical composition of individual REE minerals, although REEs typically occur in the same minerals.

REEs in the leachates of the sieved particle size fractions of Duvha and Tutuka CFA revealed an increase in the recovery of ΣREE with a decrease in particle size. In Duvha CFA, the relationship was found to be insignificant and negative with moderate correlation and was considered substantial ($R = 0.66$, $p = .108$), while in Tutuka CFA the relationship was found to be significant and negative with high correlation and deemed a dependable relationship ($R = 0.94$, $p = .002$). Similarly, the leaching efficiencies revealed the same trend where the efficiencies increased with a decrease in particle size. A positive moderate correlation was found between the α of the total REEs with particle size in Duvha CFA ($R = 0.59$, $p = .16$),

while in Tutuka CFA a very high positive correlation (R = 0.81, p = .025) was found. However, the range of α observed in the leachates of the whole (un-sieved) and particle size fractions of Duvha and Tutuka CFA were generally low. The α of HREEs was higher in both CFAs compared to that of LREEs with the highest α observed in the finest size fraction (<25 µm) in Duvha CFA (48.38 %) and the 32 -25 µm size fraction in Tutuka CFA (47.44 %). The leaching behaviour of LREEs in Duvha and Tutuka CFA may suggest that LREEs were encapsulated in mineral phases that may not have been effectively leached under the conditions applied in this study, hence, partially responsible for their low recovery in the whole (un-sieved) and particle size fractions.

The morphology of the particles of the leached CFAs was different in shape and structure compared to the raw and fused CFAs. The leached CFA residue samples appeared to have been crusted, etched and disintegrated, showing that leaching had occurred. Also, ferrospheres that were observed in the raw Tutuka CFA were not found in the leached CFA. The residue of Duvha and Tutuka CFA displayed quite similar XRD spectra. Halite and chloraluminite were minerals formed during acid leaching as they were not present in the raw CFAs. Furthermore, the XRD spectra of both CFAs showed that the abundance of quartz remained relatively unchanged compared to that in the raw CFAs. This agreed with the XRF results of the solid residues which revealed that SiO_2 and Al_2O_3 remained the major elements. This suggested that a large amount of mullite and quartz were not transformed into their active states. The analyses of the REEs retained in the leached solid residues revealed that there was minimal variation in the amounts of REEs retained between the two residues, except for Ce. The REE Ce was retained more in Tutuka compared to Duvha CFA leached residue with 88.42 ppm (44.81%) and 75.40 (34.75%) ppm retained, respectively. In order of abundance, the following REEs were most retained in the leached solid residues of both CFAs: Ce > La > Nd > Y > Sc > Pr. In addition, the order of abundance of these elements was in the same order of abundance for the raw CFA of both these CFAs. Both leached solid residues displayed to have preserved the properties of CFA that are associated with REEs and the ones that contribute towards the pozzolanic characteristic, thus, indicating that the leached residues have potential industrial value.

CHAPTER SIX: CONCLUSION AND RECOMMENDATIONS

6. Introduction

The production of products such as mobile phones, space-based satellites, communication systems, hybrid vehicles and rechargeable batteries are dependent on the unique properties of Rare Earth Elements (REEs). In recent years, there has been an increase in the demand for REEs due to the increasing number of their applications. Thus, there has been increasing interest in finding alternative sources for REEs and Coal Fly Ash (CFA) is a viable potential source. Also, there has been great interest in investigating the feasibility of recovering REEs from CFA and the possibility of optimizing the current recovery techniques. The main focus in the investigations has been to use equipment and products that are environmentally sustainable and economically efficient.

In South Africa, millions of tons of CFA is produced annually by coal-fired power plants during the generation of electricity. The management of this by-product has been a major concern due to the environmental issues associated with its disposal. There are several advantages to recovering REEs from CFA than in REE ore-bearing minerals, however, the main one is the availability of CFA as it is already mined. Furthermore, the ability to recover REEs from CFA has economic and environmental benefits as value-added products can be recovered from CFA.

6.1. Overview of the study

This study aimed to assess the effect of particle size separation on the enrichment and recovery of REEs from South African CFA. The objectives were to qualitatively and quantitatively characterize the morphology, mineral and elemental composition of Duvha and Tutuka CFA; to assess the relationship between REE with the particle size of CFA; to determine REE recovery efficiencies; and characterize, the morphology, mineral, as well as the elemental composition of solid residues produced after alkali-fusion acid leaching.

The CFA beneficiation process investigated was the recovery of REEs from CFA and as a means of optimization, the main focus was to assess the relationship between REEs and particle size. To achieve the aim and objectives of this study, several analytical techniques such as SEM-EDS, XRD, XRF, TIMA, ICP-MS and LA ICP- MS were applied to characterize the raw Duvha and Tutuka CFA, the supernatant water obtained from the alkali-fusion acid leaching of

these CFAs as well as the leached solid residues. The findings of these analyses were discussed to give a conclusive statement on the study.

6.2. Conclusion

Based on the findings of the study, the hypothesis which stated that the REE concentration increase with a decrease in particle size in CFA was proven to be true for Tutuka CFA. Therefore, the study accepts the hypothesis. Furthermore, this statement was also proven to be true in the leaching of REEs, whereby an increase in leaching efficiencies was observed with a decrease in particle size, with particle size < 25 μm showing the greatest leaching efficiency. The relationship was stronger in Tutuka CFA compared to Duvha CFA. Thus, Tutuka CFA would be better suited for particle size separation for REE enrichment and this suggests that not all CFAs may have a significant increase in REE content with particle size separation and this is in agreement with some findings in the literature. Therefore, concerning the up-scaling of REE recovery other techniques of enriching REEs should be considered.

The pozzolanic properties that were observed in the raw CFAs remained relatively unchanged in the leached solid residues even though there were differences in the mineralogical and elemental compositions. Taking into account that relatively low REE recovery efficiencies were obtained, it indicates that the alkali-fusion acid leaching conditions applied in this study were not effective at liberating the majority of the REEs. Therefore, the major mineral structures of CFA that contained REEs were not effectively decomposed. However, this also suggests that the solid waste products obtained were not more toxic than the raw CFA as they were similar in composition.

Although relatively low REE recovery efficiencies were obtained, this study has effectively demonstrated that physical separation by particle size can significantly enrich CFA with REEs in the finer size fractions. In addition, it has been confirmed that the finer particle size fractions of CFA are enriched in REE content compared to the whole (un-sieved) CFA.

6.3. Recommendations

This study has proven that physical separation by particle size can concentrate REEs in the finer size fractions for Tutuka CFA. This resulted in moderate enrichment of REEs with a decrease in particle size, however, the recovery efficiencies were relatively low. It is evident

that perhaps for better recovery efficiencies more than one separation technique is required to concentrate REEs before recovery. Thus, future studies need to focus on assessing the feasibility of combing particle, magnetic and density separation techniques in an attempt to find a fraction that is most abundant in REEs. Nevertheless, it is important to keep in mind that different CFAs will respond differently to these separation techniques; it is not a one size fits all technique. Thus, the key is to explore and develop better REE recovery techniques, especially techniques that are curated for South African CFA as this will improve the yield of REEs recovered.

Furthermore, future studies need to explore leaching the leached solid residues several times as significant amounts of REEs were retained in them. This can be approached like a sequential extraction scheme, whereby the leached solid residues are taken through several leaching stages. This will allow targeting of the majority of the retained REEs, as different leaching conditions may be applied in each stage. Also, it is recommended that the leached solid residues be considered to be used as geo-polymeric material, fly ash brick making material and as a binding material in the cement industry. This is a result of the pozzolanic properties of CFA that remained relatively unchanged in the leached solid residues. Literature has shown that the effluent produced from the acid leaching could be used to obtain gypsum by the addition of lime (CaO), which the cement will find valuable. Therefore, this can also be explored with leachates produced from South African CFA. Despite that the recovery of REEs from CFA by acid leaching raises environmental concerns due to the production of waste that may be toxic, the waste products produced have shown to have potential industrial value as they possess similar chemical properties as the raw CFAs.

REFERENCES

Abd El-Mottaleb, M., Cheira, M.F., Gouda, G.A.H., Ahmed, A.S.A., 2016. Leaching of Rare Earth Elements from Egyptian Western Desert Phosphate Rocks using HCl. Chemistry of Advanced Materials 1, 33–40.

Akinlua, A., Akinyeye, R.O., Akinyemi, S.A., Petrik, L.F., Gitari, W.M., 2011. The Leachability of Major Elements at Different Stages of Weathering in Dry Disposed Coal Fly Ash. Coal Combustion and Gasification Products 3, 28–40.

Akinyemi, S.A., Akinlua, A., Gitari, W.M., Nyale, S.M., Akinyeye, R.O., Petrik, L.F., 2012. An Investigative Study on the Chemical, Morphological and Mineralogical Alterations of Dry Disposed Fly Ash During Sequential Chemical Extraction. Energy Science and Technology 3, 28–37.

Akinyemi, S.A., Akinlua, A., Gitari, W.M., Petrik, L.F., 2011. Mineralogy and Mobility Patterns of Chemical Species in Weathered Coal Fly Ash, Energy Sources. Energy Sources 33, 768–784.

Akinyemi, S.A., Gitari, W.M., Petrik, L.F., Nyakuma, B.B., Hower, J.C., Ward, C.R., Oliveira, M.L.S., Silva, L.F.O., 2019. Environmental evaluation and nano-mineralogical study of fresh and unsaturated weathered coal fly ashes. Science of the Total Environment 663, 177–188.

Akinyemi, S.A., Gitari, W.M., Thobakgale, R., Petrik, L.F., Nyakuma, B.B., Hower, J.C., Ward, C.R., Oliveira, M.L.S., Silva, L.F.O., 2020. Geochemical fractionation of hazardous elements in fresh and drilled weathered South African coal fly ashes. Environmental Geochemistry and Health 3, 1–18.

Alegbe, J., Ayanda, O.S., Ndungu, P., Alexander, N., Fatoba, O.O., Petrik, L.F., 2018. Chemical, Mineralogical and Morphological Investigation of Coal Fly Ash Obtained from Mpumalanga Province, South Africa. Research Journal of Environmental Sciences 12, 98–105.

Ameh, A.E., Fatoba, O.O., Musyoka, N.M., Petrik, L.F., 2017. Influence of aluminium source on the crystal structure and framework coordination of Al and Si in fly ash-based zeolite NaA. Powder Technology 306, 17–25.

Anand, K.., Serajuddin, M., Rama Devi, G., Thakurta, S.G., Sreenivas, T., 2020. On the characterization and leaching of rare earths from a coal fly ash of Indian origin. Separation Science and Technology (Philadelphia) 6395, 1–18.

Bai, S., Zhou, L., Chang, Z., Zhang, C., Chu, M., 2018. Synthesis of Na-X zeolite from Longkou oil shale ash by alkaline fusion hydrothermal method. Carbon Resources Conversion 1, 245–250.

Balaram, V., 2019. Rare earth elements: A review of applications, occurrence, exploration, analysis, recycling, and environmental impact. Geoscience Frontiers 10, 1285–1303.

Bern, C.R., Yesavage, T., Foley, N.K., 2017. Ion-adsorption REEs in regolith of the Liberty Hill pluton, South Carolina, USA: An effect of hydrothermal alteration. Journal of Geochemical Exploration 172, 29–40.

Blissett, R.S., Smalley, N., Rowson, N.A., 2014. An investigation into six coal fly ashes from the United Kingdom and Poland to evaluate rare earth element content. Fuel 119, 236–239.

Braun, J.J., Pagel, M., Herbilln, A., Rosin, C., 1993. Mobilization and redistribution of REEs and thorium in a syenitic lateritic profile: A mass balance study. Geochimica et Cosmochimica Acta 57, 4419–4434.

Cao, S., Zhou, C., Pan, J., Liu, C., Tang, M., Ji, W., Hu, T., Zhang, N., 2018a. Study on Influence Factors of Leaching of Rare Earth Elements from Coal Fly Ash. Energy & Fuels 32, 8000–8005.

Cao, S., Zhou, C., Pan, J., Liu, C., Tang, M., Ji, W., Hu, T., Zhang, N., 2018b. Study on Influence Factors of Leaching of Rare Earth Elements from Coal Fly Ash. Energy and Fuels 32, 8000–8005.

Chand, P., Kumar, A., Gaur, A., Mahna, S.K., 2009. Elemental Analysis of Ash using X-Ray Fluorescence Technique, Asian Journal of Chemistry.1-8.

Choi, S.-K., Lee, S., Song, Y.-K., Moon, H.-S., 2002. Leaching characteristics of selected Korean fly ashes and its implications for the groundwater composition near the ash disposal mound. Fuel 81, 1083–1090.

Clarke, L.., Sloss, L.B., 1992. Trace elements- emissions from coal combustion and gasification, IEA Coal Research.

Dai, S., Zhao, L., Hower, J.C., Johnston, M.N., Song, W., Wang, P., Zhang, S., 2014. Petrology, mineralogy, and chemistry of size-fractioned fly ash from the Jungar power plant, Inner Mongolia, China, with emphasis on the distribution of rare earth elements. Energy and Fuels 28, 1502–1514.

Dai, S., Zhao, L., Peng, S., Chou, C.L., Wang, X., Zhang, Y., Li, D., Sun, Y., 2010. Abundances and distribution of minerals and elements in high-alumina coal fly ash from the Jungar Power Plant, Inner Mongolia, China. International Journal of Coal Geology 81, 320–332.

Dalton, A., Feig, G.T., Barber, K., 2018. Trace metal enrichment observed in soils around a coal fired power plant in South Africa. Clean Air Journal 28, 1–9.

Das, S., Gaustad, G., Sekar, A., Williams, E., 2018. Techno-economic analysis of supercritical extraction of rare earth elements from coal ash. Journal of Cleaner Production 189, 539–551.

Davison, R.L., Natusch, D.F.S., Wallace, J.R., Evans, C.A., 1974. Trace Elements in Fly Ash Dependence of Concentration on Particle Size. Environmental Science & Technology 8, 1107–1113.

de Sá Paye, H., de Mello, J.W.V., de Magalhães Mascarenhas, G.R.L., Gasparon, M., 2014. Distribution and fractionation of the rare earth elements in Brazilian soils. Journal of Geochemical Exploration 161, 27–41.

Dhawan, H., Sharma, D.K., 2019. Advances in the chemical leaching (inorgano-leaching), bio-leaching and desulphurisation of coals. International Journal of Coal Science and Technology 6, 169–183.

Eskom Holdings SOC Ltd, 2020. Power Stations [WWW Document]. URL http://www.eskom.co.za/Whatweredoing/ElectricityGeneration/PowerStations/Pages/Matimba_Power_Station.aspx (accessed 4.9.20).

Estrade, G., Marquis, E., Smith, M., Goodenough, K., Nason, P., 2019. REE concentration processes in ion adsorption deposits: Evidence from the Ambohimirahavavy alkaline complex in Madagascar. Ore Geology Reviews 112, 103027.

Etale, A., Tavengwa, N.T., Pakade, V.E., 2018. Metal Adsorption by Coal Fly Ash: The Role of Nano-sized Materials. Coal Fly Ash Beneficiation - Treatment of Acid Mine Drainage with Coal Fly Ash.1-24.

Eze, C., Nyale, S.M., Akinyeye, R.O., Gitari, W.M., Akinyemi, S.A., Fatoba, O.O., Petrik, L.F., 2013. Chemical, mineralogical and morphological changes in weathered coal fly ash: A case study of a brine impacted wet ash dump. Journal of Environmental Management 129, 479–492.

Eze, C.P., 2011. Chemical, Physical and Morphological Changes in Weathered Coal Fly Ash: a Case Study of Brine Impacted Wet Ash Dump.

Eze, C.P., 2014. Determination of toxic elements, rare earth elements and radionuclides in coal fly ash, products and waste. University of the Western Cape.

Eze, C.P., Fatoba, O., Madzivire, G., Ostrovnaya, T.M., Petrik, L.F., Frontasyeva, M. V., Nechaev,

A.N., 2014. Elemental composition of fly ash: a comparative study using nuclear and related analytical techniques / Skład pierwiastkowy popiołów lotnych: studium przypadku z wykorzystaniem metod nuklearnych i analitycznych. Chemistry-Didactics-Ecology-Metrology 18, 19–29.

Fatoba, O. O., 2007. Chemical compositions and leaching behaviour of some South African fly ashes. University of the Western Cape.

Fatoba, O.O., 2010. Chemical interactions and mobility of species in fly ash-brine co-disposal systems Ojo Olanrewaju Fatoba. University of the Western Cape.

Franus, W., Wiatros-Motyka, M.M., Wdowin, M., 2015. Coal fly ash as a resource for rare earth elements. Environmental Science and Pollution Research 22, 9464–9474.

Galbarczyk-Gasiorowska, L., 2010. Rare earth element mobility in a weathering profile-a case study from the karkonosze massif (SW Poland). Acta Geologica Polonica 60, 599–616.

Ganne, J., Feng, X., 2017. Geochemistry, Geophysics, Geosystems. Geochemistry Geophysics Geosystems 18, 1–26.

Gbor, P.K., Jia, C.Q., 2004. Critical evaluation of coupling particle size distribution with the shrinking core model. Chemical Engineering Science 59, 1979–1987.

Gitari, M.W., Fatoba, O.O., Nyamihingura, A., Petrik, L.F., Vadapalli, V.R.K., Nel, J., October, A., Dlamini, L., Gericke, G., Mahlaba, J.S., 2009. Chemical weathering in a dry ash dump: An insight from physicochemical and mineralogical analysis of drilled cores. 3rd World of Coal Ash, WOCA Conference - Proceedings.

Gitari, W.M., 2006. Evaluation of the Leachate Chemistry and Contaminants Attenuation in Acid Mine Drainage by Fly Ash and its derivatives . University of the Western Cape.

Gitari, W.M., Fatoba, O.O., Petrik, L.F., Vadapalli, V.R.K., 2009. Leaching characteristics of selected South African fly ashes: Effect of pH on the release of major and trace species. Journal of Environmental Science and Health - Part A Toxic/Hazardous Substances and Environmental Engineering 44, 206–220.

Gitari, W.M., Petrik, L.F., Etchebers, O., Key, D.L., Iwuoha, E., Okujeni, C., 2008. Passive neutralisation of acid mine drainage by fly ash and its derivatives: A column leaching study. Fuel 87, 1637–1650.

Gitari, W.M., Petrik, L.F., Key, D.L., Okujeni, C., 2010. Partitioning of major and trace inorganic contaminants in fly ash acid mine drainage derived solid residues. International Journal of Environmental Science and Technology 7, 519–534.

Gollakota, A.R.K., Volli, V., Shu, C.M., 2019. Progressive utilisation prospects of coal fly ash: A review. Science of the Total Environment 672, 951–989.

Goodarzi, F., Sanei, H., 2009. Plerosphere and its role in reduction of emitted fine fly ash particles from pulverized coal-fired power plants. Fuel 88, 382–386.

Green, J.B., Manaban, S.E., 1978. Determination of Acid-Base and Solubility Behavior of Lignite Fly Ash by Selective Dissolution in Mineral Acids, Analytical Chemistry. Interscience Publishers.

Guo, Y., Li, Y., Cheng, F., Wang, M., Wang, X., 2013. Role of additives in improved thermal activation of coal fly ash for alumina extraction. Fuel Processing Technology 110, 114–121.

Hancox, P.J., 2016. The coalfields of south-central Africa: A current perspective. Episodes 39, 407–428.

Hansen, L.D., Fisher, G.L., 1980. Elemental Distribution in Coal Fly Ash Particles. UTC.

Hansen, L.D., Silberman, D., Fisher, L., 1981. Crystalline Components of Stack-Collected, Size-Fractionated Coal Fly Ash. Environmental Science & Technology 15, 1057–1062.

Hansen, Y., Notten, P.J., Petrie, J.G., 2002. The environmental impact of ash management in coal-based power generation. Applied Geochemistry 17, 1131–1141.

Haynes, R.J., 2009. Reclamation and revegetation of fly ash disposal sites – Challenges and research needs. Environmental Management 90, 43–50.

Honaker, R.Q., Zhang, W., Werner, J., 2019. Acid Leaching of Rare Earth Elements from Coal and Coal Ash: Implications for Using Fluidized Bed Combustion to Assist in the Recovery of Critical Materials. Energy and Fuels 33, 5971–5980.

Hood, M.M., Taggart, R.K., Smith, R.C., Hsu-Kim, H., Henke, K.R., Graham, U., Groppo, J.G., Unrine, J.M., Hower, J.C., 2017. Rare Earth Element Distribution in Fly Ash Derived from the Fire Clay Coal, Kentucky. Kentucky. Coal Combustion and Gasification Products 9, 22–33.

Hower, J.C., Dai, S., Seredin, V. V, Zhao, L., Kostova, I.J., Silva, L.F.O., Mardon, S.M., 2013. A Note on the Occurrence of Yttrium and Rare Earth Elements in Coal Combustion Products. Coal Combustion and Gasification Products 5, 39–47.

Hower, J.C., Eble, C.F., Dai, S., Belkin, H.E., 2016. Distribution of rare earth elements in eastern Kentucky coals: Indicators of multiple modes of enrichment? International Journal of Coal Geology 160–161, 73–81.

Huang, Z., Fan, M., Tian, H., 2020. Rare earth elements of fly ash from Wyoming's Powder River Basin coal. Journal of Rare Earths 38, 219–226.

Hulett, L.D., Weinberger, A.J., Northcutt, K.J., Ferguson, M., 1980. Chemical Species in Fly Ash from Coal-Burning Power Plants, Source: Science, New Series.210,1356-1358.

Izquierdo, M., Querol, X., 2012. Leaching behaviour of elements from coal combustion fly ash: An overview. International Journal of Coal Geology 94, 54–66.

Jankowski, J., Ward, C.R., French, D., Groves, S., 2006. Mobility of trace elements from selected Australian fly ashes and its potential impact on aquatic ecosystems. Fuel 85, 243–256.

Jayaranjan, M.L.D., van Hullebusch, E.D., Annachhatre, A.P., 2014. Reuse options for coal fired power plant bottom ash and fly ash. Reviews in Environmental Science and Biotechnology 13, 467–486.

Jha, M.K., Kumari, A., Panda, R., Rajesh Kumar, J., Yoo, K., Lee, J.Y., 2016. Review on hydrometallurgical recovery of rare earth metals. Hydrometallurgy 165, 2–26.

Jones, K.B., Ruppert, L.F., Swanson, S.M., 2012. Leaching of elements from bottom ash, economizer fly ash, and fly ash from two coal-fired power plants. International Journal of Coal Geology 94, 337–348.

Josso, P., Roberts, S., Teagle, D.A.H., Pourret, O., Herrington, R., Ponce de Leon Albarran, C., 2018. Extraction and separation of rare earth elements from hydrothermal metalliferous sediments. Minerals Engineering 118, 106–121.

Kanazawa, Y., Kamitani, M., 2006. Rare earth minerals and resources in the world. Journal of Alloys and Compounds 408–412, 1339–1343.

Kashiwakura, S., Kumagai, Y., Kubo, H., Wagatsuma, K., 2013. Dissolution of Rare Earth Elements from Coal Fly Ash Particles in a Dilute H 2 SO 4 Solvent. Open Journal of Physical Chemistry 3, 69–75.

Kim, A.G., Kazonich, G., Dahlberg, M., 2003. Relative Solubility of Cations in Class F Fly Ash. Environmental Science & Technology 37, 4507–4511.

King, J.F., Taggart, R.K., Smith, R.C., Hower, J.C., Hsu-Kim, H., 2018. Aqueous acid and alkaline extraction of rare earth elements from coal combustion ash. International Journal of Coal Geology 195, 75–83.

Klein, D.H., Andren, A.W., Carter, J.A., Emery, J.F., Feldman, C., Fulkerson, W., Lyon, W.S., Ogle, J.C., Talmi, Y., Hook, R.I. Van, Bolton, N., Al, T., 1975. Pathways of Thirty-seven Trace Elements Through Coal-Fired Power Plant. UTC.

Kolker, A., Scott, C., Hower, J.C., Vazquez, J.A., Lopano, C.L., Dai, S., 2017. Distribution of rare earth elements in coal combustion fly ash, determined by SHRIMP-RG ion microprobe. International Journal of Coal Geology 184, 1–10.

Koukouzas, N., Ward, C.R., Papanikolaou, D., Li, Z., Ketikidis, C., 2009. Quantitative evaluation of minerals in fly ashes of biomass, coal and biomass-coal mixture derived from circulating fluidised bed combustion technology. Journal of Hazardous Materials 169, 100–107.

Kumari, A., Parween, R., Chakravarty, S., Parmar, K., Pathak, D.D., Lee, J. chun, Jha, M.K., 2019. Novel approach to recover rare earth metals (REMs) from Indian coal bottom ash. Hydrometallurgy 187, 1–7.

Kutchko, B.G., Kim, A.G., 2006. Fly ash characterization by SEM–EDS. Fuel 85, 2537–2544.

Lanzerstorfer, C., 2018. Pre-processing of coal combustion fly ash by classification for enrichment of rare earth elements. Energy Reports 4, 660–663.

Lin, R., Howard, B.H., Roth, E.A., Bank, T.L., Granite, E.J., Soong, Y., 2017. Enrichment of rare earth elements from coal and coal by-products by physical separations. Fuel 200, 506–520.

Lin, R., Stuckman, M., Howard, B.H., Bank, T.L., Roth, E.A., Macala, M.K., Lopano, C., Soong, Y., Granite, E.J., 2018. Application of sequential extraction and hydrothermal treatment for characterization and enrichment of rare earth elements from coal fly ash. Fuel 232, 124–133.

Liu, H., Sun, Q., Wang, B., Wang, P., Zou, J., 2016. Morphology and composition of microspheres in fly ash from the luohuang power plant, Chongqing, Southwestern China. Minerals 6, 1–10.

Liu, P., Huang, R., Tang, Y., 2019. Comprehensive Understandings of Rare Earth Element (REE) Speciation in Coal Fly Ashes and Implication for REE Extractability. Environmental Science and Technology 53, 5369–5377.

Luther, L., 2010. Managing Coal Combustion Waste (CCW): Issues with Disposal and Use.

Mahlaba, J.S., Kearsley, E.P., Kruger, R.A., 2011. Physical, chemical and mineralogical characterisation of hydraulically disposed fine coal ash from SASOL Synfuels. Fuel 90, 2491–2500.

Manz, O.E., 1999. Coal fly ash: A retrospective and future look. Fuel 78, 133–136.

Mardon, S.M., Hower, J.C., 2004. Impact of coal properties on coal combustion by-product quality: Examples from a Kentucky power plant. International Journal of Coal Geology 59, 153–169.

Markowski, G.R., Filby, R., 1985. Trace Element Concentration as a Function of Particle Size in Fly Ash from a Pulverized Coal Utility Boiler, Environmental Science and Technology, 19, 796-804.

Matjie, R.H., Bunt, J.R., Van Heerden, J.H.P., 2005. Extraction of alumina from coal fly ash generated from a selected low rank bituminous South African coal. Minerals Engineering 18, 299–310.

McBride, M.., 1994. Environmental Chemistry of Soils, Environmental Chemistry of Soils. Oxford University Press, New York.

Meor, Y.M.S., 2013. Rate of rare earths leaching in HCI, H2SO4 AND HNO3. Advanced Materials Research 795, 1–4.

Moldoveanu, G.A., Papangelakis, V.G., 2012. Recovery of rare earth elements adsorbed on clay minerals: I. Desorption mechanism. Hydrometallurgy 117–118, 71–78.

Muriithi, G.N., 2009. CO 2 sequestration using brine impacted fly ash Magister Scientiae in the Chemistry Department , University of the Western Cape Supervisor : Dr Leslie F . Petrik. University of the Western Cape.

Musyoka, N.M., 2009. Hydrothermal synthesis and optimisation of zeolite Na-P1 from South African coal fly ash. University of the Western Cape.

Nathan, Y., Dvorachek, M., Pelly, I., Mimran, U., 1999. Characterization of coal fly ash from Israel. Fuel 78, 205–2213.

Pan, J., Hassas, B.V., Rezaee, M., Zhou, C., Pisupati, S. V., 2021. Recovery of rare earth elements from coal fly ash through sequential chemical roasting, water leaching, and acid leaching processes. Journal of Cleaner Production 284, 124725.

Pan, J., Nie, T., Vaziri Hassas, B., Rezaee, M., Wen, Z., Zhou, C., 2020. Recovery of rare earth elements from coal fly ash by integrated physical separation and acid leaching. Chemosphere 248.

Pan, J., Zhou, C., Liu, C., Tang, M., Cao, S., Hu, T., Ji, W., Luo, Y., Wen, M., Zhang, N., 2018. Modes of Occurrence of Rare Earth Elements in Coal Fly Ash: A Case Study. Energy and Fuels 32, 9738–9743.

Pan, J., Zhou, C., Tang, M., Cao, S., Liu, C., Zhang, N., Wen, M., Luo, Y., Hu, T., Ji, W., 2019. Study on the modes of occurrence of rare earth elements in coal fly ash by statistics and a sequential chemical extraction procedure. Fuel 237, 555–565.

Peiravi, M., Ackah, L., Guru, R., Mohanty, M., Liu, J., Xu, B., Zhu, X., Chen, L., 2017. Chemical extraction of rare earth elements from coal ash. Minerals and Metallurgical Processing 34, 170–177.

Pretorius, T.B., 2007. Inferential data analysis: Hypothesis testing and decision-making. Reach Publishers, Pinetown.

Price, R.C., Gray, C.M., Wilson, R.E., Frey, F.A., Taylor, S.R., 1991. The effects of weathering on rare-earth element, Y and Ba abundances in Tertiary basalts from southeastern Australia. Chemical Geology 93, 245–265.

Renew, J.E., Huang, C., Kosson, D.S., 2017. Mass Transport Release of Heavy Metal Oxyanions from Solidified/Stabilized Co- Disposed Flue Gas Desulfurization Brine and Coal Fly Ash Monoliths. World of Coal Ash (WOCA) Conference in Lexington, KY - May 9-11.

Reynolds-Clausen, K., Singh, N., 2019. South Africa's Power Producer's Revised Coal Ash Strategy and Implementation Progress. Coal Combustion and Gasification Products 11, 1–10.

Ripfumelo, M.A., 2012. Consideration of rare earth elements (REE's) associated with coal and coal ash in South Africa. Facilitating Learning Through Humour At a Nursing Education Institution in Gauteng. University of Johannesburg.

Rosita, W., Bendiyasa, I.M., Perdana, I., Anggara, F., 2020. Sequential particle-size and magnetic separation for enrichment of rare-earth elements and yttrium in Indonesia coal fly ash. Journal of Environmental Chemical Engineering 8, 1-10.

Rowland, J., 2014. Management of coal combustion wastes, World of Coal Ash.

Rybak, Aleksandra, Rybak, Aurelia, 2021. Characteristics of some selected methods of rare earth elements recovery from coal fly ashes. Metals 11, 1–27.

Safari, V., Arzpeyma, G., Rashchi, F., Mostoufi, N., 2009. A shrinking particle-shrinking core model for leaching of a zinc ore containing silica. International Journal of Mineral Processing 93, 79–83.

Saha, A.K., 2018. Effect of class F fly ash on the durability properties of concrete. Sustainable Environment Research 28, 25–31.

Sahoo, P.K., Kim, K., Powell, M.A., Equeenuddin, S.M., 2016. Recovery of metals and other beneficial products from coal fly ash: a sustainable approach for fly ash management. International Journal of Coal Science and Technology 3, 267–283.

Saikia, N., Kato, S., Kojima, T., 2006. Compositions and leaching behaviours of combustion residues. Fuel 85, 264–271.

Scott, C., Deonarine, A., Kolker, A., Adams, M., Holland, J., 2015. Size Distribution of Rare Earth Elements in Coal Ash, World of Coal Ash.

Seames, W.S., 2003. An initial study of the fine fragmentation fly ash particle mode generated during pulverized coal combustion. Fuel Processing Technology 81, 109–125.

Seidel, A., Zimmels, Y., 1998. Mechanism and kinetics of aluminum and iron leaching from coal fly ash by sulfuric acid. Chemical Engineering Science 53, 3835–3852.

Seredin, V. V., Dai, S., 2012. Coal deposits as potential alternative sources for lanthanides and yttrium. International Journal of Coal Geology.67-93

Seredin, V. V., Dai, S., 2014. The occurrence of gold in fly ash derived from high-Ge coal. Mineralium Deposita 49, 1–6.

Seredin, V. V., Finkelman, R.B., 2008. Metalliferous coals: A review of the main genetic and geochemical types. International Journal of Coal Geology 76, 253–289.

Sharonova, O.M., Anshits, N.N., Fedorchak, M.A., Zhizhaev, A.M., Anshits, A.G., 2015. Characterization of Ferrospheres Recovered from High-Calcium Fly Ash. Energy and Fuels 29, 5404–5414.

Shemi, A., 2013. Extraction of aluminium from coal fly ash using a two step-acid leach process. University of Witwatersrand.

Singh, J., Kalamdhad, A.S., 2011. Effects of Heavy Metals on Soil, Plants, Human Health and Aquatic Life Making bricks using variety of solid waste View project Anaerobic digestion View project.

Singh, R.K., Gupta, N.C., Guha, B.K., 2012. The Leaching Characteristics of Trace Elements in Coal Fly Ash and an Ash Disposal System of Thermal Power Plants. Energy Sources 34, 602–608.

Smolka-Danielowska, D., 2010. Rare earth elements in fly ashes created during the coal burning process in certain coal-fired power plants operating in Poland - Upper Silesian Industrial Region. Journal of Environmental Radioactivity 101, 965–968.

Surender, D., 2009. Active Neutralisation and Amelioration of Acid Mine Drainage With Fly Ash. University of the Western Cape.

Taggart, R.K., Hower, J.C., Dwyer, G.S., Hsu-Kim, H., 2016. Trends in the Rare Earth Element Content of U.S.-Based Coal Combustion Fly Ashes. Environmental Sciemce and Technology 50, 5919-5926.

Taggart, Ross K., Hower, J.C., Hsu-Kim, H., 2018a. Effects of roasting additives and leaching parameters on the extraction of rare earth elements from coal fly ash. International Journal of Coal Geology 196, 106–114.

Taggart, Ross K, Rivera, N.A., Ement Levard, C., Ambrosi, J.-P., Borschneck, D., Hower, J.C., Hsu-Kim, H., 2018b. Differences in bulk and microscale yttrium speciation in coal combustion fly ash †. Environmental Science: Processes & Impacts \ 2018, 1390–1403.

Tang, M., Zhou, C., Pan, J., Zhang, N., Liu, C., Cao, S., Hu, T., Ji, W., 2019. Study on extraction of

rare earth elements from coal fly ash through alkali fusion – Acid leaching. Minerals Engineering 136, 36–42.

Teo, T.W., Tan, K.C.D., Yan, Y.K., Teo, Y.C., Yeo, L.W., 2014. How flip teaching supports undergraduate chemistry laboratory learning. Chemistry Education Research and Practice 15, 550–567.

Thompson, R.L., Bank, T., Montross, S., Roth, E., Howard, B., Verba, C., Granite, E., 2018. Analysis of rare earth elements in coal fly ash using laser ablation inductively coupled plasma mass spectrometry and scanning electron microscopy. Spectrochimica Acta - Part B Atomic Spectroscopy 143, 1–11.

Tuan, L.Q., Thenepalli, T., Chilakala, R., Vu, H.H.T., Ahn, J.W., Kim, J., 2019. Leaching characteristics of low concentration rare earth elements in Korean (Samcheok) CFBC bottom ash samples. Sustainability (Switzerland) 11, 1–11.

Vadapalli, K.V.., Petrik, L.F., Fester, V., Slatter, P., Sery, G., 2007. Effect of fly ash particle size on its capacity to neutralize acid mine drainage and influence on the rheological behavior of the residual solids. In: World of Coal Ash (WOCA). World of Coal Ash, Northern Kentucky, USA. 1–16.

Vadapalli, K.V.R., Klink, M.J., Etchebers, O., Petrik, L.F., Gitari, W., White, R.A., Key, D., Iwuoha, E., 2008. Neutralization of acid mine drainage using fly ash, and strength development of the resulting solid residues. South African Journal of Science 104, 317–322.

Valeev, D., Mikhailova, A., Atmadzhidi, A., 2018. Kinetics of iron extraction from coal fly ash by hydrochloric acid leaching. Metals 8, 533-542.

van der Merwe, E.M., Mathebula, C.L., Prinsloo, L.C., 2014. Characterization of the surface and physical properties of South African coal fly ash modified by sodium lauryl sulphate (SLS) for applications in PVC composites. Powder Technology 266, 70–78.

Vassilev, S. V., Menendez, R., 2005. Phase-mineral and chemical composition of coal fly ashes as a basis for their multicomponent utilization. 4. Characterization of heavy concentrates and improved fly ash residues. Fuel 84, 973–991.

Vassilev, S. V., Vassileva, C.G., 2007. A new approach for the classification of coal fly ashes based on their origin, composition, properties, and behaviour. Fuel 86, 1490–1512.

Vassilev, S. V, Vassileva, C.G., 2005. Methods for Characterization of Composition of Fly Ashes from Coal-Fired Power Stations: A Critical Overview. Energy and Fuel 19, 973–991.

Wagner, N.J., Matiane, A., 2018. Rare earth elements in select Main Karoo Basin (South Africa) coal and coal ash samples. International Journal of Coal Geology 196, 82–92.

Wang, Z., Dai, S., Zou, J., French, D., Graham, I.T., 2019. Rare earth elements and yttrium in coal ash from the Luzhou power plant in Sichuan, Southwest China: Concentration, characterization and optimized extraction. International Journal of Coal Geology 203, 1–14.

Wanta, K.C., Astuti, W., Perdana, I., Petrus, H.T.B.M., 2020. Kinetic study in atmospheric pressure organic acid leaching: Shrinking core model versus lump model. Minerals 10, 1–10.

Ward, C.R., 2002. Analysis and significance of mineral matter in coal seams. International Journal of Coal Geology 50, 135–168.

Wen, C.., 1968. Non-catalytic Heterogeneous Solid-fluid Reaction Models. Industrial and Engineering Chemistry 60, 34–54.

Wen, Z., Zhou, C., Pan, J., Cao, S., Hu, T., Ji, W., Nie, T., 2020. Recovery of rare-earth elements from coal fly ash via enhanced leaching. International Journal of Coal Preparation and Utilization 1–15.

Yang, X., 2019. Leaching Characteristics of Rare Earth Elements From Bituminous Coal-Based Sources. University of Kentucky.

Yang, Z., Wang, C., Liu, D., Li, Y., Ning, Y., Yang, S., Zhang, Y., Tang, Y., Tang, Z., Zhang, W., 2019. Investigation of elements (U, V, Sr, Ga, Cs and Rb) leaching and mobility in uranium-enriched coal ash with thermochemical treatment. Journal of Cleaner Production 233, 115–125.

Yao, Z.T., Ji, X.S., Sarker, P.K., Tang, J.H., Ge, L.Q., Xia, M.S., Xi, Y.Q., 2015. A comprehensive review on the applications of coal fly ash. Earth-Science Reviews 141, 105–121.

Zhang, W., Groppo, J., Honaker, R., 2015. Ash Beneficiation for REE Recovery. 2015 World of Coal Ash 11.

Zhang, W., Honaker, R., 2019. Enhanced leachability of rare earth elements from calcined products of bituminous coals. Minerals Engineering 142, 1-9.

Zhang, W., Honaker, R., 2020. Characterization and recovery of rare earth elements and other critical metals (Co, Cr, Li, Mn, Sr, and V) from the calcination products of a coal refuse sample. Fuel 267, 117236.

Zhu, K.Y., Su, H.M., Jiang, S.Y., 2019. Mineralogical control and characteristics of rare earth elements occurrence in Carboniferous bauxites from western Henan Province, north China: A XRD, SEM-EDS and LA-ICP-MS analysis. Ore Geology Reviews 114, 103144.

APPENDICES

A) TIMA scan illustrating the mineral allanite (**A**), elemental map of Ce (**B**) and EDX spectrum of allanite (**C**)

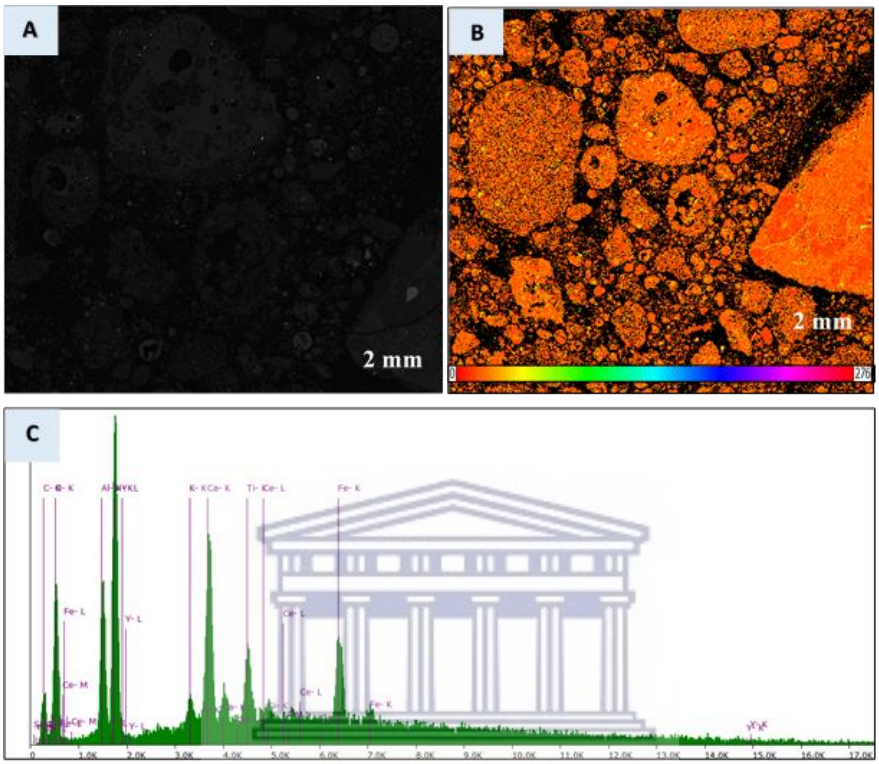

B) TIMA scan illustrating the mineral chlorite (**A**), EDX spectrum of chlorite (**B)** elemental map of **Y** (**C**) and elemental map of Nd (**D**)

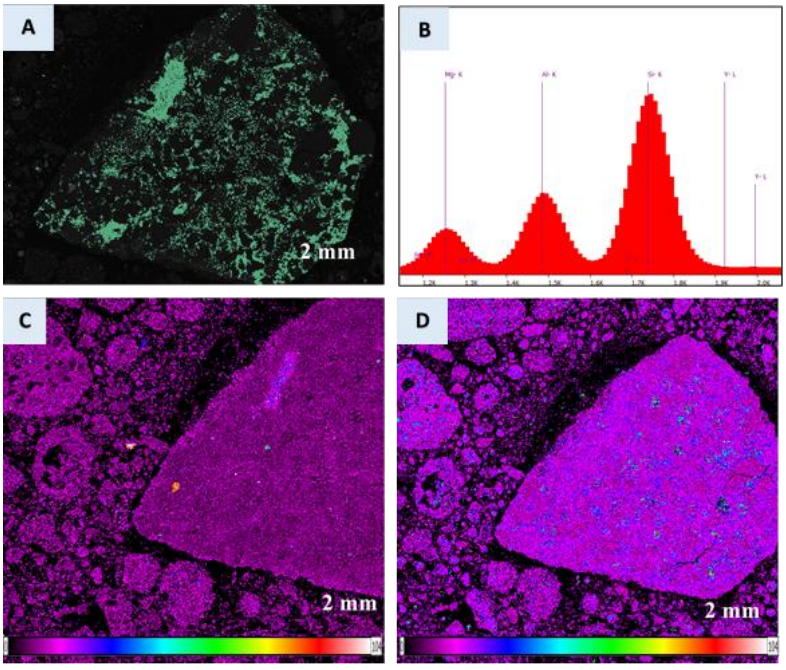

C) Summary of sieving analyses of Duvha CFA

Duvha CFA						
	Mass Retained (g)					
Size Fraction	**1**	**2**	**3**	**Arithmetic Average**	**Standard Deviation**	**Average Mass Retained %**
> 106	92.90	91.80	90.50	91.73	1.20	9.17
106 - 75	113.10	111.70	112.30	112.37	0.70	11.24
75 - 53	189.20	191.90	190.50	190.53	1.35	19.05
53 - 50	49.30	48.70	47.90	48.63	0.70	4.86
50 -32	337.10	339.80	337.90	338.27	1.39	33.83
32 - 25	81.70	80.40	82.90	81.67	1.25	8.17
< 25	122.10	120.90	121.90	121.63	0.64	12.16

D) Summary of sieving analyses of Tutuka CFA

Tutuka CFA						
	Mass Retained (g)					
Size Fraction	**1**	**2**	**3**	**Arithmetic Average**	**Standard Deviation**	**Average Mass Retained (%)**
> 106	264.40	266.50	265.10	265.33	1.07	26.53
106 - 75	177.20	176.90	175.40	176.50	0.96	17.65
75 - 53	143.80	146.10	144.60	144.83	1.17	14.48
53 - 50	31.10	29.90	30.50	30.50	0.60	3.05
50 -32	280.20	279.70	281.70	280.53	1.04	28.05
32 - 25	54.70	53.40	54.10	54.07	0.65	5.41
< 25	17.30	18.30	15.80	17.13	1.26	1.71

E) Elemental Composition (as oxides in weight %) of the various size fraction of Duvha CFA

	SiO_2	Al_2O_3	Fe_2O_3	CaO	TiO_2	P_2O_5	K_2O	Na_2O	Cr_2O_3	MgO	MnO	L.O.I.
> 106 µm	49,67	24,05	3,73	2,52	1,31	0,45	0,50	0,04	0,01	bdl	bdl	17,31
106 -75 µm	54,04	27,64	4,21	3,19	1,56	0,54	0,60	0,09	0,02	bdl	bdl	7,45
75 - 53 µm	55,26	29,29	4,07	3,52	1,67	0,58	0,64	0,11	0,02	bdl	bdl	3,90
50 - 50 µm	45,68	24,18	3,61	3,02	1,41	0,50	0,50	0,06	0,02	bdl	bdl	20,22
50 - 32 µm	55,24	30,12	3,95	3,67	1,77	0,66	0,65	0,08	0,02	bdl	bdl	3,04
32 - 25 µm	46,01	25,58	3,87	3,42	1,56	0,64	0,56	0,06	0,02	bdl	bdl	17,31
< 25 µm	52,97	30,87	4,68	3,97	1,91	0,86	0,68	0,07	0,03	bdl	bdl	3,05

F) Summary of REE composition (ppm) in the various size fractions of Duvha and Tutuka CFA

	Duvha CFA			Tutuka CFA		
	LREE	**HREE**	**Total**	**LREE**	**HREE**	**Total**
Whole	445.10	31.25	**573,77**	416.75	31.24	**546.25**
> 106 µm	340.14	28.09	442.43	378.98	27.35	477.61
106 -75 µm	411.71	34.10	536.19	402.37	28.55	505.62
75 - 53 µm	375.92	31.09	508.97	426.18	30.96	540.55
53 - 50 µm	393.82	32.59	514.23	448.45	31.73	565.13
50 - 32 µm	384.87	31.84	529.60	461.27	33.15	584.13
32 -25 µm	389.34	32.22	524.49	480.33	35.05	609.72
< 25 µm	387.11	32.03	541.07	491.88	35.62	625.85

G) Summary of Tutuka CFA SEM-EDS Analyses

Tutuka CFA SEM-EDS DATA				
Spectrum Label	**SPOT 1**	**SPOT 2**	**SPOT 3**	**SPOT 4**
O	48.30	22.90	23.11	3.97
Mg	0.82	0.35	0.15	0.27
Al	20.39	2.22	3.41	2.40
Si	23.27	1.31	2.86	2.38
P	0.31	0.14	0.48	0.00
S	0.10	0.00	0.07	0.14

Cl	0.13	0.02	0.20	0.13
K	0.71	0.05	0.00	0.00
Ca	2.39	0.78	2.22	1.20
Ti	0.83	0.15	0.13	0.09
Mn	0.00	0.01	0.01	0.00
Fe	2.71	71.70	67.37	89.37
Cu	0.04	0.36	0.00	0.04
Total	100.00	100.00	100.00	100.00

H) Summary of Duvha CFA SEM-EDS Analyses

Duvha CFA SEM-EDS					
Spectrum Label	**SPOT 1**	**SPOT 2**	**SPOT 3**	**SPOT 4**	**SPOT 5**
O	41.94	54.86	51.00	50.35	50.50
Na	0.05	0.05	0.12	0.09	0.04
Mg	0.25	0.17	0.37	0.22	0.13
Al	10.43	16.74	19.93	22.04	22.07
Si	9.91	25.49	24.87	24.56	24.61
P	0.24	0.11	0.30	0.15	0.08
S	0.00	0.14	0.03	0.00	0.08
Cl	0.05	0.00	0.00	0.00	0.08
K	0.28	0.38	0.60	1.24	0.55
Ca	0.50	0.34	1.39	0.26	0.50
Ti	0.16	0.60	0.53	0.19	0.34
Fe	36.19	1.12	0.85	0.90	1.01
Total	100.00	100.00	100.00	100.00	100.00

I) REE composition (ppm) of the raw bulk CFA of Duvha and Tutuka Power Station

Elements	Duvha CFA	Tutuka CFA
Sc	27.52	27.50
Y	69.89	70.76
La	99.41	94.27
Ce	216.98	197.33
Pr	21.59	20.60
Nd	76.67	74.16
Sm	14.64	14.53
Eu	2.68	2.76
Gd	13.15	13.10
Tb	2.06	2.02
Dy	12.27	12.13
Ho	2.37	2.35
Er	6.73	6.83
Tm	0.93	0.94
Yb	6.03	6.09
Lu	0.87	0.88
Total	**573.77**	**546.25**

J) REE composition (ppm) of the raw sieved fractions of Duvha CFA

DUVHA CFA AVERAGE CONCENTRATION (ppm)								
	DUV-Whole	**> 106**	**106 -75**	**75 - 53**	**53 - 50**	**50 - 32**	**32 -25**	**< 25**
Sc	27,52	20,59	25,14	29,66	25,35	33,65	30,97	36,33
Y	69,89	53,61	65,24	72,30	62,47	79,23	71,96	85,60
La	99,41	76,02	92,23	84,13	88,18	86,15	87,17	86,66
Ce	216,98	157,67	191,29	174,48	182,89	178,69	180,79	179,74
Pr	21,59	17,74	21,44	19,59	20,52	20,06	20,29	20,17

Nd	76,67	63,61	76,15	69,88	73,01	71,44	72,23	71,84
Sm	14,64	12,10	14,70	13,40	14,05	13,72	13,88	13,80
Eu	2,68	2,03	2,60	2,31	2,45	2,38	2,42	2,40
Gd	13,15	10,97	13,30	12,13	12,72	12,43	12,57	12,50
Tb	2,06	1,73	2,09	1,91	2,00	1,96	1,98	1,97
Dy	12,27	10,69	12,99	11,84	12,42	12,13	12,27	12,20
Ho	2,37	2,10	2,54	2,32	2,43	2,38	2,40	2,39
Er	6,73	6,07	7,35	6,71	7,03	6,87	6,95	6,91
Tm	0,93	0,89	1,10	0,99	1,04	1,02	1,03	1,02
Yb	6,03	5,75	6,99	6,37	6,68	6,52	6,60	6,56
Lu	0,87	0,87	1,04	0,95	1,00	0,97	0,98	0,98
LREE	445,10	340,14	411,71	375,92	393,82	384,87	389,34	387,11
HREE	31,25	28,09	34,10	31,09	32,59	31,84	32,22	32,03
Total	573,77	442,43	536,19	508,97	514,23	529,60	524,49	541,07

K) REE composition (ppm) of the raw sieved fractions of Tutuka CFA

TUTUKA SIEVED SIZE FRACTIONS								
	TUT-Whole	**> 106**	**106 -75**	**75 - 53**	**53 - 50**	**50 - 32**	**32 -25**	**< 25**
Sc	27,50	21,52	22,66	25,00	25,45	27,37	28,36	30,47
Y	70,76	49,76	52,05	58,41	59,51	62,34	65,98	67,87
La	94,27	87,27	92,92	97,90	103,66	106,89	111,25	113,94
Ce	197,33	178,01	188,98	200,61	211,37	217,31	225,30	232,08
Pr	20,60	18,24	19,36	20,66	21,67	22,36	23,20	23,48
Nd	74,16	67,85	71,83	76,33	79,65	81,71	85,77	87,18
Sm	14,53	13,14	13,90	14,53	15,26	15,63	16,41	16,60
Eu	2,76	2,44	2,58	2,70	2,82	2,91	3,08	3,11
Gd	13,10	12,04	12,81	13,45	14,03	14,47	15,32	15,49
Tb	2,02	1,74	1,84	1,96	2,03	2,08	2,22	2,23

Dy	12,13	10,60	11,06	11,92	12,26	12,73	13,41	13,66
Ho	2,35	2,08	2,16	2,34	2,41	2,53	2,66	2,70
Er	6,83	5,72	6,02	6,51	6,70	7,00	7,36	7,52
Tm	0,94	0,81	0,83	0,91	0,94	0,99	1,04	1,05
Yb	6,09	5,67	5,88	6,49	6,55	6,94	7,42	7,49
Lu	0,88	0,73	0,75	0,84	0,85	0,89	0,95	0,97
LREE	416,75	378,98	402,37	426,18	448,45	461,27	480,33	491,88
HREE	31,24	27,35	28,55	30,96	31,73	33,15	35,05	35,62
Total	546,25	477,61	505,62	540,55	565,13	584,13	609,72	625,85

L) REE composition (ppm) of the leachates of the sieved size fractions of Duvha CFA

DUVHA CFA LEACHATE REE CONCENTRATION (ppm)								
	DUV-Whole	**> 106**	**106 -75**	**75 - 53**	**53 - 50**	**50 - 32**	**32 -25**	**< 25**
Sc	0,79	0,52	0,79	0,69	0,77	0,97	0,91	1,09
Y	2,07	1,57	2,45	2,03	2,16	2,50	2,44	2,88
La	3,16	2,48	3,77	3,07	3,20	3,66	3,37	4,11
Ce	4,45	3,77	5,39	4,32	4,45	4,80	3,94	5,75
Pr	0,65	0,53	0,78	0,62	0,64	0,75	0,69	0,84
Nd	2,42	1,95	2,89	2,32	2,42	2,73	2,53	3,19
Sm	0,46	0,38	0,57	0,47	2,69	0,54	0,50	0,63
Eu	0,08	0,06	0,09	0,08	0,08	0,10	0,08	0,11
Gd	0,44	0,34	0,52	0,42	0,45	0,50	0,46	0,59
Tb	0,07	0,05	0,08	0,07	0,07	0,08	0,08	0,09
Dy	0,45	0,33	0,52	0,42	0,44	0,51	0,49	0,59
Ho	0,09	0,06	0,10	0,08	0,09	0,10	0,10	0,12
Er	0,24	0,19	0,29	0,24	0,26	0,30	0,28	0,34
Tm	0,04	0,02	0,04	0,03	0,04	0,04	0,04	0,05
Yb	0,22	0,16	0,26	0,22	0,24	0,26	0,26	0,32

Lu	0,03	0,02	0,03	0,03	0,03	0,04	0,03	0,04
LREE	11,66	9,51	14,01	11,30	13,94	13,07	11,57	15,21
HREE	1,14	0,85	1,32	1,09	1,17	1,33	1,28	1,55
TOTAL	15,67	12,45	18,56	15,11	18,04	17,87	16,21	20,73

M) REE composition (ppm) of the leachates of the sieved size fractions of Tutuka CFA

TUTUKA CFA LEACHATE REE CONCENTRATION (ppm)								
	TUT-Whole	**> 106**	**106 -75**	**75 - 53**	**53 - 50**	**50 - 32**	**32 -25**	**< 25**
Sc	0,63	0,58	0,82	0,88	0,97	0,99	1,11	1,15
Y	3,35	2,23	2,66	2,71	2,89	3,01	3,36	3,35
La	3,25	2,85	3,36	3,42	3,89	3,98	4,31	4,31
Ce	4,32	4,36	4,54	4,66	6,32	5,53	5,92	6,51
Pr	0,69	0,60	0,70	0,71	0,84	0,87	0,91	0,91
Nd	2,59	2,26	2,68	2,76	3,16	3,14	3,41	3,42
Sm	0,49	0,43	0,52	0,54	0,57	0,60	0,65	0,65
Eu	0,09	0,08	0,09	0,10	0,11	0,11	0,11	0,12
Gd	0,56	0,47	0,53	0,56	0,65	0,62	0,69	0,68
Tb	0,07	0,07	0,08	0,08	0,09	0,09	0,09	0,10
Dy	0,47	0,42	0,49	0,50	0,55	0,58	0,65	0,65
Ho	0,09	0,08	0,10	0,10	0,11	0,12	0,13	0,13
Er	0,28	0,24	0,28	0,29	0,31	0,33	0,37	0,37
Tm	0,04	0,03	0,04	0,04	0,05	0,05	0,05	0,05
Yb	0,25	0,21	0,25	0,26	0,28	0,31	0,34	0,34
Lu	0,03	0,03	0,03	0,03	0,04	0,04	0,04	0,04
LREE	11,98	11,06	12,43	12,75	15,52	14,85	15,99	16,60
HREE	1,23	1,08	1,27	1,30	1,43	1,51	1,66	1,68
Total	17,20	14,96	17,18	17,64	20,81	20,36	22,12	22,77

N) Summary of the total REE composition (ppm) of Duvha and Tutuka CFA in each sieved particle size fraction and LREE/HREE ratios

	Duvha CFA		Tutuka CFA	
Size Fraction	**Total [REE]**	**LREE/HREE**	**Total [REE]**	**LREE/HREE**
> 106	368,22	12,11	406,33	13,86
106 -75	445,80	12,08	430,91	14,10
75 - 53	407,01	12,09	457,14	13,77
53 - 50	426,41	12,08	480,17	14,13
50 - 32	416,71	12,09	494,42	13,92
32 -25	421,56	12,08	515,39	13,70
< 25	419,14	12,09	527,51	13,81

O) XRD analyses of raw and leached residue of Duvha CFA

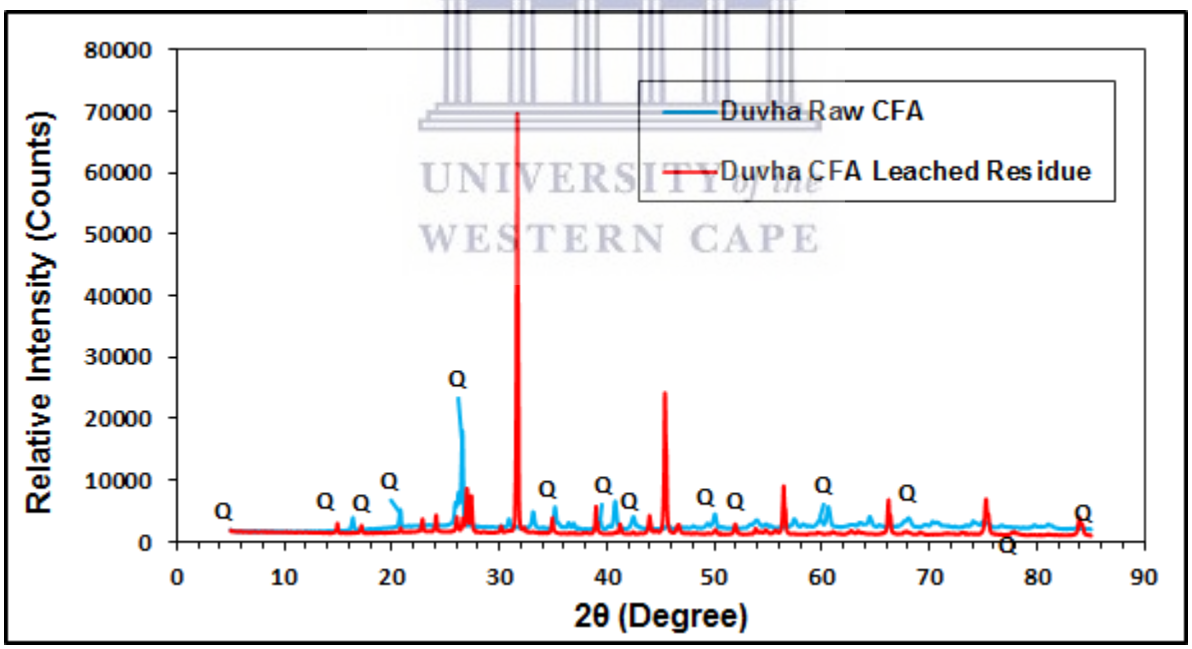

P) XRD analyses of raw and leached residue of Tutuka CFA

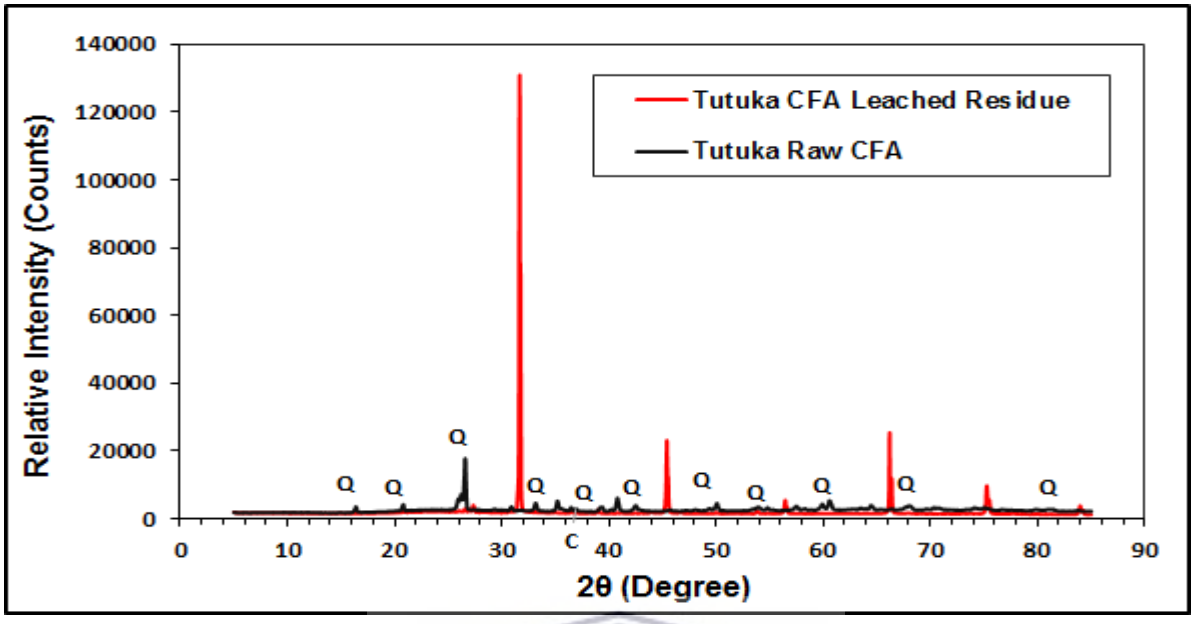

Q) REE composition (ppm) of the whole leached residues of Duvha and Tutuka CFA

	Duvha Residue	Tutuka Residue
Sc	9,89	10,42
Y	23,46	23,29
La	32,27	31,68
Ce	75,40	88,42
Pr	6,76	6,93
Nd	24,10	24,97
Sm	4,77	4,96
Eu	0,82	0,87
Gd	4,34	4,39
Tb	0,68	0,69
Dy	4,16	4,10
Ho	0,83	0,83
Er	2,45	2,34
Tm	0,35	0,34

Yb	2,19	2,25
Lu	0,32	0,31
LREE	148,47	162,23
HRE	10,98	10,87
TOTAL	192,81	206,82

R) REE composition (ppm) of Duvha CFA

	Raw CFA	**Blank Leachate**	**Acid Leachate**	**Blank Leached Residue**	**Acid Leached Residue**	**Detection Limit**
Sc	27,52	BDL	0,79	32,18	9,89	0,02
Y	69,89	BDL	2,07	78,52	23,46	0,02
La	99,41	BDL	3,16	107,77	32,27	0,00
Ce	216,98	BDL	4,45	224,01	75,40	0,01
Pr	21,59	BDL	0,65	22,23	6,76	0,00
Nd	76,67	BDL	2,42	81,17	24,10	0,00
Sm	14,64	BDL	0,46	15,65	4,77	0,02
Eu	2,68	BDL	0,08	2,68	0,82	0,01
Gd	13,15	BDL	0,44	13,77	4,34	0,02
Tb	2,06	BDL	0,07	2,29	0,68	0,001
Dy	12,27	BDL	0,45	14,02	4,16	0,02
Ho	2,37	BDL	0,09	2,79	0,83	0,01
Er	6,73	BDL	0,24	7,95	2,45	0,02
Tm	0,93	BDL	0,04	1,12	0,35	0,01
Yb	6,03	BDL	0,22	7,28	2,19	0,02
Lu	0,87	BDL	0,03	1,07	0,32	0,004
ΣREE	**573,77**		**15,67**	**614,50**	**192,81**	

S) REE composition (ppm) of Tutuka CFA

	Raw CFA	Blank Leachate	Acid Leachate	Acid Leached Residue	Blank Leached Residue	Detection Limit
Sc	27,50	0,14	0,63	10,42	31,02	0,02
Y	70,76	1,40	3,35	23,29	72,73	0,02
La	94,27	0,75	3,25	31,68	96,59	0,00
Ce	197,33	1,04	4,32	88,42	195,09	0,01
Pr	20,60	0,15	0,69	6,93	20,28	0,00
Nd	74,16	0,72	2,59	24,97	75,20	0,00
Sm	14,53	0,11	0,49	4,96	14,78	0,02
Eu	2,76	0,03	0,09	0,87	2,59	0,01
Gd	13,10	0,35	0,56	4,39	13,53	0,02
Tb	2,02	0,02	0,07	0,69	2,10	0,001
Dy	12,13	0,10	0,47	4,10	12,79	0,02
Ho	2,35	0,03	0,09	0,83	2,53	0,01
Er	6,83	0,05	0,28	2,34	7,36	0,02
Tm	0,94	0,01	0,04	0,34	1,01	0,01
Yb	6,09	0,04	0,25	2,25	6,74	0,02
Lu	0,88	0,00	0,03	0,31	0,95	0,004
ΣREE	**546,25**	**4,93**	**17,20**	**206,82**	**555,30**	